OVEREXPRESSION OF WILD-TYPE *ANXA7* TUMOR SUPPRESSOR GENE ALTERS CANCER-RELATED MICRORNAS IN HUMAN PROSTATE CANCER CELLS

YAP LIM HUI

FACULTY OF SCIENCE
UNIVERSITY OF MALAYA
KUALA LUMPUR

2013

OVEREXPRESSION OF WILD-TYPE *ANXA7* TUMOR SUPPRESSOR GENE ALTERS CANCER-RELATED MICRORNAS IN HUMAN PROSTATE CANCER CELLS

YAP LIM HUI

DISSERTATION SUBMITTED IN FULFILMENT OF THE REQUIREMENTS FOR THE DEGREE OF MASTER OF SCIENCE

FACULTY OF SCIENCE
UNIVERSITY OF MALAYA
KUALA LUMPUR

2013

Abstract

MicroRNAs (miRNAs) are endogenous 18-25nt RNAs that regulate genes at the protein translation level. They can act as tumor suppressors or oncogene and are often dysregulated in various cancers. *ANXA7* is a tumor suppressor gene that encodes for a Ca^{2+}-dependent membrane-binding protein and its expression was found to be reduced or lost in advanced androgen-independent prostate cancers. This research aims to identify miRNAs that are regulated by the *ANXA7* tumor suppressor gene and the putative pathways involved in prostate cancer. The overexpression of wild-type *ANXA7* was achieved by using a mammalian expression vector harboring the gene. From our miRNA microarray expression, a total of 16 miRNAs were found to be significantly differentially expressed in response to increased ANXA7. These include hsa-miR-874, hsa-miR-1284, hsa-miR-543 and hsa-miR-409-5p. All of these miRNAs have predicted targets that are involved in calcium signaling. In conclusion, the altered miRNA expression induced upon increased expression of ANXA7 suggests that miRNAs and the calcium signaling pathways are regulated by ANXA7 and could be manipulated for therapeutic purposes.

Abstrak

MikroRNA adalah RNA endogen dengan panjang 18-25 nukleotida yang mengawal protein pada tahap translasi. Mereka boleh mengambil tugas sebagai penindas tumor atau onkogen dan sering mengalami disregulasi dalam pelbagai kanser. *ANXA7* adalah gen untuk penindas tumor yang mengkod untuk protein bergantung-Ca^{2+} yang mengikat membrane dan tahapnya di dalam kanser prostat peringkat maju adalah kurang atau tiada sama sekali. Kajian kami ingin mengetahui apakah mikroRNA yang di kawal of *ANXA7* dan laluan biologi yang dikawal oleh mikroRNA tersebut didalam kanser prostat. Peningkatan tahap gen normal *ANXA7* dikecapi dengan vektor-ekspressi mammalia yang mengandungi gen tersebut. Dari miRNA microarray kami, mikroRNA berjumlah 16 didapati telah mengalami pengubahan ekspressi yang ketara setelah tahap ANXA7 di tingkatkan. Ini termasuk hsa-miR-874, hsa-miR-1284, hsa-miR-543 dan hsa-miR-409-5p dengan sasaran yang dijangka terlibat dalam pengisyaratan kalsium. Kesimpulannya, pengubahan ekspressi mikorRNA setelah peningkatan tahap ANXA7 mencadangkan bahawa mikroRNA dan laluan pengisyaratan kalsium yang terlibat adalah di regulasi oleh ANXA7 dan boleh dimanipulasikan untuk tujuan terapeutik.

Acknowledgements

This study was funded by University of Malaya (UM) through Postgraduate Research Allocation (PPP) (PV058-2011B and PS281-2009B) and the University of Malaya Research Grant (UMRG) (RG037-10BIO). I would like to acknowledge and thank them for their utmost generosity in terms of financing this project and making it a reality.

I would like to convey my utmost gratitude to my project supervisor Assoc. Prof. Dr. Noor Hasima Nagoor for giving me the opportunity to do this research under her group. I would also like to thank her for her guidance from the beginning of the project and making sure I'm meeting deadlines and criteria needed for the fulfillment of this thesis. She also gave me words of encouragement whenever the progress of the project did not go as well as expected to help me keep going.

Next I would also like to give my sincere thanks to other lab members in our research group and especially to Phuah Neoh Hun, Norahayu Othman and Yap Seow Hui. With them around, life in the lab throughout this project was never a dull moment. We helped each other during rough times, shared information and knowledge that we've gained to make problem solving in a relatively new field less troublesome.

A special thanks to Chong Jinq Shin. Her technical knowledge in Microsoft Excel has helped in the mining of microarray data and organization of this project. Without her assistance, the large amount of raw data generated would be difficult to handle and presented in a reader-friendly manner. In addition her motivation keeps my engine in top gear and to never give up.

Finally, I would like to extend my appreciation to my parents, family members, friends and lecturers for their support throughout this study. Most importantly I would like to thank the blessings and trials from God throughout the journey of this Masters project. Without the support and assistance from those mentioned, this project would not have been a success. Thank you!

Table of contents

Abstract ii

Abstrak iii

Acknowledgements iv

Table of contents vi

List of figures xi

List of table xiii

List of symbols and abbreviations xiv

Chapter 1: Introduction 1

Chapter 2: Literature Review 3

2.1 MicroRNAs (miRNAs) 3

2.1.1 Discovery of miRNAs 3

2.1.2 Annotation of miRNAs 5

2.1.3 Defining miRNAs 7

2.1.4(a) Biogenesis of miRNA: from the gene 7

2.1.4(b) Biogenesis of miRNA: the Microprocessor complex 10

2.1.4(c) Biogenesis of miRNA: the export to the cytoplasm 12

2.1.4(d) Biogenesis of miRNA: Dicer processing to form mature miRNAs 13

2.1.4(e) Biogenesis of miRNA: incorporation into the RISC (RNA-induced silencing complex) 14

2.1.5 Mechanism of miRNAs 16

2.2 Prostate Cancer 18

2.2.1 Facts and Figures 18

2.2.2 Defining the Prostate and Prostate Cancer 22

2.2.3 Molecular Pathway in Prostate Cancer Progression 24

2.3 Annexin VII (ANXA7) and Prostate Cancer. 26

2.4 MicroRNAs and cancer 31

2.4.1 Dysregulation of microRNAs in cancer 31

2.4.2 microRNAs as tumor suppressors and oncogenes 33

2.4.3 Regulation of microRNAs 34

2.4.4 MicroRNAs and *ANXA7* 36

2.5 Study objectives 37

Chapter 3: Methodology 38

3.1 Materials 38

3.1.1 Cancer Cell Culture Growth Media and Reagents 38

3.1.1.1 RPMI 1640 38

3.1.1.2 Fetal Bovine Serum (FBS) 38

3.1.1.3 Dulbecco's Phosphate Buffered Saline (D-PBS) 39

3.1.1.4 0.53mM EDTA solution 39

3.1.1.5 0.25% Trypsin-0.53mM EDTA solution 39

3.1.1.6 10,000 u per ml/10, 000 µg per ml Penicillin/Streptomycin solution 40

3.1.1.7 Antibiotic G-418 Sulfate 40

3.1.2 Bacterial Culture Growth Media and reagents 40

3.1.2.1 Luria-Bertani (LB) Medium 40

3.1.2.2 LB Agar 41

3.1.2.3 Antibiotics 41

3.1.2.4 Restriction enzymes (RE) and T4 DNA Ligase 42

3.1.3 Buffers and stock solutions 42

3.1.3.1 10x Tris borate EDTA buffer (TBE) 42

3.1.3.2 25x Tris acetate EDTA buffer (TAE) 42

3.1.3.3 6x DNA loading dye 43

3.1.3.4 2X RNA loading dye 43

3.1.3.5 Ethidium Bromide (EtBr) Solution 43

3.1.4 Commercial Kits 44

3.1.5 Chemical Reagents 44

3.1.6 Bacterial strains, plasmid vectors and oligonucleotides 45

3.1.6.1 Bacterial Strains 45

3.1.6.3 Oligonucleotides 48

3.1.7 DNA ladder marker 50

3.1.8 RNA ladder marker 51

3.1.9 Cancer cell lines 52

3.1.10 Normal Prostate Epithelial cDNA 52

3.2 Methods 53

3.2.1 Cell Culture 53

3.2.2 Total RNA Extraction 53

3.2.3 Agarose Gel Electrophoresis 54

3.2.3.1 DNA Agarose Gel Electrophoresis (AGE) 54

3.2.3.2 Native RNA Agarose Gel Electrophoresis (AGE) 55

3.2.4 Reverse Transcription (RT) 55

3.2.5 PCR Amplification of Annexin VII (ANXA7) gene 55

3.2.6 pENTR/ANXA7 Vector Construction and Transformation of Construct into *E. coli* 56

3.2.7 Colony PCR of Putative Clones 57

3.2.8 pcDNA3.1/ANXA7 Vector Construction and Transformation of Construct into *E. coli* 57

3.2.9 Plasmid Purification 58

3.2.10 Restriction Enzyme (RE) Digestion and Analysis 58

3.2.11 Sequencing of Plasmid Constructs and Nucleotide Sequence Analysis 59

3.2.12 Propagation of pcDNA3.1/nV5-DEST™ and pIRES2-AcGFP1 vectors 60

3.2.13 Transfer of ANXA7 gene from pcDNA3.1/ANXA7 to pIRES2-AcGFP1 vector 61

3.2.14 Stable Transfection of Cell Line 62

3.2.15 qRT-PCR of ANXA7 63

3.2.16 MicroRNA microarray expression analysis 64

3.2.17 Validation of miRNA microarray data 65

3.2.18 Bioinformatic analysis 65

3.2.19 Statistical analysis 66

Chapter 4: Results 67

4.1 Full length PCR Amplification of the *ANXA7* gene 67

4.2 Construction of pENTR/ANXA7 and pcDNA4.1/ANXA7 Vectors. 73

4.3 Transfer of *ANXA7* from pcDNA3.1/*ANXA7* to pIRES2-AcGFP1 vector 77

4.4 Stable transfection of PC-3 and DU 145 cells with pIRES2-AcGFP1-ANXA7 78

4.5 MicroRNA Profile of PC-3 and DU 145 Cells following ANXA7 Overexpression 80

4.6 Predicted Genes and Pathways Targeted by ANXA7 Dysregulated miRNAs 83

Chapter 5: Discussion 86

5.1 ANXA7 likely to Regulate a Specific Set of MiRNAs 86

5.2 Potential Regulation of Calcium Signaling by ANXA7 via Hsa-miR-874 87

5.3 Putative modulation of MEF2C by miR-1284 and miR-874 88

5.4 Hsa-miR-543 and Phospholipase A2 Group 4A (PLA2G4A) 90

5.5 MicroRNA-409-5p and Calmodulin binding transcription activator 1 (CAMTA1) 91

Chapter 6: Conclusion 94

References 96

Appendix A 110

S4.1 Full length PCR Amplification of the ANXA7 gene 110

S4.2 Construction of Cloning and Expression Vectors containing ANXA7 111

S4.3 Transfer of ANXA7 from pcDNA3.1/ANXA7 to pIRES2-AcGFP1 vector 115

S4.4 Stable transfection of PC-3 and DU 145 cells with pIRES2/ANXA7 119

S4.5 MicroRNA Profile of PC-3 and DU 145 Cells following ANXA7 Overexpression 120

S4.6 Predicted Genes and Pathways Targeted by ANXA7 Dysregulated miRNAs 121

List of figures

Figure 2.1	:	Biogenesis of microRNAs in mammals	9
Figure 2.2 a & b	:	Prostate Cancer Statistics based on Age-Standardized Rate (ASR) per 100,000 population	20
Figure 2.2 c	:	Prostate Cancer Statistics based on Age-Standardized Rate (ASR) per 100,000 population	21
Figure 2.3	:	Side view of the prostate and the male reproductive system	22
Figure 3.1	:	Map and features of pENTR™/D-TOPO® vector	46
Figure 3.2	:	Map and features of pcDNA3.1/nV5-DEST™ vector	47
Figure 3. 3	:	Map and features of pIRES2-AcGFP1 vector	47
Figure 3.4	:	Molecular weight, mass and percentage of the O'GeneRuler 1kb DNA Ladder marker fragments after an agarose gel electrophoresis	50
Figure 3.5	:	Molecular weight and mass of the RiboRuler™ High Range RNA Ladder marker fragments after a native agarose gel (left) and a formaldehyde agarose gel electrophoresis	51
Figure 4.1 a & b	:	Intact total RNA extracted from PC-3 cell line	68
Figure 4. 2 a & b	:	Determination of optimum annealing temperature (Ta) for primers flanking ANXA7	69
Figure 4. 3	:	Determination of optimum β-actin PCR amplification annealing temperature	70
Figure 4.4	:	PCR amplification of full length ANXA7 from normal prostate epithelium cDNA	72

Figure 4.5	:	Screening of clones containing the pENTR/ANXA7 construct	73
Figure 4.6		Determination of ANXA7 insert orientation in pENTR/ANXA7 construct	74
Figure 4.7 a & b	:	Analysis of sequenced ANXA7 in vector constructs using NCBI BLAST	75
Figure 4.8 a & b	:	Isolation and identification of pcDNA3.1/ANXA7 construct following transfer from pENTR/ANXA7 construct	76
Figure 4.9	:	Screening of colonies to determine presence of ANXA7 insert in pIRES2-AcGFP1 vector	77
Figure 4.10 a & b	:	Transfection of PC-3 and DU145 prostate cancer cells with pIRES2-AcGFP1-ANXA7 expression vector increased wild-type ANXA7 expression levels	79
Figure 4.11 a-c	:	Validation and correlation of selected miRNA fold-expressions between microarray and qPCR data	82
Figure 5.1	:	A hypothetical network illustrating the interaction of hsa-miR-874, hsa-miR-1284, hsa-miR-543 and hsa-miR-409-5p and their predicted targets following overexpression of wtANXA7 in PC-3 prostate cancer cells	93
Figure S4.1.1	:	PCR amplification of ANXA7 using A7P2 primer pair	111
Figure S4.2.1	:	Quality check on pENTR/ANXA7 construct sequences returned from sequencing	112
Figure S4.2.2	:	Analysis of ANXA7 sequence in pENTR/ANXA7 constructs using NCBI BLAST	113

Figure S4.2.3	:	Alignment of ANXA7 sequences with cloning construct sequences using Bioedit	114
Figure S4.2.4 a & b	:	Quality check of sequencing results and analysis of ANXA7 sequence in pcDNA3.1/ANXA7 construct	115
Figure S4.3.1	:	Cloning of the ANXA7 insert in pcDNA3.1/ANXA7 into pIRES2-AcGFP1 vector	116
Figure S4.3.2 a & b	:	Quality check of sequencing results for pIRES2/ANXA7 clones and ANXA7 sequence analysis	119
Figure S4.4.1	:	Determination of G418 antibiotic concentration for selection of stable transfected cells	120
Figure S4.4.2	:	Assessment of total RNA Integrity	121

List of tables

Table 3.1	:	Bacterial strains used	45
Table 3.2	:	Oligonucleotides used in this study	48
Table 4.1	:	List of miRNA expression fold-change alternations following the overexpression of ANXA7 on PC-3 cells	82
Table 4.2	:	List of validated miRNA gene targets and related pathways as obtained using TargetScan 6.2 software and KEGG pathway	85
Table S4.6.1	:	List of miRNA gene targets and related pathways as obtained using TargetScan 6.2 software and KEGG pathway	122

List of Symbols and Abbreviations

®	Registered
°C	degrees Celcius
β	beta
µ	micro
µg	microgram
µl	microliter
A7P2F	ANXA7 Forward Primer 2
A7P2R	ANXA7 Reverse Primer 2
A7P3F	ANXA7 Forward Primer 3
A7P3R	ANXA7 Reverse Primer 3
AGE	agarose gel electrophoresis
Ago	Argonaute
AI	androgen independent
Anx7	mouse Annexin VII
anx7	Annexin VII from other species
ANXA7	Annexin VII
AR	androgen receptor
ASR	age-standardized rate
ATCC	American Type Culture Collection
ATP	adenosine triphosphate
B3F	β-actin Forward Primer 3
B3R	β-actin Reverse Primer 3
Bak1	BCL2-antagonist/killer 1
Bcl-2	B-cell lymphocyte 2
BLAST	Basic Local Alignment Search Tool
BPH	benign prostatic hyperplasia
C. elegans	*Caenorhabditis elegans*
Ca	Calcium
CACNA1D	Calcium channel, voltage-dependent, L type, alpha 1D subunit
CACNA1E	Calcium Channel, Voltage-dependent, R type, Alpha 1E subunit
CACNB2	Calcium Channel, Voltage-dependent, Beta 2 subunit
CaM	Calmodulin
CAMTA1	calmodulin binding transcription activator 1
CaP	carcinoma of the prostate
cDNA	complementary DNA
CEFs	chicken embryo fibroblasts
ChIP	chromatin immunoprecipitation

CHP	Calcium Binding Protein P22
CLL	chronic lymphocytic leukemia
cm	centimeter
CO_2	carbon dioxide
COX	cyclooxygenase
DEPC	DiethylenePyrocarbonate
DGCR8	DiGeorge syndrome critical region gene 8
dH_2O	distilled water
DNA	deoxyribonucleic acid
dNTP	deoxy Nucleotide Triphosphate
D-PBS	Dulbecco's phosphate buffered saline
Drosophila	Drosophila melanogaster
dsRBD	dsRNA binding domain
dsRNA	double-stranded RNA
E. coli	*Escherichia coli*
EDTA	Ethylenediaminetetraacetic Acid
eIF2C	eukaryotic initiation factor 2C
EP300	E1A binding protein p300
EtBr	Ethidium Bromide
Exp5	Exportin 5
FBS	fetal bovine serum
FpcD3.1_778	pcDNA3.1/nV5-DEST Forward Primer
g	gram
GDP	guanosine diphosphate
GFP	green fluorescence protein
GTP	guanosine triphosphate
h	hour
H_2O	water
HCC	hepatocellular carcinoma
HDAC4	Histone Deacetylase 4
HETE	hydroxyeicosatetraenoic acid
HPV	human papilloma virus
HRAS	human H-*RAS* gene
hsa	*Homo sapiens*
kb	kilo base
KCl	Potassium Chloride
kDa	kilo Dalton
KEGG	Kyoto Encyclopedia of Genes and Genomes
KH_2PO_4	Potassium Dihydrogen Phosphate
Ki-MuSV	Kirsten murine sarcoma virus

KRAS	human K-*RAS* gene
L	liters
L1	larval stage 1
LB	Luria Bertani
LOH	loss of heterozygosity
LOX	lipoxygenase
m	mili
M	molar
MAPK	Mitogen-activated Protein Kinase
MEF2	Myocyte Enhancer Factor 2
MEF2C	Myocyte Enhancer Factor 2 isoform C
mg	miligram
$MgCl_2$	Magnesium Chloride
min	minutes
miRNA	microRNA
miRNP	miRNA ribonucleoprotein complex
ml	mililiter
mm	milimeter
MMPs	matrix metalloproteases
mmu	*Mus musculus*
mRNA	messenger RNA
Na_2HPO_4	Disodium Hydrogen Phosphate
NaCl	Sodium Chloride
NCBI	National Center for Biotechnology Information
NCI	National Cancer Institute
ncRNA	non-coding RNA
NFAT	Nuclear Factor of Activated T lymphocytes
NRAS	human N-*RAS* gene
nt	nucleotide
NTC	non-transfected cells
O.D	optical density
ORF	open reading frame
PBS	phosphate buffered saline
pcDNA3.1/*ANXA7*	pcDNA3.1/nV5-DEST™ containing *ANXA7* gene
PCR	Polymerase Chain Reaction
pENTR/*ANXA7*	pENTR™/D-TOPO® containing *ANXA7* gene
PG	prostaglandins
PIN	prostatic intraepithelial neoplasia
PLA2G4A	phospholipase A2, group IVA
pol	polymerase

pol II	RNA polymerase II
pol III	RNA polymerase III
polyA	polyadenylation
PPD	PAZ and PIWI domain
PPP1CA	protein phosphatase 1, catalytic subunit, alpha isozyme
pre-miRNA	precursor-miRNA
pri-miRNA	primary-miRNA
PSA	prostate specific antigen
psi	pounds per square inch
qPCR	quantitative Polymerase Chain Reaction
qRT-PCR	quantitative reverse transcription PCR
Rb	Retinoblastoma
RE	restriction enzyme
RefSeq	reference sequence
RIN	RNA Integrity Number
RISC	RNA-induced silencing complex
RNA	ribonucleic acid
RNAi	RNA interference
RNase	Ribonuclease
RpcD3.1_2790	pcDNA3.1/nV5-DEST Reverse Primer
rpm	revolutions per minute
RPMI	Roswell Park Memorial Institute
rRNA	ribosomal RNA
RT	Reverse Transcription
S.D	standard deviation
SDS	Sodium Dodecyl Sulfate
siRNA	short interfering RNA
smRNA	small regulatory RNA
snRNA	small nuclear RNA
SOC	super-optimal catabolite repression
SOX5	SRY-box5
stRNA	small temporal RNA
STS	steroid sulfatase
T_a	annealing temperature
TAE	Tris Acetate EDTA
TBE	Tris Borate EDTA
TGF-β	Transforming Growth Factor-Beta
TMA	tissue microarray
tncRNA	tiny non-coding RNA
tRNA	transfer RNA
TRPM8	Transient Receptor Potential Cation Channel, subfamily M,

	member 8
TSG	tumor suppressor gene
™	Trademark
u	unit
UTR	untranslated region
V	volt
v/v	volume per volume
VEGF	Vascular Endothelial Growth Factor
w/v	weight per volume
Wnt	Wingless-int
wtANXA7	wild-type ANXA7

Chapter 1: Introduction

MicroRNAs (miRNAs) are endogenous 18-25nt RNAs that regulate genes at the post transcriptional level via complementary base-pairing with mRNAs and the triggering of two posttranscriptional events; mRNA cleavage and translational repression (Bartel, 2004). MicroRNAs are known to play key roles in carcinogenesis and their expression is often dysregulated in various cancers (Calin et al., 2002; Michael et al., 2003, Takamizawa et al., 2004; Metzler et al., 2004). MicroRNAs can also act as tumor suppressors (Takamizawa et al., 2004) or oncomirs (Meng et al., 2007) in cancer. The expression of miRNAs are regulated by various transcription factors such as c-Myc (O'Donnell et al., 2005) and p53 (Suzuki et al., 2009) in addition to epigenetic factors (Lodygin et al., 2008) or hormones (Shi et al., 2007).

Prostate cancer is the second most frequent cancer to occur in men worldwide after lung cancer (Ferlay et al., 2008). Even though current treatment options such as surgery and radiation therapy are effective against early stages of prostate cancer, patients with hormone-independent advanced stage prostate cancers typically faces a poor prognosis with limited treatment options (Damber and Aus, 2008). Therefore there is a need to search for alternative therapeutic options.

Human ANXA7, located at chromosome 10q21 was recently identified as a tumor suppressor gene in prostate cancer and various cancers (Srivastava et al., 2007). ANXA7 levels were decreased markedly or even lost in metastatic and recurrent hormone-independent CaP, while still remaining high in less advance stages (Srivastava et al., 2001b).

Our study aimed to look at whether the tumor suppressive effect of ANXA7 in prostate cancer involves regulation of miRNAs and whether the miRNAs regulated are involved in distinct signaling pathways. In order to do so, we tried to restore the wild-type ANXA7 (wtANXA7) function in hormone-independent prostate cancer cell lines by transfecting the cells with a mammalian expression vector harboring the *wtANXA7* gene. A global expression pattern of miRNAs was then obtained using miRNA microarrays. Genes potentially targeted by the dysregulated microRNAs was predicted *in silico* and putative signaling pathways involved were identified.

Chapter 2: Literature Review

2.1 MicroRNAs (miRNAs)

2.1.1 Discovery of miRNAs

Before the discovery of small regulatory ribonucleic acids (RNA), we only know the existence and functions of the messenger RNA (mRNA), transfer RNA (tRNA) and ribosomal RNA (rRNA). However, researchers realized that the picture was still incomplete when Fire *et al* in 1998 discovered that the introduction of double-stranded RNA (dsRNA) into the nematode *Caenorhabditis elegans* (*C. elegans*) interfered with functions of endogenous gene expression. Therefore, the term RNA interference (RNAi) was coined. This then led to many more classes of RNAs being discovered; short interfering RNAs (siRNAs), tiny non-coding RNAs (tncRNAs), small regulatory RNAs (smRNAs) and also microRNAs (miRNAs) (Novina and Sharp, 2004).

The first member of what is considered now a growing class of miRNAs was the *lin-4* RNA which was discovered by Victor Ambros and colleagues (Lee, Feinbaum and Ambros, 1993). They found that the *lin-4* gene code for a pair of small RNAs but does not code for protein. This gene is involved in the translational repression of the *lin-14* mRNA. The *lin-14* gene is involved in the transition of early larval stage 1 (L1) to L2 (Wightman *et al*., 1991). The developmental transition occurs due to the sharp change of relatively high levels of *lin-14* gene activity during L1 to lower levels. This is to allow the switch to L2.

The second member of this family is the *let-7* miRNA which was also discovered in *C. elegans* long after the discovery of *lin-4* (Reinhart *et al.*, 2000). This miRNA is also involved in the heterochronic pathway (temporal control of developmental events) similar to *lin-4*. Loss of *let-7* causes the larval cell fates to be reproduced during the adult stage while overexpression of *let-7* causes early expression of adult cell fates during larval stages. There are five heterochronic genes namely *lin-14*, *lin-28*, *lin-41*, *lin-42* and *daf-12* that were identified as *let-7* targets suggesting its (*let-7*) role in regulating their expression. In the same year, Pasquinelli and colleagues found the expression of *let-7* RNAs in a wide range of species but not the *lin-4* expression (Pasquinelli *et al*., 2000). This indicates that some miRNAs can be highly conserved and plays a significant role in development. *lin-4* and *let-7* were called small temporal RNAs (stRNAs).

A year after the discovery of *let-7*, researchers discovered an abundant number of highly conserved miRNA genes in both vertebrates and invertebrates (Lagos-Quintana *et al.*, 2001). In this study, they identified 16 novel *Drosophila melanogaster* (Drosophila) miRNAs and 21 novel human miRNAs, strengthening the idea of a large class of small non-coding RNAs (ncRNAs) with regulatory roles. Several of the miRNAs exist in clusters and some have repeated genomic copies. Besides regulation of developmental timing, miRNAs are suggested to have tissue specification functions as well. This is due to the absence of expression of some miRNAs in some tissue types while present in others. In the same issue of the journal, two other groups also reported their findings on such small regulatory RNAs. The first group discovered more than 50 new miRNAs in *C. elegans* (Lau *et al*., 2001) while the second group reported the identification of 15 novel miRNA genes in the nematode (Lee and Ambros, 2001). The three groups together at that time put forth about nearly a hundred new miRNAs through various cloning, sequencing and

informatics approaches. They proposed that more miRNA genes were yet to be uncovered as their screening had yet to reach saturation levels.

More rigorous screening efforts have indeed yielded an abundant class of miRNA gene in most model eukaryotic species such as *Arabidopsis thaliana* (Llave *et al.*, 2002a; Park *et al*., 2002; Reinhart *et al.*, 2002), mouse (Lagos-Quintana *et al*., 2002, 2003), zebrafish (Giraldez *et al*., 2005; Wienholds *et al*., 2005) and in humans (Lagos-Quintana *et al*., 2003; Bentwich *et al*., 2005). From then onwards, the pace of miRNA discovery has been increasing. Until the year 2009, the miRNA count in miRBase database reached almost a total (all genomes included in the database) of 1500 with 721 miRNAs found in humans (Griffiths-Jones *et al*., 2006).

2.1.2 Annotation of miRNAs

In order to avoid confusion and distinguish miRNAs from other molecules in the genome, there has to be a set of guidelines for researchers to follow in identifying and naming miRNAs. Therefore the annotation of miRNAs will be discussed here briefly in two parts; the criteria required for a molecule to be identified as miRNA and the nomenclature of the miRNA itself. Readers are referred to these papers (Ambros *et al*., 2003; Griffiths-Jones *et al*., 2003; Griffiths-Jones, 2004; Griffiths-Jones *et al*., 2006) for more details on the subject.

In identifying a miRNA from a sample of size-fractioned RNA, one must address the issue of distinguishing an authentic miRNA sequence from other ncRNAs such as rRNA, tRNA, small nuclear RNA (snRNA) and some mRNA. Filtering away of such

ncRNAs from possible miRNA sequences can be done through informatics screening in available established databases. The more difficult part would be to differentiate a miRNA from a siRNA sequence and annotating sequences based on evolutionary conservation as addressed by Ambros *et al*. The criteria for a sequence to be identified as a miRNA comes not from its functions and biochemical compositions (both indistinguishable from those of siRNAs) but from its biological synthesis and expression. These set of criteria are stated in detail in the mentioned paper (Ambros *et al*. 2003). The criteria are based on the fact that precursor miRNAs are endogenous transcripts that have fold-back (hairpin) structures. The hairpins are processed in a way where miRNAs are only formed from one arm of the hairpin molecule (siRNAs are formed from both arms). In addition, precursor molecules can be in the form of multiple hairpins where each hairpin produces a different miRNA.

In naming miRNAs, scientists have agreed to use the letter prefix "miR" to designate mature miRNAs while "mir" is used for precursor hairpins for example primary transcripts are pri-mir while precursor transcripts are pre-mir. Following the letter prefix, miRNAs are also given unique numerical identifiers and in sequence for example miR-1, miR-2, miR-3 and so on. In order to show which species the miRNA originated from, there are also letter prefixes preceding the miR designation. For example, human miR-1 would be written as hsa-miR-1 (hsa stands for *Homo sapiens*) and mouse miR-1 as mmu-miR-1(mmu stands for *Mus musculus*) (Griffiths-Jones *et al*., 2006). The naming system also takes into account orthology and paralogy. MiRNA genes that are orthologous and very similar in sequence can be given the same number (for example hsa-miR-101 and mmu-miR-101) while paralogs can also be given the same number but in addition are given a letter after the same number designated (for example mmu-miR-10a and mmu-miR-10b).

However, naming can be complicated and in the end it (miRNA name) comes down to the decision of the authors who submit the sequence (Griffiths-Jones *et al*., 2006).

2.1.3 Defining miRNAs

MicroRNAs are a class of small regulatory RNAs that have a size of 20-23 nucleotides. They are transcribed from endogenous genes but as mentioned before, they do not code for a protein like other genes. Some miRNAs are found within an intron while a number of them are in polycistronic transcription units. MiRNAs also show evolutionary conservation within closely related species such as human and mouse (Lagos-Quintana *et al*., 2003) and distant lineages such as *C. elegans* and human (Lim *et al*., 2003). The definitive feature of a miRNA would be its interaction with mRNAs via complementary base-pairing and the triggering of two posttranscriptional events; mRNA cleavage and translational repression (Bartel, 2004). The two events make miRNAs one of the most abundant classes of regulatory genes in human. Prediction studies show that about 30% of protein-coding genes are miRNA-regulated (Lewis *et al*., 2005).

2.1.4(a) Biogenesis of miRNA: Transcription

The synthesis of a mature miRNA molecule from its endogenous gene involves a flow of cellular processes, intermediate molecules such as primary-miRNA (pri-miRNA) and precursor-miRNA (pre-miRNA) and the participation of key molecules (Figure 2.1). The first step involved in the synthesis is the transcription of the miRNA gene by a RNA

polymerase to produce a long pri-miRNA transcript. However, there was no evidence of which RNA polymerase that played a major role in miRNA transcription and initially it was thought to be RNA polymerase III (pol III). This view was conceived from the observation that pol III was involved in the transcription of most small RNAs like tRNAs, 5S rRNA and U6 snRNA (Lee *et al*., 2004).

In contrast, there were several findings from experiments that disputed pol III as the main player in miRNA transcription. First, pri-miRNA transcripts can be quite long (~1kb) and are longer than what pol III normally transcribes. The long transcripts therefore contain stretches of Uridine and this would lead to the formation of prematurely terminated pri-miRNAs by pol III (Lee *et al*., 2002). Second, differential expression of many miRNAs during development is often observed for RNA polymerase II (pol II) and not pol III products (Bartel, 2004). Third, a couple of studies done on miRNA regulation proposed that the miRNA precursors are 5' capped, polyadenylated and spliced (Aukerman and Sakai, 2003; Tam, 2001) which are typical of pol II gene processing. Direct evidence to show that miRNA genes are transcribed by RNA pol II then came in 2004 by Lee and colleagues. Through affinity purification they were able to selectively enrich capped and polyadenylated pri-miRNAs from mammalian total RNA (Lee *et al*., 2004). They also confirmed that treatment of α-amanitin (a pol II inhibitor) on cells directly decreased the expression of pri-miRNAs while expression of pol I- and pol III–transcribed genes were not affected. In addition, chromatin immunoprecipitation (ChIP) assays confirmed the physical presence of pol II on promoter regions of a pri-miRNAs.

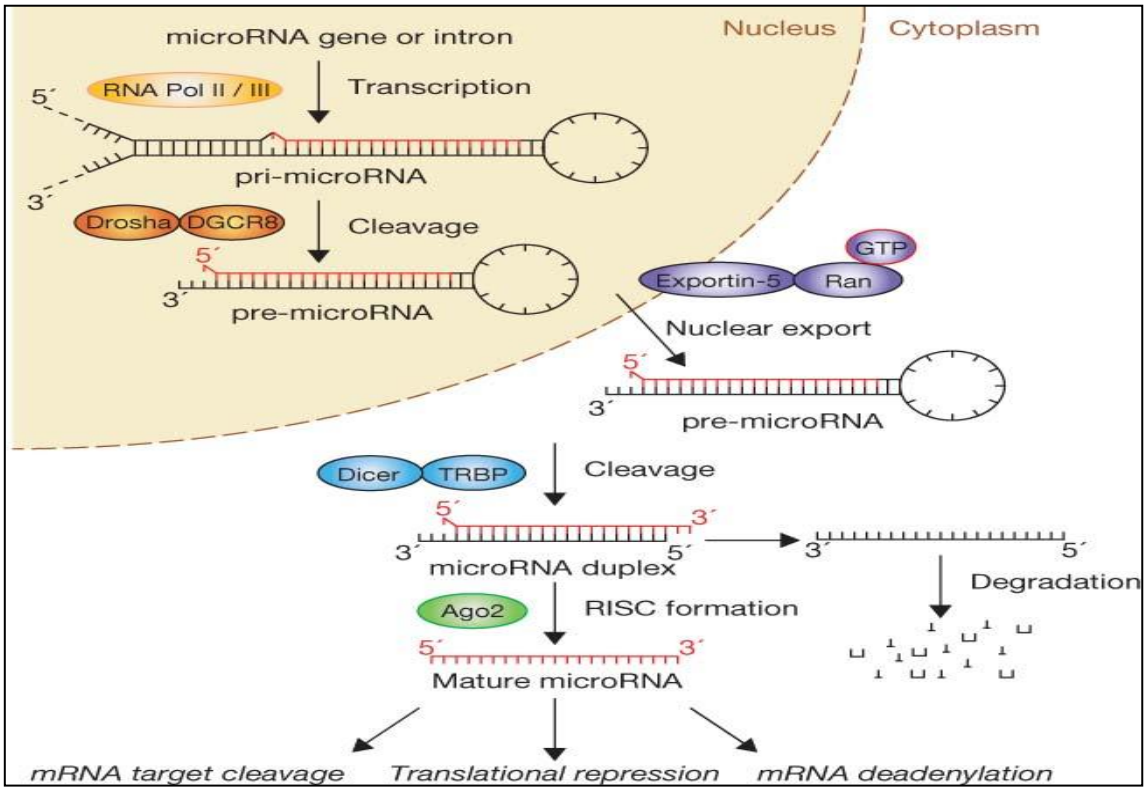

Figure 2.1: Biogenesis of microRNAs in mammals. The processing of miRNA from its gene in the nucleus into a mature miRNA that is incorporated into the RISC to form a miRNA ribonucleoprotein (miRNP) complex in the cytoplasm that exerts its function in mRNA regulation and the involvement of intermediate molecules is shown. Adapted from Winter *et al.*, 2009.

Two years later, a paper published (Borchert *et al*., 2006) provided evidence that pol III is needed for miRNA transcription instead of pol II. They found a miRNA cluster to be dispersed among Alu repeats and transcription of these repeats required pol III. ChIP and cell-free transcription assays also revealed the presence of pol III on the miRNA genomic sequence and not pol II. In addition, other miRNAs were also found to be located within Alu repeats and other repetitive elements, proving the significance of pol III in miRNA transcription.

As evidence accumulates, we will see studies supporting both pol II and pol III being equally important in miRNA transcription. MiRNA transcription appears to be a process that seems to be carried out without the restriction to only one type of RNA polymerase.

2.1.4(b) Biogenesis of miRNA: the Microprocessor complex

Pri-miRNA, which can be in the range of several hundred to several kilobases, are predicted to form a hairpin secondary structures which will undergo further processing to form a pre-miRNA. The biogenesis of miRNAs requires this important pri-miRNA processing step as it predetermines the sequence of the final mature miRNAs (Lee *et al*., 2003).

The processing is initiated by a nuclear RNase III called Drosha (Lee *et al*., 2003). Drosha belongs to the class II of RNase III endonuclease family where they bind and cleave dsRNA in a staggered manner. Precursor molecules that undergo *in vitro* processing with immunoprecipitated Drosha gave fragments of 60-70 nt which correlate to pre-miRNAs. RNAi on Drosha resulted in the accumulation of pri-miRNAs and decrease in pre-miRNA (Lee *et al.,* 2003). The paper also proposed a model whereby Dicer functions to process substrates provided by Drosha and both enzymes work in a stepwise manner. This stepwise model is supported by the evidence that Drosha and Dicer are differentially localized in the nucleus (Wu *et al*., 2000) and cytoplasm (Provost *et al*., 2002), respectively. In addition, the model allows for both enzymes to work synergistically and

increases the efficiency and accuracy of miRNA production as compared to the Dicer working alone.

In the following year, Denli's group found that Drosha functions in a complex along with other proteins. They named this complex as the Microprocessor due to its role in microRNA processing. Their study in *Drosophila* cells identified a dsRNA binding protein called Pasha (Partner of Drosha) together with Drosha in a functional 500kDa Microprocessor (Denli *et al*., 2004). In the same issue of *Nature*, Gregory's group also found evidence that human Drosha associates with other proteins to carry out its biological role (Gregory *et al*., 2004). In addition, human Drosha was also found in two forms; a large complex and a small complex. The former might have a function in other RNA processing reactions but for pri-miRNA processing the smaller complex is the major player. It consists of Drosha and a protein called DGCR8 (DiGeorge syndrome critical region gene 8). This smaller complex is known as the Microprocessor in humans and is needed for the processing of pri-miRNAs as the lost of both Drosha and DGCR8 results in pri-miRNA accumulation and absence of either one result in inefficient processing. In order to identify the mechanism of action of Drosha, Han and colleagues conducted site-directed mutagenesis studies of key residues on both Ribonuclease (RNase) III domains (a and b) of human Drosha. They identified two residues important for catalytic staggered cleavage of the pri-miRNA hairpin where one cleaves at the 3' site while the other at the 5' site (Han *et al*., 2004). Besides that, they concluded that Drosha works in a complex together with DGCR8 which supports the findings of others (Gregory *et al*., 2004) and the complex might contain multiple copies of both Drosha and DGCR8. Due to their association with Drosha, Pasha and DGCR8 might have similar functions and hence there is a possibility of

them being orthologs but nonetheless, their role in pri-miRNA processing is undeniably important.

2.1.4(c) Biogenesis of miRNA: Export to the cytoplasm

Once the pri-miRNA has been processed by the Microprocessor to become a pre-miRNA, it will be exported from the nucleus to the cytoplasm for further downstream processing by Dicer. Exchange of substances between the nucleus and the cytoplasm proceeds through nuclear pore complexes either by passive diffusion or facilitated translocation. The second mode of exchange involves mediators known as exportins and importins, as their names suggest, function in exporting substances to the cytoplasm and importing them to the nucleus, respectively.

The key player in pre-miRNA export from the nucleus is Exportin5 (Exp5) (Lund *et al*., 2004). The export occurs in a RanGTP-dependent manner just as how other smaller cellular RNAs are exported as depletion of RanGTP results in export inhibition (Lund *et al*., 2004 and Bohnsack *et al*., 2004). Exp5 binds to pre-miRNAs without any sequence specificity to dsRNAs (Bohnsack *et al*., 2004) and efficient export might depend on the precise ends of the pre-miRNA produced by Drosha (Lund *et al*., 2004).

Another group examined the structural requirements for pre-miRNA binding by Exp5 (Zeng and Cullen, 2004). They found that a minimum pre-miRNA stem length of 18bp is required for high-affinity binding and the presence of a 5’ overhang at the stem inhibited binding to Exp5. In addition, the formation of a pre-miRNA/Exp5/RanGTP complex protected the pre-miRNA from digestion by cellular RNases. This “protecting complex” ensures the delivery of the pre-miRNA to the cytoplasm in an intact form.

2.1.4(d) Biogenesis of miRNA: Dicer processing to form mature miRNAs

After going through the nuclear pore, dissociation of pre-miRNA from Exp5 is triggered by the hydrolysis of RanGTP to RanGDP in the cytoplasm (Cullen 2004). The process of miRNA maturation is then continued by another enzyme called Dicer, due to its ability to "dice" dsRNA into small RNAs uniformly (Bernstein *et al*., 2001). It belongs to the third class of RNase III enzymes and has two RNase III (RIIIa and RIIIb) domains and an amino-terminal helicase domain. The Dicer family is evolutionarily conserved as homologues and are found in *C. elegans*, *Arabidopsis*, *Schizosaccharomyces pombe* and in humans. Bernstein's group first identified Dicer to be involved in the initiation of the RNAi pathway in Drosophila.

The Dicer homolog in *C. elegans* known as *dcr-1* (K12H4.8) was proposed by two groups (Grishok *et al*., 2001 and Ketting *et al*., 2001) to be involved in RNAi and also the maturation of small RNAs related to developmental timing in the worm. A similar study in Drosophila, led by Hutvagner presented evidence of the *let-7* stRNA being produced by cleaving a precursor RNA in a RNA interference-like fashion. They then found that an RNase III was involved in the processing of this stRNA due to the existence of a terminal structure with 5' monophosphate and 2'- and 3'-terminal hydroxyls. This terminal structure is a characteristic of RNase III-cleaved products. The involvement of Dicer in miRNA maturation was then confirmed when siRNA knockdown of Dicer resulted in the accumulation of *pre-let-7* in Drosophila (Hutvagner *et al*., 2001).

A single processing center model was then proposed for Human Dicer where the RIIIa and RIIIb domains functions as an intramolecular dimer. Both domains contribute to the processing center while the catalytic activity of each domain is independent. The PAZ domain and the dsRNA binding domain (dsRBD) domain are both involved in helping Dicer function where the former is responsible in recognizing the 3' overhang of the Drosha-processed substrate (Zhang *et al*., 2004).

2.1.4(e) Biogenesis of miRNA: Incorporation into the RISC (RNA-induced silencing complex)

Once the pre-miRNA has been processed by Dicer, the miRNA now has a duplex miRNA:miRNA* structure. Central mismatches in the duplex favor RISC loading while seed region or 3'-mid mismatches promote unwinding (Yoda *et al*., 2010). The miRNA strand or the 'guide strand' will then be retained to form the mature RISC while the miRNA* strand or the 'passenger strand' will be discarded and degraded (Kawamata and Tomari 2010).

This complex (RISC) known as miRNA ribonucleoprotein (miRNP) complex was first reported by Mourelatos *et al*. The complex consists of Gemin3, Gemin4 , eukaryotic initiation factor 2C (eIF2C) 2 as the major components with the possible involvement of other proteins as well (Mourelatos *et al*., 2002). The eIF2C2 being a human Argonaute(Ago) homolog was found together with eIF2C1 in a RISC complex, supporting the association of RISC with miRNAs (Martinez *et al*., 2002).

In determining the canonical pathway of human RISC assembly involving miRNAs, there were two events that were in question. The first was whether small RNA duplexes unwind before or after it has bound to Ago proteins and how it is unwound. The next was whether the process of dicing and RISC formation is coupled or independent (Kawamata and Tomari 2010; Yoda *et al*., 2010).

There are two models to explain when small RNA duplexes unwind during RISC assembly. One is the 'helicase' model and another, the 'duplex-loading' model. For the first model, a putative ATP-dependent helicase is proposed to unwind the small RNA duplexes before loading the guide strand to Ago2 (Bartel, 2004). However, the existence of such helicase has not been validated. The second model with supporting evidence by some groups (Kawamata *et al*., 2009; Rand *et al*., 2005) suggests that the miRNA:miRNA*duplex and siRNA duplex is loaded onto Ago1 and Ago2 proteins in *Drosophila*, respectively. The mechanism of unwinding probably could be through a slicer-independent unwinding (Matranga *et al*.,2005). Considering the similarities in feature between fly Ago1 and human Ago2 (Yoda *et al*., 2010), this model would more likely suit the human pathway.

Previously, it was proposed that the process of pre-miRNA dicing and RISC formation are both coupled in humans (Gregory *et al*., 2005; Maniataki and Mourelatos, 2005). A more recent study (Yoda *et al*., 2010) reexamined the RISC assembly process and reported that dicing and RISC assembly are uncoupled and independent of each other. They also found that RISC loading requires ATP but is not necessary for unwinding of the small RNA duplexes. This finding is contrary to previous evidence that show an ATP-independent RISC assembly. The reason could be due to the usage of a 'bypass pathway'

that can function only with single-stranded RNAs (reviewed in Kawamata and Tomari, 2010).

RISC assembly is still a process that warrants more study due to the discovery of many proteins that associates with this complex such as Mov10, Imp8 and GW182 (Carthew and Sontheimer, 2009). Elucidation of the function of these proteins would provide a better understanding on this process.

2.1.5 Mechanism of miRNAs

A microRNA is able to exert its function of posttranscriptional gene regulation by guiding the RISC in the cytoplasm to the target mRNA. In most cases, the miRNA will bind to the 3' untranslated region (UTR) region of the mRNA via complementary base-pairing. Gene regulation could also be achieved by binding of the microRNA to the 5' UTR or the open reading frame (ORF) of the gene (Lewis *et al*., 2005). There is a region in the miRNA that consists of 2 to 8 nucleotides known as the seed region which binds to the target mRNA (Carthew and Sontheimer, 2009). The target mRNA could either be cleaved or translationally repressed. The factor that determined one of the two regulatory events to occur would be the degree of miRNA complementarity to the target mRNA.

In order for a target mRNA to be cleaved, the miRNA has to be an exact complement to the target sequence. The structure of the miRNA precursor and the intrinsic sequence of the miRNA produced do not prevent the miRNA from entering the RNAi pathway (Hutvagner and Zamore, 2002). The nuclease activity of the miRNA *let-7* was

confirmed *in-vitro* and *in-vivo*. This siRNA-like event was found to involve the PPD (Paz and Piwi Domain) protein eIF2C2. This PPD protein is found associated to the RISC and RISC-like complexes in other organisms and associated to miRNP complex. Hence, the proposed involvement of RISC programmed by miRNAs in the cleavage of target RNAs in an RNAi fashion. The miRNA-programmed cleavage site of the target RNA occurs in between nucleotides pair 10 and 11 which is identical to the site during siRNA-directed cleavage (Llave *et al*., 2002b). After the target mRNA has been cleaved, the miRNA can be reused again to guide the cleavage of additional target mRNAs (Hutvagner and Zamore, 2002).

Translational repression occurs when the miRNA:target complex forms bulges due to central mismatches. The quantity of the target mRNA will not decrease unlike in the above mechanism. Only the expression of the target mRNA-encoded protein will be reduced. A concern for this mechanism was whether the repression occurs during initiation or after initiation (postinitiation). Experimental evidences showed that either event could occur during translational repression (Carthew and Sontheimer, 2009). Several models were also proposed by different groups to explain how the repression would work *in vivo* such as i) miRNA competition for binding at mRNA cap or poly(A) tail (Humphreys *et al*., 2005) ii) premature ribosomal dropping from translational complex (Petersen *et al*., 2006), iii) prevention of the circularization of the mRNA during translation (Wakiyama *et al*., 2007) However, each model also suffers contradiction from other studies and hence the when and how translational repression occurs still remain as questions unanswered.

2.2 Prostate Cancer

2.2.1 Facts and Figures

Prostate cancer is the second most frequent specified cancer to occur in men worldwide after lung cancer in the year 2008 and is the sixth leading cause of death due to cancer in men (Figure 2.2a). Prostate cancer is the fifth most frequent cancer to occur in both men and women worldwide (Figure 2.2b). The incidence of prostate cancer in Asia with an age-standardized rate (ASR) of 7.2 per 100,000 and in Southeast Asia (ASR of 8.3 per 100,000) is among the lowest in the world (Figure 2.2c). This is probably due to the less widespread use of prostate specific antigen (PSA) testing as compared to other more developed regions. However, mortality rates are similar between less developed and more developed regions (Ferlay *et al*., 2008).

In Malaysia, the number of reported cases of prostate cancer for the years 2002, 2003, 2003-2005 and 2006 were 671, 602, 2150 and 735 cases, respectively. As for the ASR, the data also showed no obvious pattern of increase or decrease with age-standardized rates of 11.6, 10.3, 12 and 11 for the same years (National Cancer Registry 2002-2006). Although both total number of incidence and ASR shows fluctuation, a pattern of increase is expected for the following years. This is because the life expectancy at birth of male increased from 70.8 years in 2002 to 71.6 years in 2008 and the number of population that exceeds the age of 65 shows an increase from 993,900 in 2002 to 1,286,200 in 2009 (Depart of Statistics Malaysia, 2009) which put Malaysian males at a higher risk of getting prostate cancer since old age is the main risk factor.

Even though current treatment options such as surgery and radiation therapy are effective against early stages of prostate cancer, patients with hormone-independent advanced stage prostate cancers typically face a poor prognosis with limited treatment options (Damber and Aus, 2008) and therefore the need to search for alternative therapeutic options.

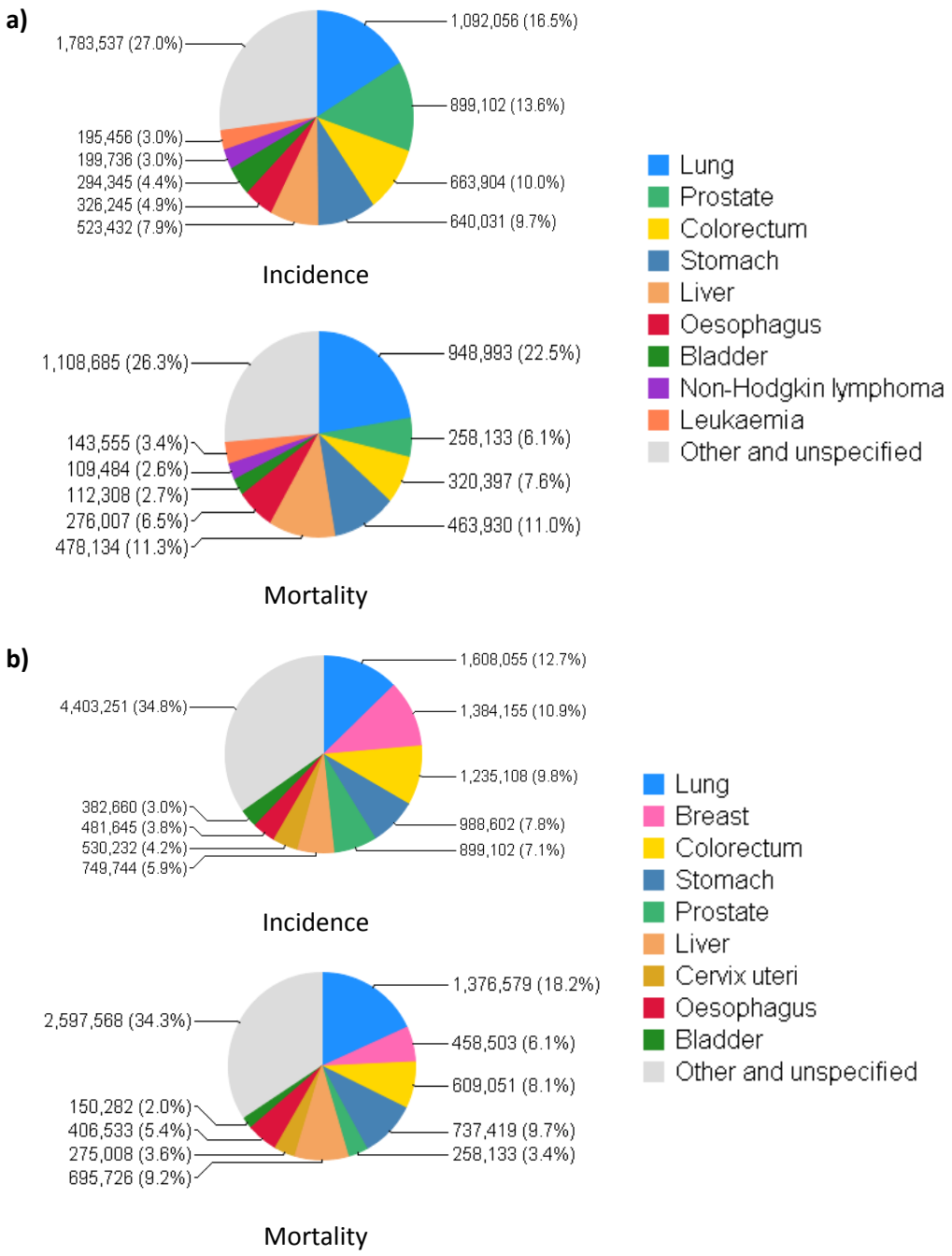

Figure 2.2 a & b : Prostate Cancer Statistics based on Age-Standardized Rate (ASR) per 100,000 population. a) Prostate cancer incidence and mortality in men worldwide among various other cancers. b) Prostate cancer incidence and mortality compared with various cancers in both men and women worldwide. Figure adapted from GLOBOCAN 2008. http://globocan.iarc.fr/factsheet.asp . Retrieved September 26, 2013.

c)

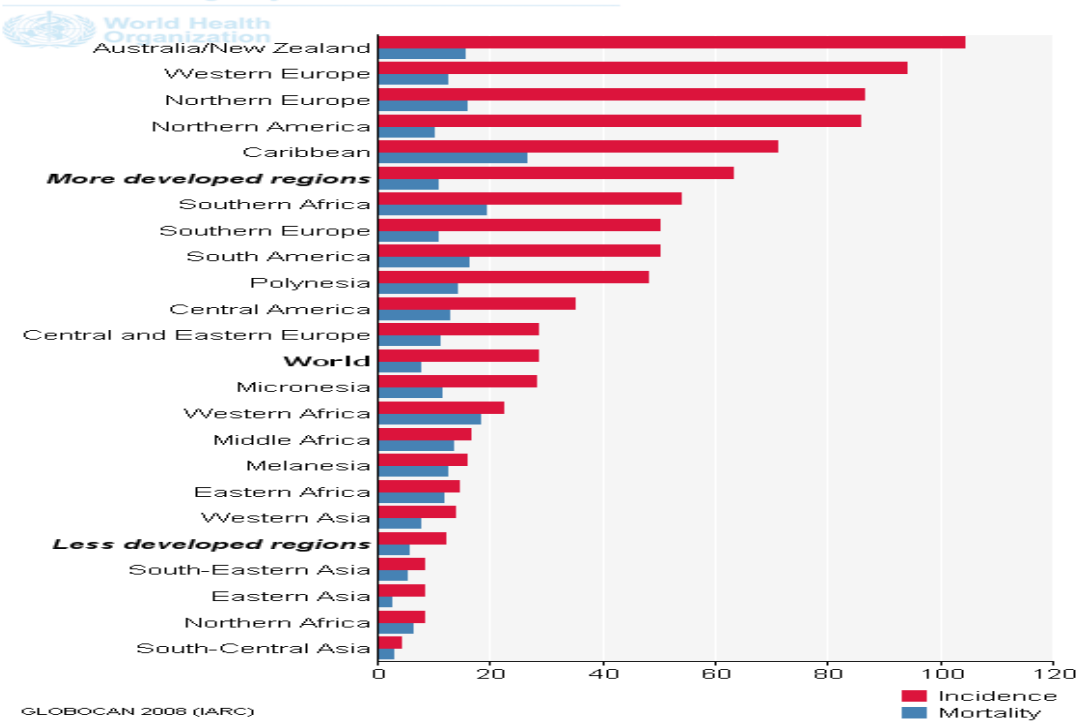

Figure 2. 2 c: Prostate Cancer Statistics based on Age-Standardized Rate (ASR) per 100,000 population. c) Prostate cancer incidence and mortality among different populations. Figure adapted from GLOBOCAN 2008. http://globocan.iarc.fr/factsheet.asp Retrieved September 26, 2013

2.2.2 Defining the Prostate and Prostate Cancer

According to the National Cancer Institute (NCI), prostate cancer or also known as carcinoma of the prostate (CaP) is a cancer that forms in the tissues of the prostate (National Cancer Institute, 2008). The prostate is a small walnut-sized gland found in the male reproductive system (Figure 2.3).

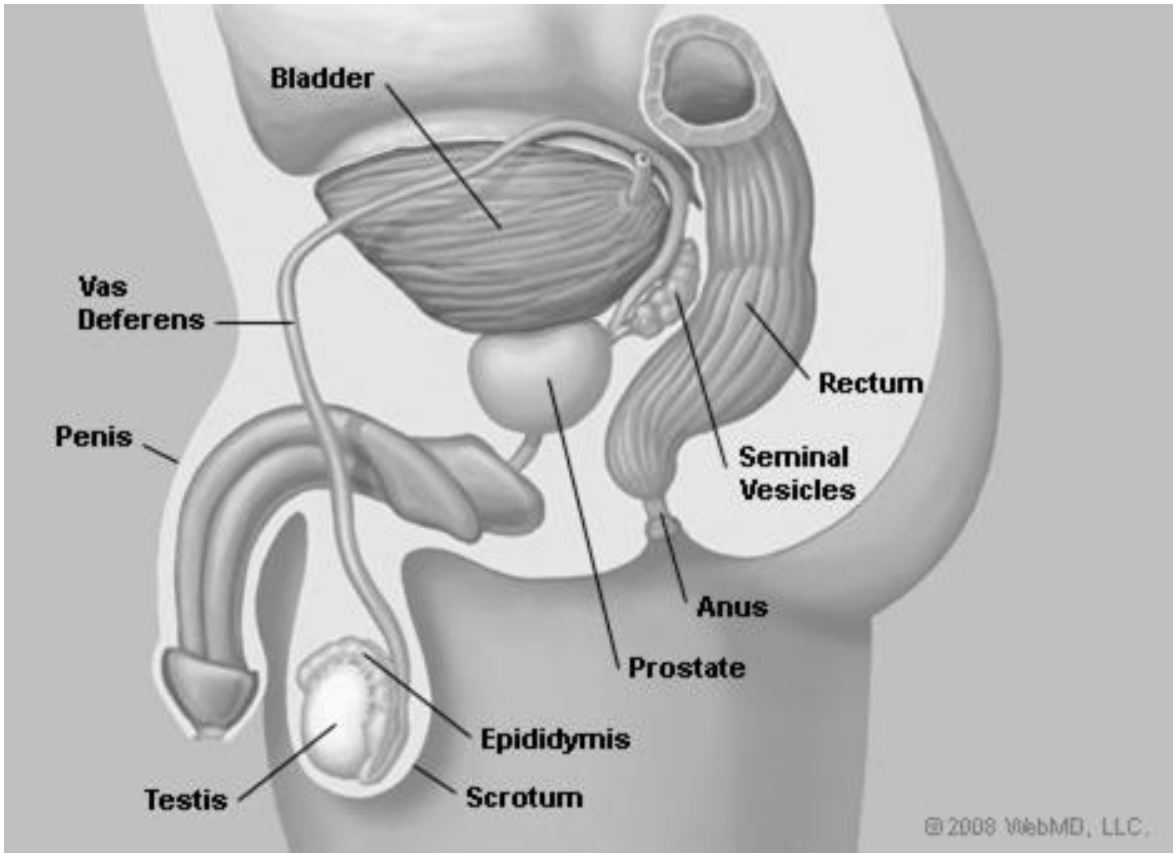

Figure 2.3: Side view of the prostate and the male reproductive system. Adapted from http://www.webmd.com/urinary-incontinence-oab/picture-of-the-prostate. Retrieved September 26, 2013.

It envelops the section of the urethra that carries the urine from the bladder to the penis. The gland is also divided into peripheral and transition zones with the former being near the rectum. The gland has a function of producing a thick clear fluid which becomes an important component for the semen (Cancer Research UK, 2010; Prostate Cancer Foundation, 2010). There are at least three types of cells that can be found in the epithelium of the prostate: i) Secretory luminal epithelial cells- the predominant androgen-dependent cells that secrete prostatic proteins, (ii) neuroendocrine cells- the small population androgen-independent cells dispersely located at the same stratum with the basal cells and believed to provide paracrine signals that support the growth of luminal cells, iii) basal cells- situated in between the first cell type layer and the basement membrane. Each cell type in the prostate also expresses specific molecules that allow for their molecular characterization. The fourth cell type would be prostate cancer stem cells which are yet proven to exist (Abate-Shen and Shen, 2000; Lee *et al*., 2008).

Prostate cancer should not be confused with benign prostatic hyperplasia (BPH) or the enlargement of the prostate. BPH is a non-cancerous condition which starts from the transition zone and it grows inwards to the core of the prostate. The growth forces the urethra to constrict, resulting in pain. On the other hand, prostate cancer originates from the outer peripheral zone and it grows outward, invading neighbouring tissue (Prostate Cancer Foundation, 2010).

2.2.3 Molecular Pathway in Prostate Cancer Progression

There are many factors associated with prostate cancer. Some of the factors that might increase a person's risk of getting prostate cancer would be; i) old age. ii) family history of prostate cancer iii) diet iv) diabetes v) ethnicity. Early stages of prostate cancer are often curable by conventional treatments such as surgery and radiotherapy. However, most cases of prostate cancer remain relatively benign or 'silent' and this poses a high risk of only detecting it when it is at an advanced stage, often fatal within 24 months. Such aggressive and hormone-independent stage, as a result of androgen-ablation therapy, is often associated with seminal vesicles invasion and followed by a lethal stage of metastasis, primarily to the bone. (Altieri *et* al., 2009; Abate-Shen and Shen, 2000).

In order for carcinogenesis to occur and progress to more aggressive states, it requires multiple molecular changes. A study by Rhim *et al*. clearly shows the evidence to support this multistep pathway. They transfected normal prostate epithelial cells with a plasmid containing the human papilloma virus (HPV) 18 genome and it resulted only in the immortalization of the cells but not malignancy. Cells only become tumorigenic after a second oncogene, Ki-*ras* was introduced via Kirsten murine sarcoma virus (Ki-MuSV) infection (Rhim *et al*., 1994).

Chromosomal aberrations are often the event that can be observed in most prostate cancer tissue. Some of the common chromosomal abnormalities include losses at chromosome, 6q (Cooney *et al*., 1996), 7q (Takahashi *et al*., 1995; Zenklusen *et al*., 1994), 8p (Nupponen *et al*., 1998), 10q (Isaacs and Carter, 1991), 13q (Hyytinen *et al*., 1999), 16q (Latil *et al*., 1997), 17p and 18q (Latil *et al*., 1994). Besides chromosomal losses, gains in

chromosome 7p, 7q, 8q, and Xq are also associated with prostate cancer (Nupponen *et al*., 1998).

Such aberrations are proposed to contribute to carcinoma of the prostate (CaP) due to existence of putative tumor suppressors or oncogenes in these regions. It is suggested by several groups that alteration of each region and its associated gene/s are involved in each stage of CaP, from initiation to progression and finally to advance carcinoma and metastasis (Isaacs and Kainu, 2001; Abate-Shen and Shen, 2000).

The event preceding prostate cancer initiation involves the formation of prostatic intraepithelial neoplasia (PIN). PIN lesions form once basal cells are lost and luminal cells start to invade to the periphery zone (Lee *et al*., 2008). Prostate cancer initiation is strongly associated to loss of chromosome 8p12-21 and 8p22 which occurs in high percentage (~80%) of prostate tumors and other cancers (Chang *et al*., 1994; Matsuyama *et al*., 1994). A putative tumor suppressor gene (TSG), *NKX3.1* is suggested to reside in this chromosomal region and its loss causing prostate cancer initiation (Bhatia-Gaur *et al*., 1999).

Several factors are thought to be involved in the progression stage of CaP. Some of them include i) the loss of chromosome 10q and the *PTEN* candidate gene, ii) loss of chromosome 13q and the *Retinoblastoma* (*Rb*) gene, iii) Change of expression in cell-cycle regulatory genes such as *p27* and *p16*, iv) Telomere length and telomerase dysfunction (Abate-Shen and Shen, 2000).

Progression of CaP to advance carcinoma and metastatic state involves androgen receptor (AR) signaling. Androgen ablation therapy is the common treatment for advance prostate cancer and it could provoke the recurrence of a more aggressive androgen-independent state of CaP in most cases, possibly through the selection for survival of

androgen-independent cells (Gingrich *et al*., 1997; Huggins and Hodges, 1941). Androgen independence could also be acquired through changing AR function by making it more sensitive to low androgen levels or allowing it to bind to other steroid hormones (Elo *et al*., 1995; Veldscholte *et al*., 1992). In addition, AR was also found to be activated by various growth factors in prostate tumors (Culig *et al*., 1994). Loss of chromosome 17p and the residing *p53* gene is also an event detected in advance and metastatic CaP (Saric *et al*., 1999) although the frequency of *p53* mutation in CaP is less common compared to other cancers (Kleihues *et al*., 1997). Such an observation could be explained by the possibility that most patients die from other carcinoma before CaP develops. It could also be due to difficulty in detecting frequenct *p53* mutations occurring in more aggressive forms and in hard to get tissues (Abate-Shen and Shen, 2000). Another feature found in advanced, hormone-refractory CaP would be the alteration of the *Bcl2* gene. Overexpression of the gene was found to confer resistance to apoptosis (Colombel *et al*., 1993) and also resistance to chemotherapy (Tu *et al*., 1995).

2.3 Annexin VII (ANXA7) and Prostate Cancer.

Annexin VII (ANXA7) or also known as synexin was first discovered and reported in 1978 by Creutz and colleagues. The protein was isolated from the bovine adrenal medulla. Synexin got its name from the Greek word *synexis* which means “meeting” due to its ability of making chromaffin granules aggregate or “meet” (Creutz *et al*., 1978). The

human synexin was later on isolated and its sequence and structure elucidated by Burns *et al*. (Burns *et al*., 1989). Synexins was also then identified in different organisms such as the frog *Xenopus laevis* (Srivastava *et al*., 1996), mouse (Zhang-Keck *et al*., 1993) and *Dictyostelium* slime mold (Doring *et al*., 1991).

In order to distinguish the different origins of Annexin VII, the gene in human is written in italics and with uppercase letters (*ANXA7*) while the gene from mouse in italics and first letter uppercase (*Anx7*). The gene from other species is written in italics with lowercase letters (*anx7*) (Srivastava *et al*., 2001).

Human *ANXA7* gene is located at chromosome 10q21 and has a molecular weight of approximately 51 kilo Dalton (kDa) (Srivastava *et al*., 2001). When compared with human ANXA7, proteins such as endonexin II, bovine calpactin I heavy chain, lipocortin I, protein II and calelectrin 67K, all belonging to a family of calcium-dependent membrane binding proteins showed major homology. This could mean that ANXA7 also belonged to this group of membrane binding proteins. ANXA7 has a unique N-terminal region that is hydrophobic with repetitive motifs in the protein sequence that may act as "structural stabilizers". The C-terminal is more conserved and has four imperfect repeats which do not have any known function but due to its highly anionic character, the repeats could be the calcium binding sites (Burns *et al*., 1989). The synexin did not follow the usual structure of membrane channel proteins formed by non-amphipathic helical regions, therefore a secondary structure for the ANXA7 was proposed by Burns and colleague which places the hydrophobic regions exposed to and the hydrophilic regions hidden from the membrane. The model accounts for the voltage gating feature of the synexin (Burns *et al*., 1989). ANXA7 was proposed to be involved in exocytosis as an intracellular receptor for Ca^{2+} from the observation of calcium-dependent aggregation of chromaffin granules (Creutz *et*

al., 1978). Direct association of ANXA7 with calcium occurs when ANXA7 undergoes self-association in the presence of calcium. This correlates with chromaffin granule aggregation (Creutz *et al*., 1979). Involvement of ANXA7 in exocytosis was confirmed when it catalyzed the fusion of phospholipid vesicles (Hong *et al*., 1981) and fusion of specific phospholipid membranes (Hong *et al*., 1982). ANXA7 membrane fusion activity was augmented by binding to GTP and deactivated upon GTP hydrolysis (Caohuy *et al*., 1996). This finding suggest that ANXA7 is a Ca^{2+}-dependent GTP binding protein and further supports its role as a direct mediator of exocytosis in cells.

A study conducted to find out the involvement of ANXA7 in pancreatic β-cell Ca^{2+} signaling produced two types of *Anx7* mutant mouse, one with a null(-/-) mutation and the other a heterozygous (+/-) mutation. The null mutant was found to be lethal while the heterozygous mutant was viable with hyperplastic islets of Langerhans and β cell hypertrophy phenotypes (Srivastava *et al*., 1999). Production of this *Anx7*(+/-) knockout mouse brought about the notion that it (*Anx7*) is involved in carcinogenesis due to the high frequency of tumor formation in older mice (Srivastava *et al*., 2001a). Another study carried out in the same year looked at the possible role of *ANXA7* as a tumor suppressor gene (TSG) in prostate cancer. It showed that *ANXA7* was able to suppress growth of various tumor cell lines with effects comparable to well known TSG, *p53*. An inverse correlation was seen between ANXA7 protein expression and CaP progression. ANXA7 levels were decreased markedly or even lost in metastatic and recurrent hormone-independent CaP, while still remained high in less advance stages. The pattern observed in the gene expression correlated with other TSGs such as *p53*, CD44, KAI-1 and PTEN. In addition, loss of heterozygosity (LOH) and even homozygous deletion of the gene was

found in CaP tissues tested. Several of these observed features strongly support the idea of *ANXA7* as a TSG crucial in prostate cancer progression pathway (Srivastava *et al*., 2001b).

Further investigations have been carried out to determine the mechanism of tumor formation driven by mutation in the *Anx7* gene. The Knudson two-hit model and the haploinsufficiency model was tested. From their data, Srivastava *et al.* observed the presence of normal *Anx7* allele even in hepatocellular carcinoma heterozygous mice and this suggests that happloinsufficiency is the more suitable model. Several prominent *Anx7* downstream targets have been identified from cDNA microarray experiments which include BRCA1 and BRCA2, WT1 and DCC (significantly down-regulated) and APC, TSG101 and VHL (up-regulated) in malignant tissue as compared to normal tissue. Genetic instability and abnormalities in the DNA-repair mechanism is a result from *Anx7* haploinsufficiency. Such widespread effect of *Anx7* loss and other characteristics of the gene strongly suggest it as a TSG with "gatekeeper" features (Srivastava *et al*., 2003).

ANXA7 is also involved in breast carcinogenesis and was found to be significantly up-regulated in metastatic and HER-2 negative breast cancers as compared to primary breast tumors. This led to the suggestion that ANXA7 expression is associated with the most aggressive forms of HER-2 negative breast cancers. Thus it is postulated to be used as a biomarker for early detection of this form of breast cancer by monitoring the levels of ANXA7 in those suspected of having breast cancer. (Srivastava *et al*., 2004). However, the increased expression levels of ANXA7 in breast cancers conflicts with its TSG role in prostate cancers. A possible explanation for this could be the different types of ANXA7 that is expressed in HER-2 negative breast cancers and in prostate cancers. HER-2 negative breast cancers could be expressing high levels of non-functional ANXA7. In prostate cancers the ANXA7 might be still functional but its expression is inhibited.

The role of *ANXA7* as a TSG and a biomarker was further supported by a large scale study involving 4061 samples. The study aimed at looking into the involvement of *ANXA7* in hormonal dysregulation in prostate and breast cancer (Srivastava *et al*., 2007). By using human tissue microarrays (TMA), the group found that most of the neoplastic tissue types had reduced ANXA7 protein levels as compared to their normal counterparts and reduction increases as the tumor progresses to more advance stages. The reduced expression supports the role of *ANXA7* as a TSG. ANXA7 expression that does not follow this pattern would probably reflect its other functions such as exocytosis and membrane fusion being exerted on those tissues. Reduced ANXA7 expression was also seen in tumors of glandular and non-glandular origin when compared to their respective normal tissues, supporting its tumor suppressive function. In comparing the ANXA7 expression between carcinoid (neuroendocrine derived) tumors and non-carcinoid tumors, they found that carcinoids have high expression level of ANXA7 while non-carcinoid tumors have varied expression levels from undetectable in some to present at high levels in others (Srivastava *et al*., 2007). This suggests a more probable association between ANXA7 and neuroendocrine biomarkers and not epithelial type biomarkers. Identification of several NKX binding sites in the analysis of the *ANXA7* promoter suggests that the gene was coregulated by *NKX3.1*. However, further analysis via cDNA microarray of both *ANXA7* and *NKX3.1* did not support this notion. Instead two other genes involved in steroidogenesis, *steroid sulfatase* (*STS*) and *SRY-box5* (*SOX5*) were suspected to be involved in the same transcriptional program as *ANXA7*. This correlation together with the presence of lipid and steroid hormone regulatory sites found in the *ANXA7* promoter strongly points to the hormone-dependent tumor suppression features of *ANXA7*.

2.4 MicroRNA and cancer

2.4.1 Dysregulation of microRNAs in cancer

One of the foremost evidences of miRNAs being involved in tumorigenesis was the discovery of frequent deletion of miR15 and miR16 at a region in chromosome 13 of chronic lymphocytic leukemia (CLL) patients where previous studies failed to identify other coding genes in the region (Calin et al., 2002). From then on, many more findings directly linking miRNAs and various cancers such as colorectal neoplasia (Michael et al., 2003), lung (Takamizawa et al., 2004) carcinomas and Burkitt's lymphoma (Metzler et al., 2004) were reported. A large scale genome analysis conducted in 2004 revealed that miRNA genes are non-randomly distributed in the genome and are frequently found in chromosomal fragile sites or near HPV integration sites (Calin et al., 2004). In addition to the dysregulation of individual miRNAs, clusters of miRNAs could also be dysregulated as well. MiR-17-92 cluster located in chromosome 13 that consists of seven miRNAs was found to be significantly overexpressed in lung cancers (Hayashita et al., 2005). These studies show the relevance of miRNAs in the process of tumorigenesis.

In order to study the global expression of genes, microarray and gene profiling techniques are used. Similarly, the expression of hundreds or even thousands of miRNAs can also be simultaneously determined with miRNA microarrays and various profiling methods to get a more comprehensive list of the miRNAs that are dysregulated. A large scale profiling study of miRNAs in several types of human tissues and tumors was carried

out by Lu and colleagues. They profiled the expression of 217 miRNAs in 334 samples using a bead-based profiling system. Results from their study showed that miRNA expression profiles could be used to identify tumor origin and distinguish normal from cancerous tissue accurately (Lu et al., 2005). A microarray-based expression profiling of lung, breast, stomach, prostate, colon and pancreatic tumors was carried out on a total of 363 samples and 177 normal samples. Data analysis showed that the miRNA signature tested in a majority of the tumors shared expression of several miRNAs (Volinia et al., 2006). A compelling miRNA expression pattern was also observed in microarray profiles of primary glioblastomas tissues and cell lines (Ciafre et al., 2005). Likewise, other cancers such as lymphomas (Metzler et al., 2004), thyroid cancers (He et al., 2005) and liver cancers (Murakami et al., 2006) also have dysregulated miRNA expression profiles. Real-time PCR is also another technique that has been used for miRNA expression profiling. A total of 222 human miRNA precursors were profiled from 32 human cell lines from prostate, lung, colorectal, breast, hematologic, pancreatic and head and neck cancers. The study introduced a new method to quantify individual members of identical miRNA isoforms (Jiang et al., 2005).

Several miRNA expression profiling has been conducted using the microarray platform to study prostate cancer (Mattie et al., 2006; Ozen et al., 2008; Porkka et al., 2007; Ambs et al., 2008). However, the data does not agree with one another and some of the miRNAs even show opposite expression. This could partly be due to the different measurement platforms used, selection of samples and purification of the RNA from the samples (reviewed by Schaefer et al., 2009). These confounding data might also be due to intricate relationships in the regulatory networks in the cells that we have yet to understand.

2.4.2 microRNAs as tumor suppressors and oncogenes

Once the idea of various cancers having widespread dysregulation of miRNAs was established, studies moved on to elucidate the function of these (ncRNAs). MiRNAs can act as tumor suppressors by negative regulation of oncogenes or as oncogenes (also known as oncomirs) by inhibiting tumor suppressors (Morris and McManus, 2005). One of the early evidences of a miRNA being a tumor suppressor was the *let-7* family of miRNA. Johnson and colleagues found that there were *let-7* complementary binding sites in the 3' UTR of the *let60/ras* which is a nematode ortholog for the human *Ras* genes and this led them to discover similar sites in all three human *RAS* (*HRAS*, *KRAS* and *NRAS*) 3' UTRs. They then went on to experimentally prove the negative regulation of *Ras* by *let-7* (Johnson *et al*., 2005). Concurrently, an inverse correlation was observed between *let-7* and *Ras* expression in lung cancers (Takamizawa *et al*., 2004). Another example of miRNAs acting as tumor suppressors would be the modulation of c-Myc-induced proliferation by *miR-17-5p* and *miR-20a* in a negative feedback loop mechanism. Both miRNAs tightly control cell proliferation induced by *c-Myc* by limiting the expression of a transcription factor, E2F1. This transcription factor which is involved in the promotion of cell cycle progression is also a target of c-Myc (O'Donnell et al., 2005).

Since miRNAs were found to be tumor suppressors, it raises the question of whether this class of small RNAs could also act as oncogenes? A study carried out by Tam and colleagues hint to the possibility for miRNAs to be oncogenes. Their study found that *bic*, a gene that codes for a ncRNA (Tam, 2001) is a collaborator of *c-Myc* during oncogenesis. The coexpression of both *bic* and *c-Myc* increased the proliferation of chicken embryo fibroblasts (CEFs) (Tam *et al*., 2002). The well studied *miR-21* is a fine example of

an oncomir. It was found that this miRNA was overexpressed in hepatocellular carcinoma (HCC) as compared to normal liver tissue and targets the tumor suppressor gene, *PTEN*. By down-regulating *PTEN*, phosphorylation of downstream targets such as FAK and Akt increases and expression of matrix metalloproteases (MMPs) 2 and 9 which leads to cell growth, invasion and migration (Meng *et al*., 2007). A couple of other examples of oncomirs are *miR-10b* that promotes metastasis by suppressing HOXD10 (Ma *et al*., 2007) and the *miR-17-92* cluster where its overexpression promotes proliferation, angiogenesis and cell survival while inhibiting differentiation (Olive *et al*., 2010).

There is no doubt that the list of miRNAs that belong to the class of tumor suppressors and oncogenes will increase as research intensifies but it should be cautioned that the characterization of miRNAs by just comparing their expression between cancer and normal cells are inaccurate. This is because some miRNAs could have both tumor suppressive and oncogenic functions in different cancers. Several miRNAs that have this duality of function are *miR-125b* (Le *et al*., 2009; Ozen *et al*., 2008), *miR-181a*, *miR-181c* and *miR-220* (Fabbri *et al*., 2007). Therefore it is important to specify their function specific to the types of cancer (Cortez *et al*., 2011).

2.4.3 Regulation of microRNAs

As the role of microRNA in cancer becomes more evident, studies moved on to unveil the complex regulatory circuit of these small RNAs. This was done by identifying members of the genome that were regulating the miRNAs or being regulated by the miRNAs. The first account of a transcription factor being involved in regulating miRNAs was reported by

O'Donnell *et al*. Their examination of c-Myc, a transcription factor often dysregulated in cancers, revealed the activation of 6 miRNAs by this oncoprotein. Acitivation was achieved by direct binding of c-Myc to the miRNA cluster *in vivo*. The group then found E2F1 transcription factor to be the target of two miRNAs; miR-17-5p and miR-20a. This led them to propose a model where precise gene modulation is achieved via transcription activation and translation inhibition (O'Donnell *et al*., 2005). Another transcription factor that was identified to regulate miRNAs is the TSG p53. Doxorubicin-induced increase of p53 expression also saw the upregulation of several mature miRNAs while knockdown of p53 by siRNAs saw the predictable weakened expression of those miRNAs. Following DNA damage, several miRNAs are also post-transcriptionally upregulated in a p53-dependent and p68/p72-dependent manner. Processing of pri-miRNAs is promoted by the association of p53 to Drosha or p68 (Suzuki *et al*., 2009). Besides transcription factors, other epigenetic factors such as aberrant CpG methylation was also found to be able to affect miRNA expression in cancers. CpG methylation of the miR-34a (a known p53 target) promoter was found in multiple types of cancer cell lines (Lodygin *et al*., 2008). Hormones such as androgens also affect miRNA expression in different stages of CaP (Shi *et al*., 2007).

MiRNA targets are genes that are regulated post-transcriptionally by miRNAs. One example is the *Bcl-2* gene that is often found to be overexpressed in several cancers. The *Bcl-2* expression was repressed by direct interaction of miR-15 and miR-16 with the 3' UTR of the gene. Repression of *Bcl-2* results in apoptosis via the intrinsic pathway in leukemic cells (Cimmino *et al*., 2005). The proapoptotic Bak1 is another example of a miRNA target. It was found to be regulated by miR-125b in CaP. Downregulation of Bak1

together with other miR-125b targets can cause androgen independent (AI) cell growth (Shi *et al*., 2007).

The findings reveal the complexity of the miRNA regulatory circuit in cancer and more studies should be carried out to complete this circuit and relate it to other regulatory networks for a deeper understanding of cancer.

2.4.4 MicroRNAs and *ANXA7*

Currently there are no reports associating the regulation of miRNAs to the expression of *ANXA7*. Expression of miRNAs could be affected by various factors such as epigenetics and hormone regulation, thus it is postulated that dysregulation in homeostatic cellular processes such as calcium signaling would also affect the expression of miRNAs. ANXA7 is a Ca^{2+}-dependent mediator of exocytosis and a hormone-dependent tumor suppressor. Therefore it is postulated that the dysregulation of *ANXA7* in prostate cancers would also dysregulate the global miRNA expression pattern.

2.5 Study Objectives

The roles of microRNAs in cancer regulation are growing. Future applications in the treatment of cancer as biotherapeutics and biomarkers are promising. It is our hope that this study brought new insights into the role of a recently discovered tumor suppressor gene, ANXA7 in the regulation of prostate cancer through the regulation of microRNAs. We also hoped that the global microRNA expression profile obtained from the altered expression of ANXA7 would reveal non-canonical target genes and signaling pathways that are dysregulated in prostate cancer. Hence, our objectives for this study were:

1. To overexpress wild-type ANXA7 in PC-3 and DU 145 cells.
2. To investigate the effect of *ANXA7* overexpression on the global microRNA expression in PC-3 cells.
3. To predict genes that are targeted by microRNAs that have altered expression due to overexpression of ANXA7.
4. To postulate putative cancer-related pathways associated with microRNAs and ANXA7.

Chapter 3: Methodology

3.1 Materials

3.1.1 Cancer Cell Culture Growth Media and Reagents

3.1.1.1 RPMI 1640

RPMI 1640 liquid medium (1x) with phenol red (containing 2.05mM L-Glutamine) was purchased from a commercial supplier (HyClone®, USA). The medium was supplemented with 10% (v/v) Fetal Bovine Serum (JR Scientific, Inc., USA) and 100 u/100 μg Penicillin/Streptomycin and stored in 4°C.

The RPMI 1640 culture medium used during stable transfection was prepared the same way as above except the Penicillin/Streptomycin was replaced with G-418 sulfate solution to a final working concentration of 0.8mg/ml.

3.1.1.2 Fetal Bovine Serum (FBS)

Fetal Bovine Serum was purchased from a commercial manufacturer (JR Scientific, Inc., USA). Aliquots were made and stored in -20°C.

3.1.1.3 Dulbecco's Phosphate Buffered Saline (D-PBS)

A 1L 10x D-PBS stock solution was prepared, filtered, autoclaved and stored in room temperature. The stock consists of 26.67mM KCl, 14.71mM KH_2PO_4, 1379.31mM NaCl and 80.6mM Na_2HPO_4. The pH of the stock was adjusted to pH 7.4. A 1x working solution was made by dissolving 1/10 of stock with dH_2O and autoclaved at 121°C, 15psi for 15 minutes to sterilize.

3.1.1.4 0.53mM EDTA solution

A 0.53mM (w/v) EDTA solution in 1L was prepared by dissolving 197.3mg EDTA (Gibco®, USA) in 1L of 1X PBS solution and autoclaved at 121°C, 15psi for 15 minutes to sterilize.

3.1.1.5 0.25% Trypsin-0.53mM EDTA solution

Trypsin of porcine pancreas origin was purchased from manufacturer (SAFC Biosciences, USA). The trypsin comes in 10x concentration of 2.5% (v/v). A 0.25% (v/v) Trypsin, 0.53mM EDTA working solution was prepared by diluting the 10x stock in 0.53mM EDTA solution under aseptic conditions and stored in room temperature.

3.1.1.6 10,000 u per ml/10, 000 µg per ml Penicillin/Streptomycin solution

The Penicillin/Streptomycin antibiotic solution was purchased from manufacturer (Lonza, USA). The antibiotic solution comes in 100x concentration of 10,000 u/ml of Penicillin and 10, 000 µg/ml of Streptomycin. The antibiotic solution was added into RPMI 1640 medium as shown above.

3.1.1.7 Antibiotic G-418 Sulfate

The antibiotic G-418 Sulfate was purchased from a commercial supplier (Promega, USA) in powder form and was stored in room temperature. A 50mg/ml stock solution was prepared by dissolving the powder in distilled H_2O and sterile filtered before being stored at -20°C. The stock solution was used to prepare RPMI 1640 culture medium (Section 3.1.1.1) for antibiotic selection during stable transfection.

3.1.2 Bacterial Culture Growth Media and reagents

3.1.2.1 Luria-Bertani (LB) Medium

The LB medium (Laboratorios CONDA, Spain) was purchased from a distributor. The LB medium contained 1% (w/v) Tryptone, 0.5% (w/v) Yeast Extract and 0.5% (w/v) NaCl with final pH 7.0 ± 0.2 at 25°C. The powdered media was dissolved in 1 Liter distilled water (dH_2O) and sterilized by autoclaving at 121°C, 15psi for 15 minutes. The medium was stored in 4°C for up to a month.

3.1.2.2 LB Agar

The LB Agar was obtained from the same manufacturer as the LB medium. The components are all the same with the addition of 1.5% (w/v) bacteriological agar. LB Agar was also dissolved in 1 Liter dH_2O and autoclaved at 121°C, 15psi for 15 minutes. It was then cooled to approximately 50°C and added with antibiotics if necessary before being poured into plates. Plates were then sealed and stored upside down in 4°C for up to a month.

3.1.2.3 Antibiotics

Stock 100x liquid Kanamycin Sulfate (GIBCO®, USA) with a concentration of 10mg/ml was purchased, aliquot and stored in -20°C, in the dark. Growth media and agar plates were supplemented with 50μg/ml Kanamycin and stored in 4°C for up to a month.

Powder Ampicillin Sodium Salt (GIBCO®, USA) was purchased. The Ampicillin powder was rehydrated in sterile dH_2O to obtain a concentration of 10mg/ml and stored in 4°C. Growth media and agar plates were supplemented with 100μg/ml Ampicillin and stored in 4°C for up to a month.

3.1.2.4 Restriction enzymes (RE) and T4 DNA Ligase

FastDigest® *BamHI*, FastDigest® *BglII*, FastDigest® *EcoRV* and FastDigest® *NotI* restriction enzymes were purchased from manufacturer (Fermentas, Canada) and stored in -20°C. The T4 DNA Ligase enzyme was bought from the supplier in the form of 20,000 units (New England Biolabs, USA) and stored in -20°C. *EcoRI* enzyme was obtained from Vivantis Technologies, Malaysia.

3.1.3 Buffers and stock solutions

3.1.3.1 10x Tris borate EDTA buffer (TBE)

The TBE buffer was bought in a 10x liquid concentrate form (Amresco®, USA). A 1x working solution was prepared by dissolving in DEPC-treated H_2O. The 1x working TBE buffer contains 89mM Tris, 89mM Borate and 2mM EDTA.

3.1.3.2 25x Tris Acetate EDTA buffer (TAE)

The TAE buffer was obtained in a 25x liquid concentrate form (Amresco®, USA). A 1x working solution was prepared by dissolving in dH_2O. The 1x working TAE buffer contains 40mM Tris-Acetate and 1mM EDTA.

3.1.3.3 6x DNA loading dye

The 6x Orange DNA loading dye was purchased from manufacturer (Fermentas, Canada) and stored in -20°C.

A loading dye with denaturing conditions were made by adding 1% SDS solution into the 6x Orange DNA loading dye and stored in -20°C. This loading dye is used to resolve products of ligation.

3.1.3.4 2X RNA loading dye

The 2X RNA loading dye was obtained from Fermentas, Canada and stored in -20°C.

3.1.3.5 Ethidium Bromide (EtBr) Solution

Ethidium Bromide stock solution was bought from the manufacturer (Sigma-Aldrich, USA) in a concentration of 10mg/ml (v/v). The EtBr working solution is prepared by dissolving the stock solution in dH_2O (for DNA agarose gel) or DEPC-treated H_2O (for RNA agarose gel) into a working concentration of 0.5µg/ml (v/v).

3.1.4 Commercial Kits

Commercial Kits obtained and used for this study were:

1. RNeasy Plus Mini Kit (Qiagen, Germany).
2. High Capacity cDNA Reverse Transcription Kit (Applied Biosystems, USA).
3. GoTaq® Flexi DNA Polymerase Kit (Promega, USA).
4. *Pfu* DNA Polymerase (Fermentas, Canada).
5. QIAquick Gel Extraction Kit (Qiagen, Germany).
6. pENTR™/D-TOPO® Cloning Kit (Invitrogen, USA).
7. PureYield™ Plasmid Miniprep System (Promega, USA).
8. pcDNA3.1/nV5-DEST™™ Gateway™™ Vector Pack (Invitrogen, USA).
9. Agilent RNA 6000 Nano Kit (Agilent Technologies, USA).
10. FlashTag™ Biotin RNA Labelling Kit for Affymetrix® GeneChip® miRNA Arrays (Genisphere, USA).
11. GeneChip® miRNA Array (Affymetrix, USA)
12. *mir*Vana™ qRT-PCR miRNA Detection Kit (Ambion, USA)

3.1.5 Chemical Reagents

Chemical Reagents were purchased from various manufacturers which include Sigma-Aldrich®, USA; Promega Corp., USA; Merck, Germany; Thermo Fisher Scientific, USA; GIBCO® Invitrogen, USA; AMRESCO, USA and Roche, Germany.

3.1.6 Bacterial strains, plasmid vectors and oligonucleotides

3.1.6.1 Bacterial Strains

The bacterial strains used in this study is shown in the table below:

Table 3.1: Bacterial strains used.

Name	Description	Reference/Source
One Shot® TOP10 *E. coli*	F- *mcr*A Δ(*mrr-hsd*RMS-*mcr*BC) Φ80*lac*ZΔM15 Δ*lac*X74 *rec*A1 *ara*D139 Δ(*araleu*) 7697 *gal*U *gal*K *rps*L (StrR) *end*A1 *nup*G	Invitrogen, USA
Library Efficient® DB3.1™ *E. coli*	F^- *gyr*A462 *end*A1 Δ(sr1-*rec*A) *mcr*B *mrr hsd*S20(r_B-, m_B-) *sup*E44 *ara*-14 *gal*K2 *lac*Y1 *pro*A2 *rps*L20(Sm^R) *xyl*-5 λ- l*eu mtl*1	Invitrogen, USA

The plasmid vectors used for this research are pENTR™/D-TOPO® (Invitrogen, USA), pcDNA3.1/nV5-DEST™ (Invitrogen, USA) and pIRES2-AcGFP1 (Clontech USA). Maps of the plasmids are as follow:

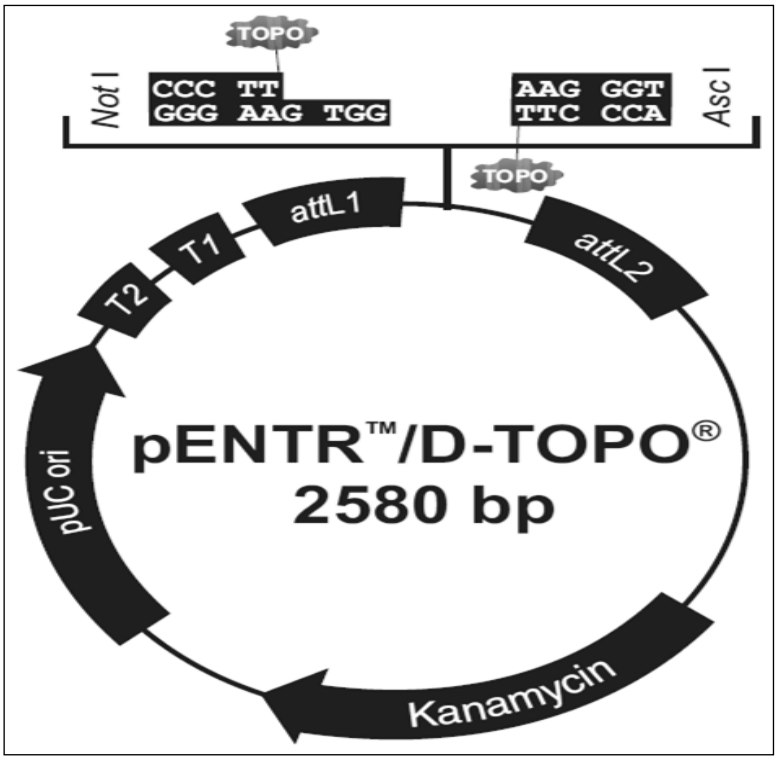

Figure 3.1: Map and features of pENTR™/D-TOPO® vector (www.Invitrogen.com)

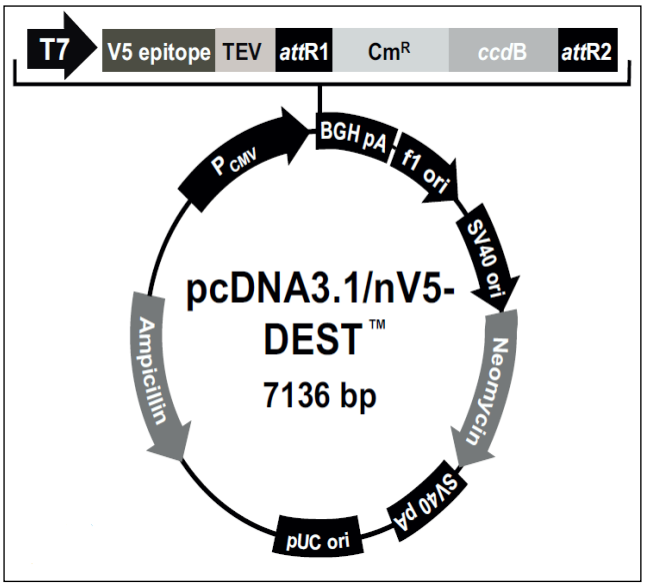

Figure 3.3: Map and features of pcDNA3.1/nV5-DEST™ vector (www.Invitrogen.com)

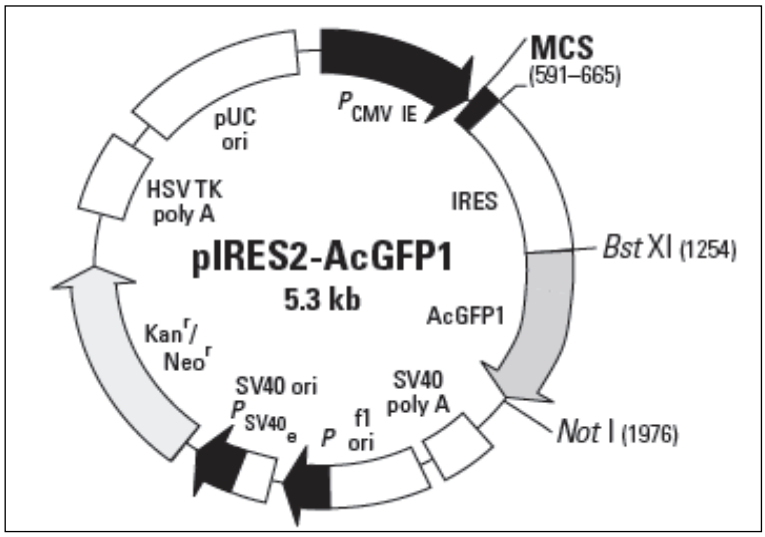

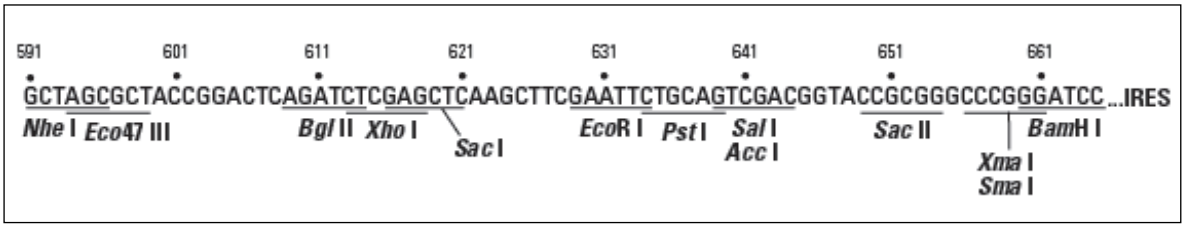

Figure 3.2 Map and features of pIRES2-AcGFP1 vector (www.Clontech.com)

3.1.6.3 Oligonucleotides

Oligonucleotides were designed using Primer3 and Primer-BLAST software and synthesized by commercial manufacturer (First BASE Laboratories, Malaysia).

Table 3.2: Oligonucleotides used in this study. Underlined sequence represents a RE recognition site.

Name	**Sequence 5' to 3'**	**Length and Description**
ANXA7 Forward Primer 2 (A7P2F)	CACCAGAATGTCATACCCAGGCTA	24nt
ANXA7 Reverse Primer 2 *(*A7P2R*)*	TTACCCTGATACGGTCCTTGACAG	24nt
ANXA7 Forward Primer 3 (A7P3F)	CACCTGGGCTGTGACGCTGCT	21nt
ANXA7 Reverse Primer 3 (A7P3R)	CCCTCCTACTGGCCCACAATAGCC	24nt
F_EcoRI_pcDNA3.1/ANXA7	TAACATGAATTCTGGGCTGTGACGCTGCTGCT	32nt
R_BamHI_pcDNA 3.1/ANXA7	ATTCCTGGATCCCCCTCCTACTGGCCCACAATA	33nt
β-actin Forward Primer 3 (B3F)	AGCCTCGCCTTTGCCGATCC	20nt
β-actin Reverse Primer 3 (B3R)	GGGCAGCGGAACCGCTCATT	20nt

pcDNA3.1/nV5-DEST Forward Primer (FpcD3.1_778)	GCGGTAGGCGTGTACGGTGG	20nt
pcDNA3.1/nV5-DEST Reverse Primer (RpcD3.1_2790)	AAGGAAGGCACGGGGGAGGG	20nt
F_pIRES2_528	GCGGTAGGCGTGTACGGTGG	20nt
R_pIRES2_1029	ACGTGGCACTGGGGTTGTGC	20nt
M13F (-20)	GTAAAACGACGGCCAGT	17nt Universal Primer
M13R-pUC (-26)	CAGGAAACAGCTATGAC	17nt Universal Primer
T7 promoter	TAATACGACTCACTATAGGG	20nt Universal Primer
BGH reverse	CTAGAAGGCACAGTCGAGGC	20nt Universal Primer

Table 3.2, continued

3.1.7 DNA ladder marker

The DNA ladder marker used was the O'GeneRuler™ 1 kb DNA Ladder, ready-to-use (Thermo Scientific, USA) unless stated otherwise and had fragment sizes from 250 bp to 10,000 bp. The marker was stored in -20°C. The ladder is as shown in Figure 3.4.

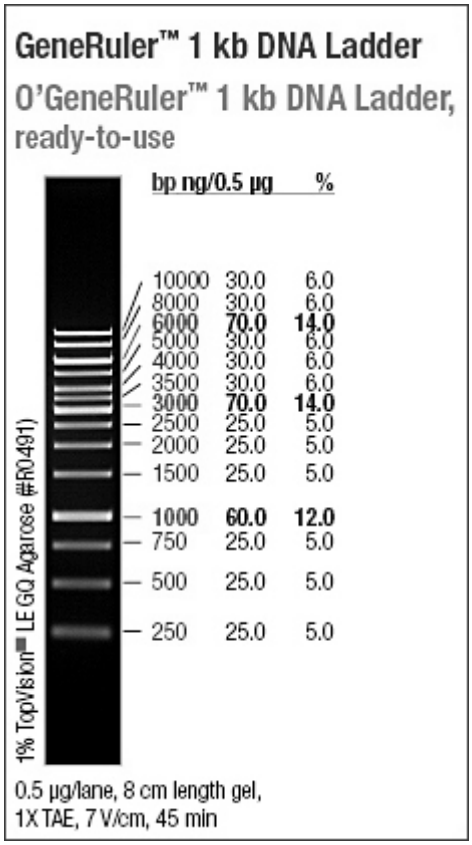

Figure 3.4: Molecular weight, mass and percentage of the O'GeneRuler 1kb DNA Ladder ready-to-use marker fragments after an agarose gel electrophoresis. Adapted from http://www.thermoscientificbio.com/nucleic-acid-electrophoresis/generuler-1-kb-dna-ladder-ready-to-use-250-to-10000-bp/ . Retrieved September 27, 2013.

3.1.8 RNA ladder marker

The RNA ladder marker used was the RiboRuler™ High Range RNA Ladder, ready-to-use (Thermo Scientific, USA) unless stated otherwise. It had fragment size ranging from 200bp to 6000bp. The marker was stored in -20°C. The ladder is as shown in Figure 3.5.

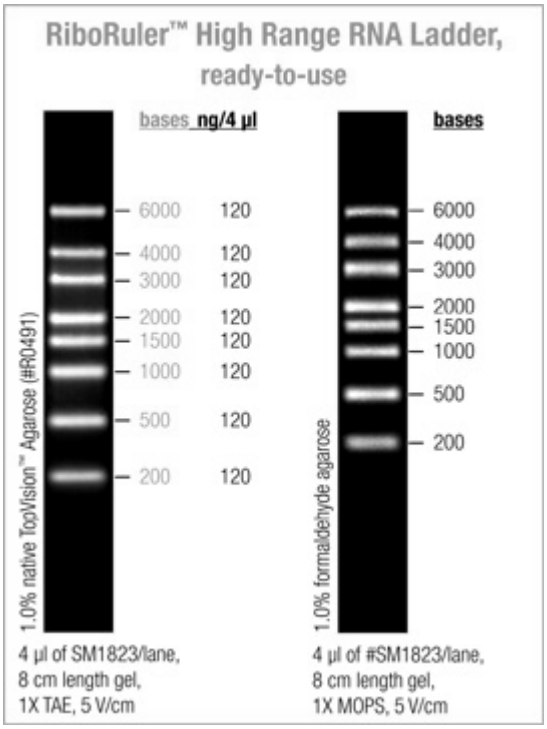

Figure 3.5: Molecular weight and mass of the RiboRuler™ High Range RNA Ladder, ready-to-use marker fragments after a native agarose gel (left) and a formaldehyde agarose gel (right) electrophoresis. Adapted from http://www.thermoscientificbio.com/nucleic-acid-electrophoresis/riboruler-high-range-rna-ladder-ready-to-use/ . Retrieved September 27, 2013.

3.1.9 Cancer cell lines

PC-3 (cat. no. CRL-1435) and DU 145 (cat. no. HTB-81) prostate cancer cell lines were purchased from American Type Culture Collection (ATCC). PC-3 cell line originated from the bone metastasis of a prostatic adenocarcinoma from a 62 years old Caucasian male and the cells are epithelial adherent cells. Meanwhile, DU 145 cell line originated from a brain metastasis of a prostate carcinoma from a 69 years old Caucasian male and the cells are also adherent epithelial cells.

3.1.10 Normal Prostate Epithelial cDNA

Human Prostate Epithelial Cell cDNA [HPrEpiC cDNA] (cat. no. 4414) was purchased from ScienCell™ Research Laboratories. The cDNA was prepared by reverse transcription of RNA extracted from normal human primary cells.

3.2 Methods

3.2.1 Cell Culture

Cells were cultured according to supplier's protocol. Briefly, cells were cultured in RPMI 1640 with 10% FBS and 100 u/100 µg Penicillin/Streptomycin, at 37°C in a humidified, 5% CO_2 environment for 2 to 3 days until about 70-80% confluency before being used for downstream work or subcultured. Subculturing into a new flask was performed after media was discarded and cells washed twice with 1x PBS. Trypsin-EDTA was used as the dissociating agent.

3.2.2 Total RNA Extraction

Total RNA was isolated using two methods. The first method was by using the RNeasy Plus Mini Kit (Qiagen, Germany) and according to manufacturer's recommendation. The second method was by using the TRIZOL reagent according to manufacturer's instructions (Invitrogen, USA). Purity and integrity of RNA was determined by spectrophotometry and Tapestation 2200 (Agilent Technologies, Inc, USA) respectively.

3.2.3 Agarose Gel Electrophoresis

3.2.3.1 DNA Agarose Gel Electrophoresis (AGE)

Agarose gels were prepared according to previously (Sambrook and Russell., 2001). Briefly, a solution of agarose in 1x TAE at a percentage appropriate to separate the DNA fragments of the expected size was prepared. For example, a 1% (w/v) gel was prepared by dissolving 300mg of agarose powder in 30ml of 1x TAE. Agarose in the solution was then dissolved by heating in a microwave and cooled to 55°C before the gel was poured into a casting tray. Once the gel hardens after about 45 minutes, a small amount of buffer was poured on the gel and the comb removed carefully. The gel was then placed in the electrophoresis tank and covered in sufficient buffer to a depth of approximately 1mm.

DNA samples are mixed with the 6x Orange DNA loading dye (Fermentas, Canada). After mixing, the sample was loaded carefully into the slots of the prepared gel. The O'GeneRuler™ 1kb DNA Ladder (Fermentas, Canada) was then loaded into the left or right slots of the gel. The gel was then run at 1-5V/cm length of the gel until the dye front has reached the appropriate distance through the gel. Gels were stained in EtBr solution for 10 minutes and destained with dH_2O for 15 minutes. The gel was then viewed and annotated with AlphaImager® 2200 Gel Documentation System (Cell Biosciences, USA).

3.2.3.2 Native RNA Agarose Gel Electrophoresis (AGE)

The Agarose Gel was prepared according to DNA Agarose Gel method except that the buffer is substituted with 1x TBE. The RNA samples were mixed with the 2x RNA Loading Dye (Fermentas, Canada). The RiboRuler™ High Range RNA Ladder (Fermentas, Canada) was use as size standards. Eletrophoresis settings and staining are according to DNA AGE. Viewing is also done with the same gel documentation system as in section 3.2.3.1.

3.2.4 Reverse Transcription (RT)

The total RNA was reverse transcribed to cDNA using the High Capacity cDNA Reverse Transcription Kit (Applied Biosystems, USA) and according to manufacturer's protocol. The concentration of total RNA used for each RT-PCR reaction was 0.1µg/µl, obtained by diluting stock total RNA extracted with nuclease-free H_2O.

3.2.5 PCR Amplification of Annexin VII (ANXA7) gene

PCR amplification of the human *ANXA7* gene was first optimized from the cDNA obtained from the RT reaction of PC-3 total RNA. Once conditions were optimized, amplification was then carried out on the normal human prostate epithelium cDNA purchased commercially (Sciencell, USA). The oligonucleotide primers used were: Forward primer (A7P3F) - 5' CAC CTGGGCTGTGACGCTGCT 3' and Reverse primer

(A7P3R) - 5' CCCTCCTACTGGCCCACAATAGCC 3'. All PCR was carried out in 0.20mM dNTPs, 2.0mM $MgSO_4$, 0.1μM of each primer and 0.625u of *Pfu* DNA Polymerase (Fermentas, Canada) in a final reaction volume of 25μl. Amplification was performed with an initial denaturation temperature of 94°C for 3min followed by 30 cycles: denaturation at 94°C for 1min, annealing at 61°C for 1min, extension at 72°C for 4min and 1 cycle of final extension at 72°C for 15min. PCR products were resolved by agarose gel electrophoresis and purified with QIAquick Gel Extraction Kit (Qiagen, Germany) according to manufacturer's protocol.

3.2.6 pENTR/ANXA7 Vector Construction and Transformation of Construct into *E. coli*

The *ANXA7* PCR product was inserted to pENTR™/D-TOPO® vector according to manufacturer's instructions (Invitrogen, USA) and will be known as pENTR/*ANXA7*. Briefly, purified *ANXA7* PCR product was mixed with the vector and incubated at room temperature for 30 minutes. The mix was then added into a vial of chemically competent One Shot® TOP10 *E. coli* and was incubated on ice for 30min. Cells were heat shocked before being added with S.O.C. medium or LB medium. Cells were then incubated at 37°C with shaking for 1 hour before being spread on a prewarmed LB selective plate. Plate was incubated overnight at 37°C before being checked for presence of single colonies.

3.2.7 Colony PCR of Putative Clones

Colony PCR was carried out on transformed clones found on the selective plates. The PCR was carried out in 0.3mM dNTPs, 3mM $MgCl_2$, 0.1µM of each A7P3F and A7P3R primers and 0.5u of GoTaq® Flexi DNA Polymerase (Promega, USA) in a final volume of 20µl. Using a sterile pipette tip, a colony was picked and rubbed on the bottom of the PCR reaction tube. The cells sticking to the wall of the tube acted as the template for the PCR reaction. Amplification was carried with initial denaturation temperature of 95°C for 5min, followed by 30 cycles: denaturation at 95°C for 1min, annealing at 55°C for 1min, extension at 72°C for 2min and 1 cycle of final extension at 72°C for 5min. PCR products were resolved with agarose gel electrophoresis and positive transformant/s (putative clones) were identified and selected to be used in downstream steps.

3.2.8 pcDNA3.1/ANXA7 Vector Construction and Transformation of Construct into *E. coli*

The pcDNA3.1/nV5-DEST™ expression vector containing the *ANXA7* gene (pcDNA3.1/*ANXA7*) was constructed via a recombination reaction according to manufacturer's protocol (Invitrogen, USA) and transformed into One Shot® Chemically Competent TOP10 *E. coli* cells according to section 3.2.6. Positive transformants were then screened using colony PCR according to section 3.2.7.

3.2.9 Plasmid Purification

Positive putative *E. coli* clones were cultured overnight in LB medium with added antibiotics, shaking at approximately 225rpm and at a temperature of 37°C for about 16 hours (until the $O.D._{600}$ of a tenfold dilution of the culture was 0.1-0.35) before the plasmids were isolated using the PureYield™ Plasmid Miniprep System according to manufacturer's recommendations (Promega, USA). Briefly, cells were collected by centrifugation and resuspended again in water before being lysed with lysis buffer. Neutralization buffer was added to neutralize the lysis buffer in the lysate. Lysate was then collected and plasmids were bound on the membrane in the spin column. The endotoxin removal wash step and column wash step was each incubated for 1 minute at room temperature. The plasmid was then eluted from the column membrane with water.

3.2.10 Restriction Enzyme (RE) Digestion and Analysis

Based on the Restriction Map of pENTR™/D-TOPO® vector obtained from www.invitrogen.com and analysis using the NEBcutter V2.0 software (New England BioLabs, USA), restriction endonucleases that cut once in the vector and once in the *ANXA7* gene fragment were chosen for ease of downstream analysis and in this case *EcoRV* was selected.

Restriction enzyme digestion of 0.25µg or 0.5µg of purified plasmid was carried out using half the volume recommended of the FastDigest® *EcoRV* enzyme (Fermentas, Canada) in a final reaction volume of 20µl. The product of the RE digest was then resolved with agarose gel electrophoresis and its restriction pattern determined.

3.2.11 Sequencing of Plasmid Constructs and Nucleotide Sequence Analysis

Constructs extracted from liquid culture of putative clones confirmed to have the *ANXA7* gene cloned in the correct orientation with RE digest were then sent to a sequencing facility (First BASE Laboratories, Malaysia). The forward and reverse sequencing primers used to sequence the *ANXA7* gene in the cloning constructs were the M13F (-20) and the M13R-pUC (-26) universal primers, respectively. The forward and reverse sequencing primers used to sequence the *ANXA7* gene in the pcDNA3.1/nV5-DEST™ vector were the T7 promoter and the BGH reverse universal primers, respectively. All universal primers were provided by the sequencing facility. The primers to sequence *ANXA7* construct inserted into the pIRES2-AcGFP1 vector were forward (F_pIRES2_528) – 5' GCGGTAGGCGTGTACGGTGG 3' and reverse (R_pIRES2_1029) – 5' ACGTGGCACTGGGGTTGTGC 3'.

To view the chromatogram and check the quality of the sequences returned, the Sequence Scanner version 1.0 software was used (Applied Biosystems, USA). After analyzing the chromatogram, the nucleotide sequences were trimmed and aligned using the BioEdit software (Hall., 1999). The nucleotide sequences was then compared to two genomic contig assemblies (Accession number NT 030059.13 and NW 001837987.2) in

the National Center for Biotechnology Information (NCBI) database (www.ncbi.nlm.nih.gov) using their BLAST program. Sequences were also manually compared to GenBank reference sequences i) *Homo sapiens* annexin A7, transcript variant 1, mRNA (asession number: NM_001156.3) and ii) *Homo sapiens* annexin A7, transcript variant 2, mRNA (asession number: NM_ 004034.2) using Bioedit software to check whether or not sequences were identical to the reference sequence. Clones containing vector with sequence identical to the reference sequence will be used for further downstream work.

3.2.12 Propagation of pcDNA3.1/nV5-DEST™ and pIRES2-AcGFP1 vectors

The pcDNA3.1/nV5-DEST™ vector (Invitrogen, USA) was transformed into Library Efficient® DB3.1™ competent *E. coli* (Invitrogen, USA) while the pIRES2-AcGFP1 vector (Clontech, USA) was transformed into One Shot® TOP10 *E. coli* (Invitrogen, USA) according to manufacturer's protocol. Briefly, the vector was added to thawed competent cells. The cells were then incubated on ice for 30 minutes before being heat shocked and returned to ice for 2 minutes. Cells were then cultured in S.O.C. medium or LB medium for 1 hour with shaking at 37°C before it was spread on a prewarmed selective plate and incubated overnight at 37°C. Colonies were observed the next day and picked for screening via colony PCR according to section 3.2.7 with some modifications.

The PCR to screen for pcDNA3.1/nV5-DEST™ vector was carried out using forward primer (FpcD3.1_778) - 5' GCGGTAGGCGTGTACGGTGG 3' and reverse primer (RpcD3.1_2790) - 5' AAGGAAGGCACGGGGGAGGG 3'.

The PCR to screen for pIRES2-AcGFP1 vector meanwhile uses F_pIRES2_528 forward and R_pIRES2_1029 reverse primers with a 58°C annealing temperature and an extension time of 3min each cycle for a PCR reaction of 25 cycles.

Positive transformants were further cultured and the expression vector isolated according to section 3.2.9.

3.2.13 Transfer of ANXA7 gene from pcDNA3.1/ANXA7 to pIRES2-AcGFP1 vector

The *ANXA7* gene inserted into pcDNA3.1/nV5-DEST™ was PCR amplified according to section 3.2.5 but using F_EcoRI_pcDNA3.1/ANXA7 and R_BamHI_pcDNA3.1/ANXA7 forward and reverse primers, respectively. These primers are designed with an RE recognition site within each; *EcoRI* on the forward primer and *BamHI* on the reverse primer (Table 3.3 under Materials). The RE site facilitates the cloning of the PCR product into the corresponding RE sites in the pIRES2-AcGFP1 vector. The cycling conditions were the same except for the annealing temperature used which was between 53-68°C and amplification was done with 35 cycles.

A 0.2µg of purified *ANXA7* PCR product were restricted with FastDigest® *BamHI* (Fermentas, Canada) and *EcoRI* (Vivantis Technologies, Malaysia) in a 30µl reaction incubated in FastDigest® buffer for 1 hour in 37°C while 0.2µg of pIRES2-AcGFP1 vector were also restricted with both enzymes in a 20µl reaction under the same conditions. Enzymes were inactivated by heat at 80°C for 20min. Ligation was then carried out in a 20µl reaction with 1µl of T4 DNA Ligase (New England Biolabs, USA) mixed with restricted *ANXA7* PCR product and restricted pIRES2-AcGFP1 vector in a 3:1 insert to

vector molar ratio. Reaction was incubated in room temperature for 1 hour and the product of the ligation was resolved with agarose gel electrophoresis. Ligation product was then transformed into *E.coli* according to Section 3.2.6 and colony PCR was carried out to confirm the presence of pIRES2-AcGFP1 vector with *ANXA7* insert according to Section 3.2.7 but using F_pIRES2_528 forward and R_pIRES2_1029 reverse primers. The annealing temperature used was 58°C and the time for the extension step was 3min each cycle and the PCR was carried out for 25 cycles. Products of the PCR were resolved with agarose gel electrophoresis.

Clones containing the desired construct (pIRES2-AcGFP1-ANXA7) were cultured and plasmids were then purified according to Section 3.2.9. The plasmids were subjected to *BamHI* digestion in 20µl reaction incubated at 37°C for 1 hour and analyzed using agarose gel electrophoresis. Plasmids were then sent for sequencing according to Section 3.2.11.

3.2.14 Stable Transfection of Cell Line

PC-3 cells and DU 145 cells were seeded at 1 x 10^5 cells/well and 2 x 10^5 cells/well, respectively in a 6-well plate, in 2 ml of growth medium and cultured for about 48 h until 90% confluency. Transfection was performed using X-tremeGENE HP transfection reagent (Roche, Penzberg, Germany). The ratio between transfection reagents and vectors were optimized using the empty vector pIRES2-AcGFP1 (Roche, Penzberg, Germany), and was found that a ratio of 3:1 for PC-3 cells and a ratio of 2:1 for DU 145 yielded maximum transfection efficiency. Cells were transfected for approximately 48 h and expression of green fluorescence protein (GFP) was observed. Cells were then selected with medium

containing G418 (Promega, Madison, WI, USA) at 600 μg/ml. for 14 days or longer until a stable population of cells was established. Cells that were transfected with empty vectors were used as negative controls. Total RNA was extracted and used for miRNA microarray, qRT-PCR analysis.

3.2.15 RT-qPCR of ANXA7

Total RNA was extracted from cells using TRIzol reagent (Invitrogen, Carlsbad, CA, USA) according to manufacturer's protocol. The integrity of the total RNA was determined with the Agilent 2200 Tapestation (Agilent Technologies, Santa Clara, CA, USA) and samples with RIN value of ≥7 were used. For ANXA7 mRNA detection, RT-qPCR was performed with SuperScript III SYBR Green One-Step RT-qPCR Kit with ROX (Invitrogen, Carlsbad, CA, USA) in 10 μl reactions with CFX96™ Real Time PCR Detection System (Bio-Rad, Hercules, CA, USA). β-actin mRNA levels were detected for normalization and quantification purposes. PCR primers used were: (ANXA7 forward)-5'-TTACCCTAGTCAGCCTGCCA-3',

(ANXA7 reverse)-5'-GCCTGCTCATCTGTCCCAAA-3',

(β-actin forward)-5'-AAGCCACCCCACTTCTCTCTAA-3' and

(β-actin reverse)-5'-ACCTC CCCTGTGTGGACTTG-3'.

All RT-qPCR experiments were performed with two biological replicates and three technical replicates.

3.2.16 MicroRNA microarray expression analysis

MiRNA expression profiles were obtained using GeneChip miRNA Array (Affymetrix, Santa Clara, CA, USA) according to manufacturer's protocol. Each array containing 46,228 probes, representing over 6703 miRNA sequences (71 organisms) from the Sanger miRNA database v. 11. Briefly, 1 μg of PC-3 total RNA was extracted from cells transfected with pIRES2-AcGFP1-ANXA7 (sample group) and cells transfected with empty vector (reference group). The total RNA was poly (A) tailed and biotinylated. Labeled RNA samples were hybridized on arrays at 48°C and 60 rpm for 16 h. A total of 4 arrays (2 for pIRES2-AcGFP1-ANXA7-transfected cells and 2 for empty vector-transfected cells) were washed, stained and scanned by GeneChip scanner 3000 7G (Affymetrix, USA). Scanned images were subjected to quality control checks using the miRNA QC tool (Affymetrix, USA). Significant differentially expressed miRNAs between the sample group arrays and the reference group were generated using 1-way ANOVA analysis in Partek Genomics Suite 6.6. An unadjusted p-value of <0.05 and a fold expression threshold of ≥ 1.5-folds between samples overexpressing *ANXA7* and samples transfected with empty vectors were used. MicroRNA microarray was performed with two biological replicates.

3.2.17 Validation of miRNA microarray data

MiRNAs were first reversed transcribed from PC-3 and DU 145 total RNA using Taqman® miRNA Reverse Transcription Kit in 10 µl reactions (Applied Biosystems, Carlsbad, CA, USA). A miRNA qPCR was then performed using the Taqman® Fast Advanced Master Mix together with Taqman® miRNA assays (hsa-miR-1284 assay ID: 002903, hsa-miR-409-5p assay ID: 002331, hsa-miR-543 assay ID: 002376). Expression of all miRNAs were normalized to the small nuclear RNA RNU6B (assay ID: 001093) (Applied Biosystems, Carlsbad, CA, USA). Amplification was performed at 50°C for 2 min with an initial enzyme activation temperature of 95°C for 20 sec followed by 45 cycles of denaturation at 95°C for 3 sec and an annealing/extension step at 60°C for 20 sec using the CFX96™ Real Time PCR Detection System (Bio-Rad, Hercules, CA, USA). All miRNA qPCR experiments were performed with two biological replicates and three technical replicates.

3.2.18 Bioinformatic analysis

Gene targets of dysregulated miRNAs were predicted with the online algorithm TargetScan Release 6.2 using default settings (http://www.targetscan.org) (Lewis *et al*., 2005). Shortlisted miRNA targets with total context score of ≤ -0.25 were then selected for gene enrichment involving cancer-related pathways using the online Database for Annotation, Visualization and Integrated Discovery (DAVID v6.7) functional annotation tool (http://david.abcc.ncifcrf.gov/tools.jsp) using default settings of minimum gene count

threshold of 2 and maximum EASE score/P-value threshold of 0.1 (Huang *et al*., 2009a & 2009b) and Kyoto Encyclopedia of Genes and Genomes (KEGG) pathway tool (http://www.genome.jp/kegg/pathway.html) (Kanehisa and Goto, 2000; Kanehisa *et al*., 2012).

3.2.19 Statistical analysis

Statistically significant comparisons were performed using the Student's T-test. A *p*-value threshold of ≤ 0.05 was set for all experiments with the exception of DAVID v6.7 gene target analysis and qPCR validation of shortlisted miRNAs, where a ≤ 0.10 *p*-value cutoff threshold was used. Validation of miRNA microarray data using qPCR was performed using the Pearson's correlation coefficient value. All experiments were performed on a minimum of two biological replicates and two technical replicates, and presented as mean ± S.D.

Chapter 4: Results

4.1 Full length PCR Amplification of the *ANXA7* gene

High grade prostate tumors have a low ANXA7 protein expression (Srivastava *et al*., 2001) and therefore the prostate cancer cell lines PC-3 and DU 145 were chosen for this study. Due to the limited amounts of normal prostate epithelium cDNA that was obtained from the commercial supplier (Sciencell, USA), the PCR amplification of the *ANXA7* gene was first optimized using cDNA obtained from PC-3 cells. Intact and pure total RNA extracted from PC-3 cell line was observed using agarose gel electrophoresis (Figure 4.1a and b) and was used for the reverse transcription and PCR reaction.

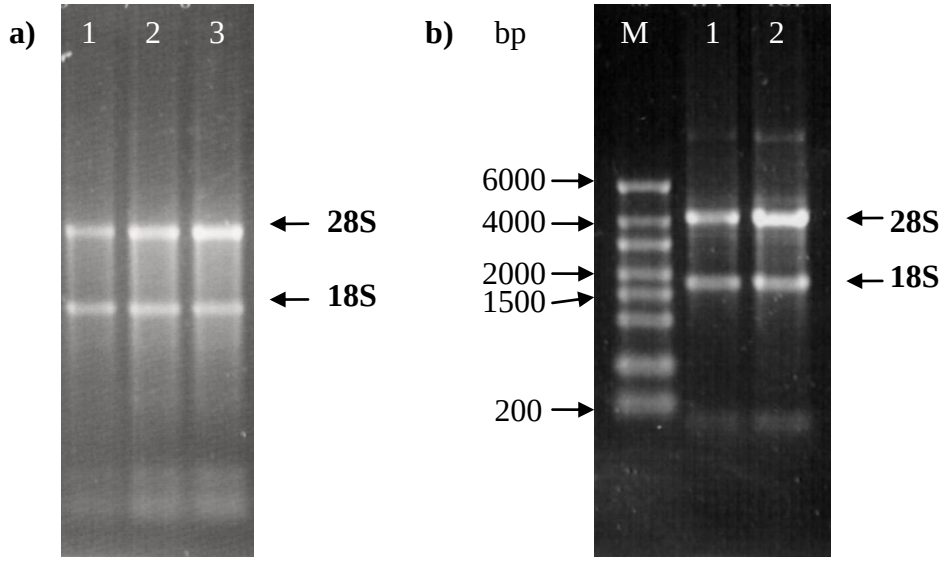

Figure 4.1 a & b: Intact total RNA extracted from PC-3 cell line. a) Total RNA was extracted using the TRIZOL reagent and different amount of RNA was loaded, with increasing amounts from lane 1 to lane 3. b) Two samples of RNA was extracted using the RNeasy Plus Mini Kit and ran beside a RiboRuler™ High Range RNA Ladder with sizes of marker (in bp) shown on the left. RNA samples were resolved by 1% TBE agarose gel electrophoresis. The expected pattern of two distinct bands were observed; 28S rRNA (top) and 18S rRNA (bottom) with an intensity ratio of 2:1.

In order to determine the optimal conditions for the full length amplification of the ANXA7 from a cDNA template, a range of annealing temperatures (T_a) for the two pair of primers designed (A7P2 and A7P3) was tested (Figure 4.2a & b). The different temperatures tested for A7P2 gave similar yield of the product except for Ta of 62°C which had lesser yield (Figure 4.2a). For the case of A7P3, all the annealing temperatures were able to give satisfactory yield.

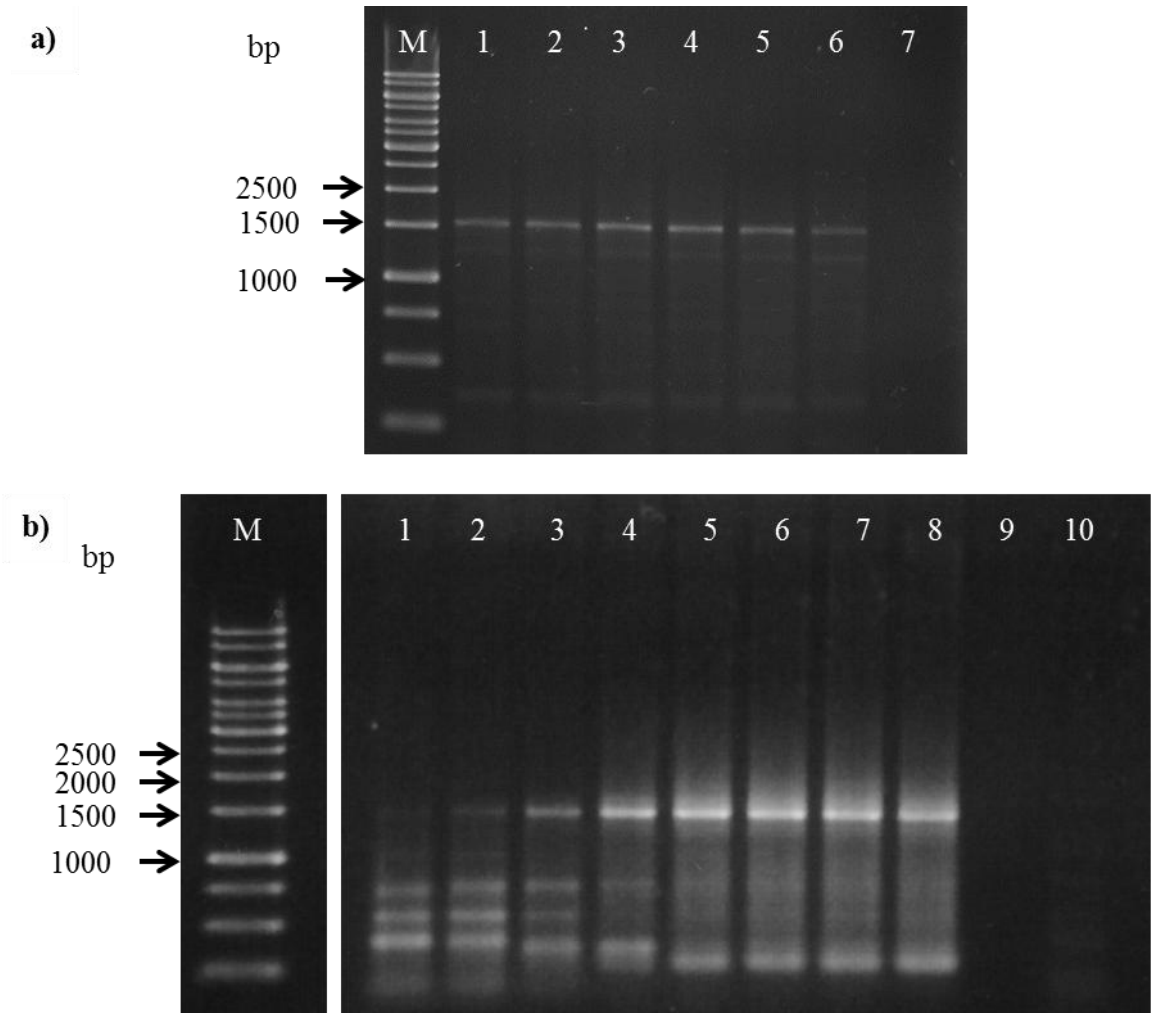

Figure 4.2 a & b: Determination of optimum annealing temperature (Ta) for primers flanking ANXA7. The annealing temperatures for two primer pairs; A7P2 (a) and A7P3 (b) designed to amplify ANXA7 were tested. **a)** The annealing temperatures tested were 50.0 ºC (lane 1), 52.5 ºC (lane 2), 54.8 ºC (lane 3), 57.9 ºC (lane 4), 60.4 ºC (lane 5) and 62.0 ºC (lane 6). **b)** The annealing temperatures tested were 45.0 ºC (lane 1), 46.2 ºC (lane 2), 48.9 ºC (lane 3), 52.7 ºC (lane 4), 57.6 ºC (lane 5), 61.6 ºC (lane 6), 63.8°C (lane 7) and 65°C (lane 8). The expected product size is approximately 1500 bp. A no-template amplification acted as negative control (lane 7 in a and lane 10 in b). Lane 9 was left empty.

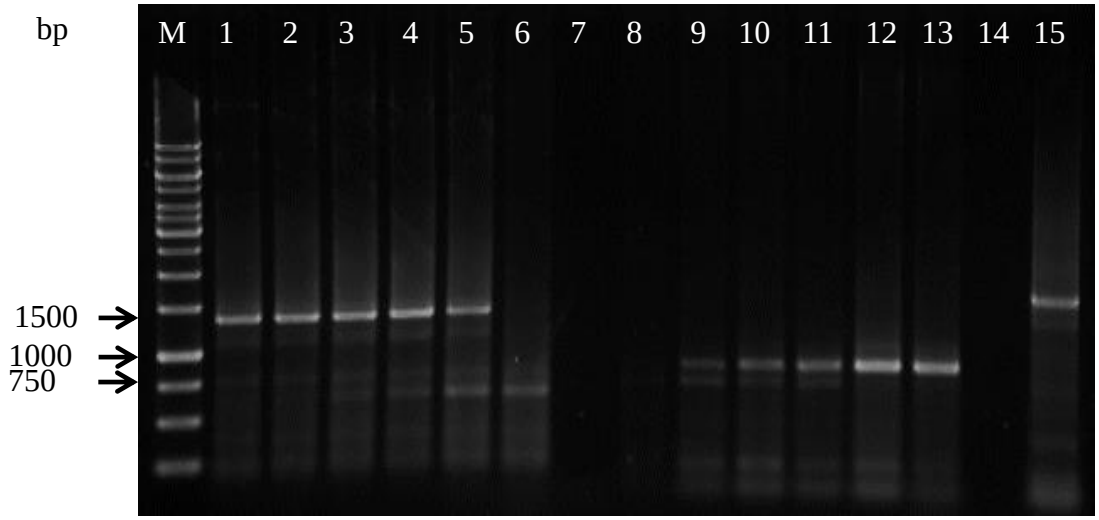

Figure 4.3: Determination of optimum β-actin PCR amplification annealing temperature. Amplification of β-actin gene using primer pair B1 (lanes 1-6) and primer pair B3 (lanes 8-13) with different annealing temperatures. The annealing temperatures tested were 49°C (lanes 1 & 8), 52°C (lanes 2 & 9), 55°C (lanes 3 & 10), 57°C (lanes 4 & 11), 59°C (lanes 5 & 12) and 63°C (lanes 6 & 13). A no-template amplification acted as negative controls (lane 7) for primer pair B1 and (lane 14) primer pair B3. Amplification of diluted PCR products from previous ANXA7 amplification acted as a positive control (lane 15).

To establish a positive control for the subsequent amplifications of *ANXA7* gene, two pair of primers (B1 and B3) were designed to amplify a housekeeping gene, β-actin. Different annealing temperatures (49°C - 63°C) were also tested for these set of primers to determine the optimal conditions for the amplification of this control gene (Figure 4.3). Primer pair B1 was able to amplify β-actin with the expected product size of ~1400bp from T_a of 49°C-59°C. At T_a 63°C, the expected product size was not seen. However, amplification was not specific and multiple bands were observed in all the T_a tested. Hence, primer pair B1 was not used in subsequent PCR reactions. Primer pair B3 was not able to amplify β-actin with the expected product size of ~800bp at T_a of 49°C but successful amplification was observed from T_a of 52°C-63°C. Primer pair B3 was chosen for

following downstream PCR reactions as it produced less multiple bands compared to primer pair B1 and a T_a of 62°C (one degree lower) were chosen as it has less non-specific amplification compared to other temperatures tested.

After optimizing the conditions for PCR amplification of full length *ANXA7* gene was done using prostate cancer cell line cDNA, the normal prostate epithelium cDNA was then used as a template for PCR. Amplification using both pair of primers were carried out but the yield obtained using A7P2 primer pair was not satisfactory (Figure S4.1.1), whereas amplification using A7P3 primer pair gave reasonable yield of the desired product. However, no amplification was observed on a replicate reaction that was performed (Figure 4.4).

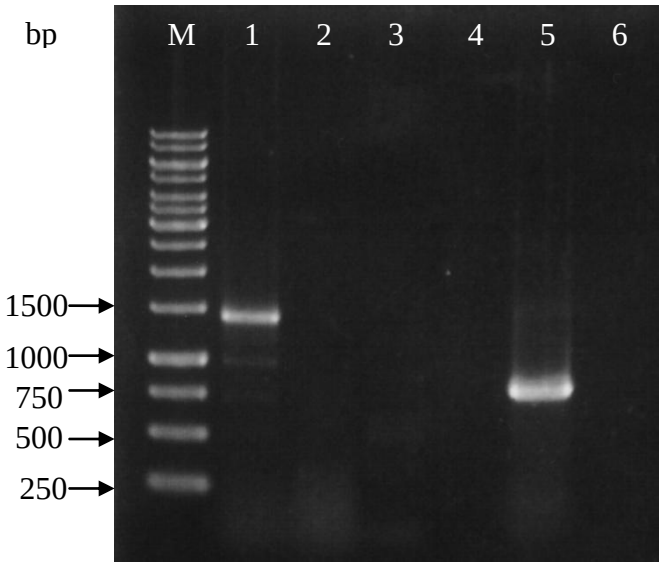

Figure 4.4: PCR amplification of full length ANXA7 from normal prostate epithelium cDNA. Primer pair A7P3 was able to amplify ANXA7 from the normal prostate epithelium cDNA (lane 1). A replicate reaction was also carried out (lane 2) but no amplification was observed. Amplification of β-actin acted as a positive control for the PCR reaction (lane 5) while no-template amplification acted as negative controls (lane 3 & 6). Lane 4 was left empty.

4.2 Construction of pENTR/*ANXA7* and pcDNA4.1/*ANXA7* Vectors.

Once the full length *ANXA7* was inserted into the cloning vector (pENTR™/D-TOPO®, screening of clones that contained the pENTR/*ANXA7* vector was done using colony PCR. All the clones picked for colony PCR showed the presence of the vector (Figure 4.2.1). Once the colonies picked were confirmed to contain the construct (Figure 4.5), the orientation of the *ANXA7* inserted in the construct was determined with a restriction enzyme (RE) digestion on some of the cultured colonies.

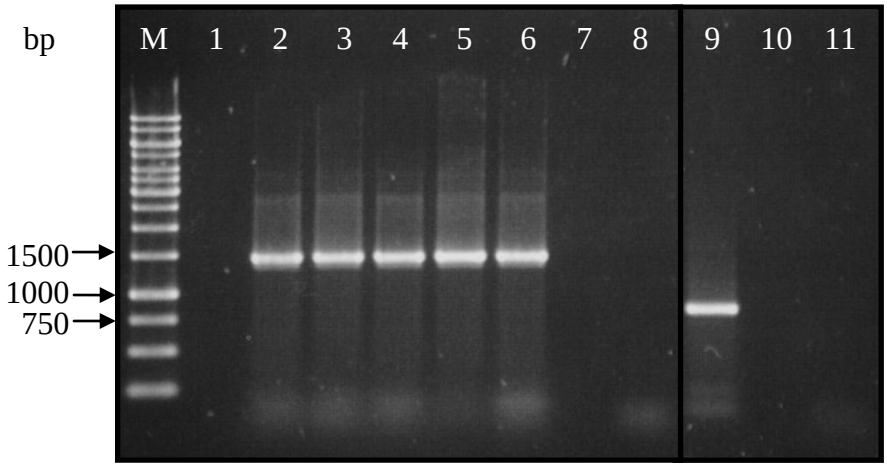

Figure 4.5: Screening of clones containing the pENTR/ANXA7 construct. Several colonies found on the plate containing the transformed E. coli were picked for colony PCR. Primers flanking ANXA7 were used and positive transformants were indicated by an amplified product at ~1500bp (lanes 2-6). Amplification of β-actin acted as a positive control (lane 9) and no-template amplification acted as negative controls (lanes 8 & 11). Lanes 1, 7 & 10 was left empty.

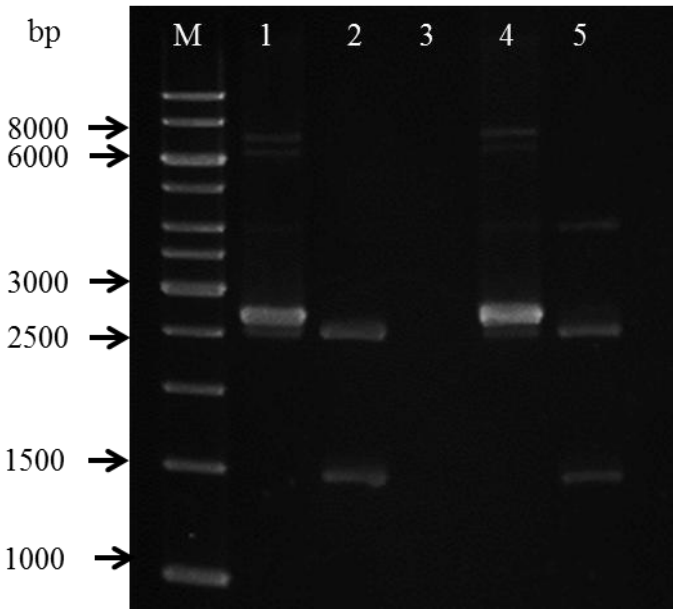

Figure 4.6: Determination of ANXA7 insert orientation in pENTR/ANXA7 construct. Plasmid extraction was carried out to obtain the construct from colonies cultured in liquid media (lanes 1 & 4). The constructs in lanes 1 and 4 were then subjected to EcoRV restriction enzyme digestion to give the expected bands with size of about 2500bp and 1500bp in lanes 2 and 5, respectively. Lane 3 was left empty.

pENTR/*ANXA7* constructs with *ANXA7* inserted in the correct orientation were then sequenced (Figure S4.2.1). The full sequence of the *ANXA7* insert was analyzed and found to match a region in chromosome 10 of the human genome. The sequence was found to contain features of both *ANXA7* mRNA variant 1 and *ANXA7* mRNA variant 2 (Figure 4.7a & Figure S4.2.2). Manual alignment of construct sequences with both *ANXA7* variants using Bioedit software showed that the sequence inserted in the construct was *ANXA7* variant 1 (Figure S4.2.3). The insert in the pENTR/*ANXA7* was then transferred to an expression vector (pcDNA3.1/nV5-DEST™) to generate a pcDNA3.1/*ANXA7* construct.

a)

T5c1 (1443 letters)

Query ID	lcl|35599	**Database Name**	Human Genome (all assemblies) (3 databases)
Description	T5c1	**Description**	▷See details
Molecule type	nucleic acid	**Program**	BLASTN 2.2.26+ ▷Citation
Query Length	1443		

Sequences producing significant alignments:

Accession	Description	Max score	Total score	Query coverage	E value	Max ident
NT_030059.13	Homo sapiens chromosome 10 genomic contig, GRCh37.p5 Pri	379	2718	99%	2e-102	100%
NW_001837987.2	Homo sapiens chromosome 10 genomic contig, alternate asse	379	2718	99%	2e-102	100%

b)

LR1b4 full sequence (1439 letters)

Query ID	lcl|13425	**Database Name**	Human Genome (all assemblies) (3 databases)
Description	LR1b4 full sequence	**Description**	▷See details
Molecule type	nucleic acid	**Program**	BLASTN 2.2.26+ ▷Citation
Query Length	1439		

Sequences producing significant alignments:

Accession	Description	Max score	Total score	Query coverage	E value	Max ident
NT_030059.13	Homo sapiens chromosome 10 genomic contig, GRCh37.p5 Pri	379	2716	99%	2e-102	100%
NW_001837987.2	Homo sapiens chromosome 10 genomic contig, alternate asse	379	2716	99%	2e-102	100%

Figure 4.7 a & b: Analysis of sequenced ANXA7 in vector constructs using NCBI BLAST. The sequence of the pENTR/ANXA7 cloning construct, T5c1 in **(a)** and the pcDNA3.1/ANXA7 expression construct, LR1b4 in **(b)** was compared to sequences in the Human BLAST Assembled RefSeq Genomes. Both sequence had a complete match (Max ident: 100%) to a region in Homo sapiens chromosome 10. The human genome build 37.3 with two genomic contig assemblies was used as a reference during the analysis (Accession number NT 030059.13 and NW 001837987.2).

The construct was also sent for sequencing after screening via colony PCR and RE digestion analysis (Figure 4.8a & b). Sequence analysis showed that the *ANXA7* sequence in pcDNA3.1/*ANXA7* construct was identical to a region in human chromosome 10 (Figure 4.7b & Figure S4.2.4a & b). Thus, the sequence was successfully subcloned without errors.

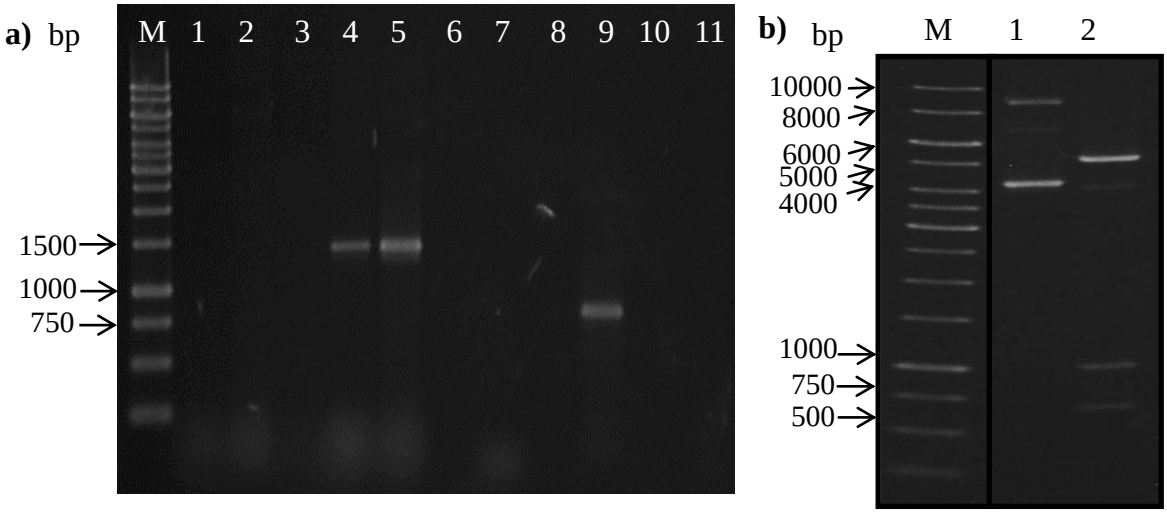

Figure 4.8 a & b: Isolation and identification of *ANXA7* from pcDNA3.1/ANXA7 construct following transfer from pENTR/ANXA7 construct. **(a)** Colonies (lanes 1-5) picked for colony PCR to screen for the presence of ANXA7 in pcDNA3.1/ANXA7 construct (lanes 4 & 5) transferred from the cloning construct via a recombination reaction. No-template amplification (lanes 7 & 11) and β-actin amplification (lane 9) was carried out as positive control for the PCR reaction. Lanes 6, 8 & 10 were left empty. **(b)** Purified expression construct from a liquid culture of colony 5 in (a) (lane 1) was then double digested with BglII and NotI (lane 2) to give three expected bands with sizes of approximately 5000bp, 1000bp and 700bp. A 0.7% agarose gel was used.

4.3 Transfer of *ANXA7* from pcDNA3.1/*ANXA7* to pIRES2-AcGFP1 vector

In order to conveniently determine whether successful transfection occurred and the transcripts in the vector was expressed, a vector that also expresses a fluorescent protein such as GFP was acquired and in this case a pIRES2-AcGFP1 vector. The *ANXA7* sequence in pcDNA3.1/*ANXA7* was cloned into the *EcoRI* and *BamHI* sites of the pIRES2-AcGFP1 vector (Figue 4.9 & Figure S4.3.1a-d) and *ANXA7* sequence was found to be identical to the reference sequence (asession number: NM_001156.3) of *Homo sapiens* annexin A7, transcript variant 1, mRNA (Figure S4.3.2a & b). Therefore the *ANXA7* in the pIRES2-AcGFP1-ANXA7 construct generated was error-free and could be used for further downstream work.

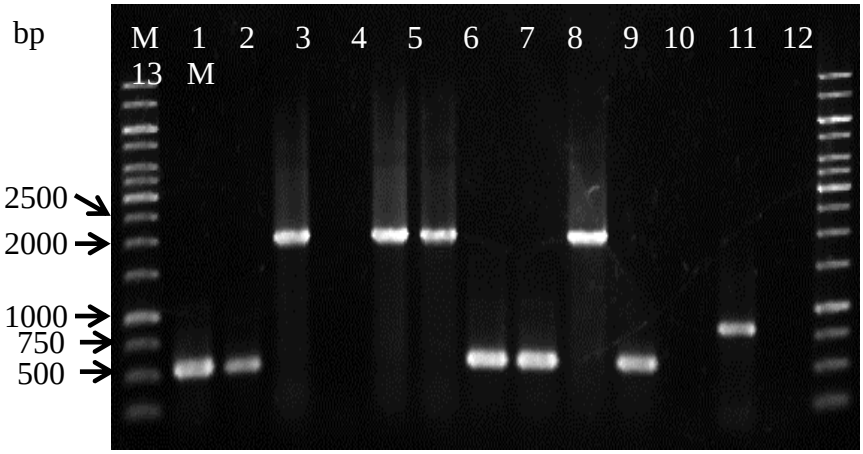

Figure 4.9: Screening of colonies to determine presence of ANXA7 insert in pIRES2-AcGFP1 vector. Colonies (lanes 3, 5, 6 and 9) that contained the insert with the correct size have the expected band size of about 2kbp and colonies (lanes 1, 2, 7, 8, 10) that did not have any insert have the expected band size of about 500bp. No template amplification (lanes 11 & 13) and β-actin amplification (lane 12) was carried out as PCR reaction negative and positive controls, respectively.

4.4 Stable transfection of PC-3 and DU 145 cells with pIRES2-AcGFP1-ANXA7

Once the pIRES2-AcGFP1-ANXA7 construct was obtained, it was transfected into PC-3 and DU 145 cells. Successful transfection was observed through the expression of GFP after 48h using fluorescence microscopy (Figure 4.10a).

The concentration of G418 antibiotic needed to be used for selecting cells containing the expression vector (antibiotic-resistant) was determined using untransfected PC-3 and DU 145 cells (Figure S4.4.1). The minimum concentration that killed all untransfected cells after incubation in G418 for 7 days was 600 μg/ml for both PC-3 and DU 145 cells. After the successful transfection of cell lines was confirmed using fluorescence microscopy, the selection was carried out until stable populations of antibiotic resistant cells were obtained. In order to confirm that expression of ANXA7 was elevated in these cells, qRT-PCR assay quantifying *ANXA7* transcripts was performed. The purified RNA was confirmed based on a RNA Integrity Value (RIN) of ≥7 before using the RNA for other downstream work (Figure S4.4.2). A significant increase in *ANXA7* expression was observed in both ANXA7 expression vector (pIRES2-AcGFP1-ANXA7) transfected cell lines, whereby a 4.8-fold and 1.6 fold increase was recorded in the PC-3 and DU 145 cells, respectively. No increase in expression was observed in untransfected cells and empty-vector transfected cells (pIRES2-AcGFP1) (Figure 4.10b).

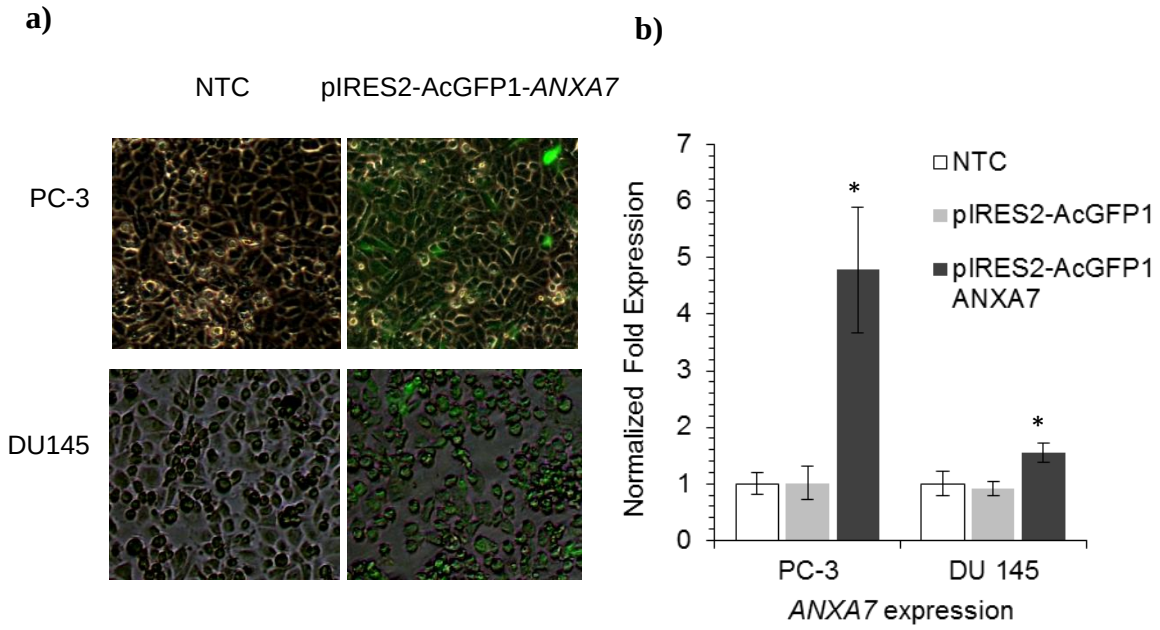

Figure 4.10 a & b: Transfection of PC-3 and DU145 prostate cancer cells with pIRES2-AcGFP1-ANXA7 expression vector increased ANXA7 expression levels. (a) Transfection was performed using the X-tremeGENE HP transfection reagent, followed by the observation of GFP expression after 48 h. NTC denotes untransfected control. All representative images were taken under 100X magnification. **(b) A** significant increase in the expression of ANXA7 mRNA in PC-3 cells transfected with vector carrying ANXA7 was observed using qRT-PCR. All experiments were performed in biological triplicates with two technical replicates, and presented as mean normalized fold expression ±S.D. Statistically significant differences in expression between *ANXA7*-transfected cells and empty vector control groups was confirmed (*$p \leq 0.05$).

4.5 MicroRNA Profile of PC-3 and DU 145 Cells following ANXA7 Overexpression

Once the increased expression levels of *ANXA7* was confirmed, the same purified RNA samples were hybridised in a microRNA microarray to identify altered miRNAs due to increased levels of *ANXA7*. A list of dysregulated miRNAs in *ANXA7*-overexpressed PC-3 cells as compared to cells transfected with the empty vector was constructed (Table 4.1). A total of 16 miRNAs were found to be dysregulated where eight of them were up-regulated and eight of them were down-regulated. Hsa-miR-346 showed the highest up-regulation with a 4.8-fold increase in expression while hsa-miR-543 showed the most down-regulation with a 2-fold decrease in expression. In order to validate the miRNA microarray results, miRNA qPCR was performed for three miRNAs (hsa-miR-1284, hsa-miR-409-5p and hsa-miR-543) in PC-3 stably transfected cells. The miRNA qPCR results positively correlated with the microarray results ($R = 0.8413$ and $R^2 = 0.71$) (Figure 4.11a). All the microRNAs tested showed a significant change in expression either being up-regulated (hsa-miR-1284) or down-regulated (hsa-miR-409-5p and hsa-miR-543) as compared to the empty vector-transfected cells (Figure 4.11b). The expression pattern of the three miRNAs was also determined in DU 145 cells using miRNA qPCR. All three miRNAs also showed a significant change in expression levels as compared to the empty vector-transfected cells (Figure 4.11c). However, when the expression patterns of the three miRNAs were compared between both cell lines, only hsa-miR-1284 had the same pattern of up-regulated expression. Hsa-miR-409-5p and hsa-543 on the other hand had opposing expression patterns (Figure 4.11b & c).

Table 4.1: List of miRNA expression fold-change alterations following the overexpression of ANXA7 on PC-3 cells. Experiments were performed using Affymetrix® GeneChip® miRNA arrays followed by data analysis using the Partek® Genomics Suite™ 6.6. † Positive values denote up-regulation, while negative values denote down-regulation relative to groups transfected with empty vectors, fold change threshold was set at 1.5. ‡ p-values ≤ 0.05 were considered significant.

miRNA	**miRBase No.**	**Fold change**†	***p*-value**‡
hsa-miR-346	MI0000826	4.77 ± 2.16	0.030
hsa-miR-1237	MI0006327	2.18 ± 0.00	0.010
hsa-miR-363	MI0000764	2.14 ± 0.38	0.035
hsa-let-7b	MI0000063	1.69 ± 0.39	0.045
hsa-miR-874	MI0005532	1.91 ± 0.48	0.039
hsa-miR-133a	MI0000450	1.56 ± 0.14	0.036
hsa-miR-551a	MI0003556	1.56 ± 0.17	0.025
hsa-miR-1284	MI0006431	1.52 ± 0.02	0.027
hsa-miR-448	MI0001637	-1.50 ± 0.00	0.009
hsa-miR-382	MI0000790	-1.50 ± 0.09	0.028
hsa-miR-487b	MI0003530	-1.60 ± 0.01	0.005
hsa-miR-940	MI0005762	-1.60 ± 0.12	0.045
hsa-miR-376a	MI0000784	-1.70 ± 0.00	0.008
hsa-miR-193a-3p	MI0000487	-1.80 ± 0.04	0.008
hsa-miR-409-5p	MI0001735	-1.80 ± 0.00	0.026
hsa-miR-543	MI0005565	-2.0 ± 0.10	0.029

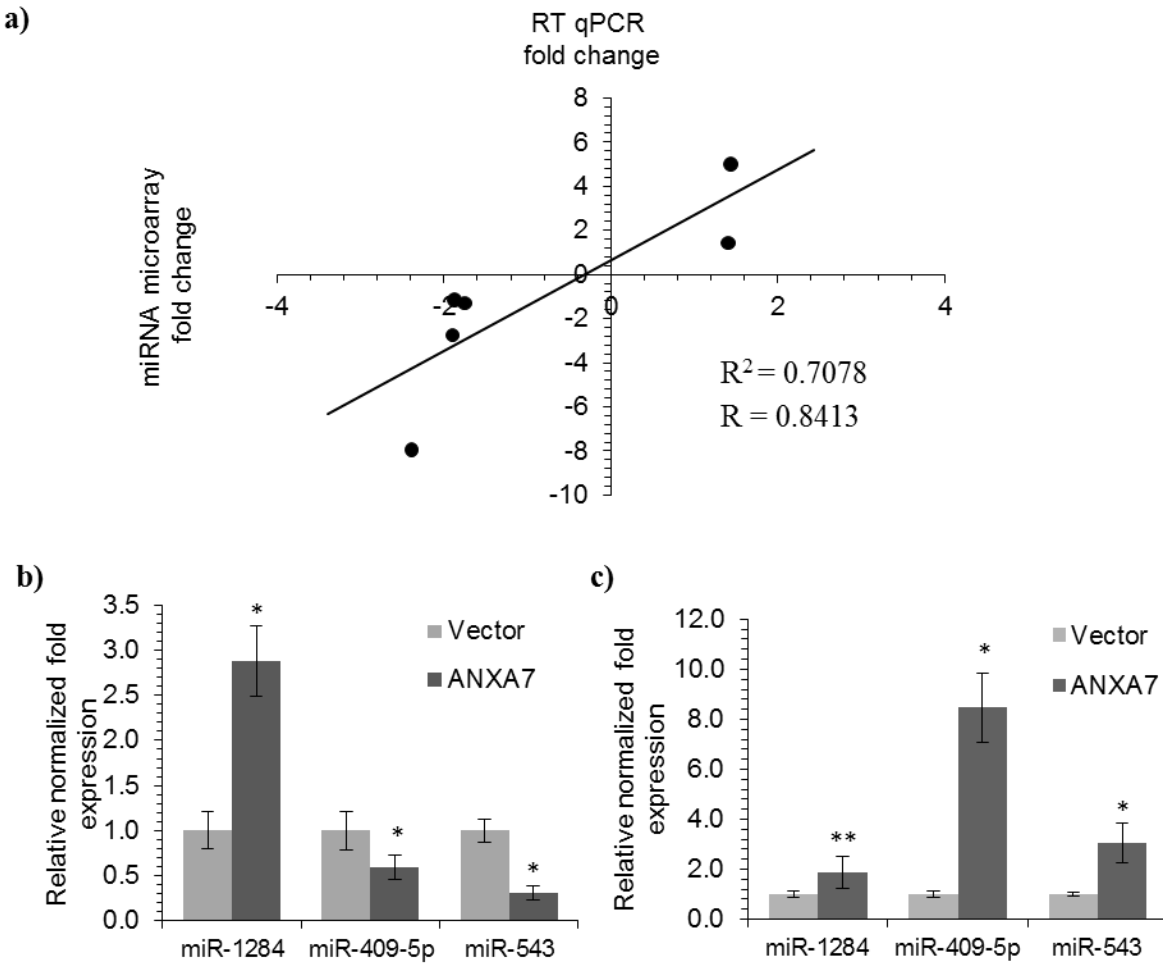

Figure 4.11 a- c: Validation and correlation of selected miRNA fold-expression between microarray and qPCR data. (a) Pearson correlation coefficient value, R was 0.8413 with an R^2 of 0.7078, indicating a positive correlation between both sets of data. A total of three significantly differentially expressed miRNAs were selected and expressed as relative normalized fold change expression values using qPCR in **(b)** PC-3 cells, and **(c)** DU-145 cells. Statistically significant differences between the empty vector control cells and transfected cells are presented as (*$p \leq 0.05$) and (**$p \leq 0.1$).

4.6 Predicted Genes and Pathways Targeted by *ANXA7* Dysregulated miRNAs.

Each miRNA in the list of dysregulated miRNAs were subsequently subjected to *in silico* target prediction and pathway enrichment analysis (Table 4.2). In order to identify miRNAs that were most relevant to this study, miRNAs that did not show involvement in cancer-related pathways after gene enrichment were not used for further analysis. After filtering, five of the up-regulated miRNAs and six of the down-regulated miRNAs passed our selection. Short listing of miRNA targets according to their target gene binding strength were conducted by eliminating those with a context score of > -0.25. A lower context score indicates a higher binding strength between the miRNA and the predicted target. Among the cancer-related pathways enriched for these miRNAs were the MAPK, Wnt, TGF-β, Notch and VEGF signaling pathways. Several miRNAs such as hsa-miR-133a, hsa-miR-1284, hsa-miR-448, hsa-miR-940 and hsa-miR-193a-3p were predicted to be involved in multiple pathways while others such as hsa-miR-874 and hsa-miR-543 were predicted to be involved in a single pathway targeting one or several genes (Table 4.2 & Table S4.6.1). Since four out of five predicted target genes for hsa-miR-874 were involved in forming calcium voltage-gated channels and calcium binding, we also postulated the possible implications of the calcium signaling pathway. ANXA7 is a Ca^{2+}-dependent membrane-binding protein involved in exocytosis. Its tumor suppression role would thus potentially involve the regulation of calcium signals and therefore our focus was on predicted targets that are related to calcium signaling. Hsa-miR-543 was predicted to interact with a calcium-dependent enzyme known as phospholipase A2, group IVA (PLA2G4A). Hsa-miR-409-5p targets were not enriched in any cancer-related pathways but it was predicted to bind strongly to calmodulin binding transcription activator 1 (CAMTA1). Since miRNAs are

negative gene regulators, these highlighted gene targets are expected to be downregulated by these upregulated miRNAs.

Table 4.2: List of validated miRNA gene targets and related pathways as obtained using TargetScan 6.2 software and KEGG pathway. A full list of validated and unvalidated miRNAs can be found in Table S4.6.1. * Targets obtained from TargetScan 6.2, with total context scores ≤ -0.2. ** Pathways obtained from KEGG Pathway Database.

† Strength of binding, -0.25 ≥ + ≥ -0.39, -0.40 ≥ ++ ≥ -0.59. †† False discovery rate, with FDR ≤ 50.0

miRNA	Target Genes (Gene symbol) *	Total Context Score *	Binding Strength†	KEGG Pathways**	FDR ††
hsa-miR-874	calcium channel, voltage-dependent, beta 2 subunit (CACNB2); R type, alpha 1E subunit (CACNA1E); L type, alpha 1D subunit (CACNA1D)	-0.4 / -0.36 / -0.39	++ / + / +	hsa04010:MAPK signaling pathway	0.38
	calcium binding protein P22 (CHP)	-0.31	+		
	protein phosphatase 5, catalytic subunit (PPP5C)	-0.35	+		
hsa-miR-1284	notch 3 (NOTCH3)	-0.34	+	hsa04330:Notch signaling pathway hsa04010:MAPK signaling pathway hsa04310:Wnt signaling pathway hsa04350:TGF-beta signaling pathway	0.84
	E1A binding protein p300 (EP300)	-0.28	+		0.91
	myocyte enhancer factor 2C (MEF2C)	-0.43	++		2.56
	TAO kinase 1 (TAOK1)	-0.43	++		40.99
	frizzled family receptor 5 (FZD5)	-0.29	+		
	inhibitor of DNA binding 4, dominant negative helix-loop-helix protein (ID4)	-0.28	+		
hsa-	phospholipase A2, group	-0.26	+	hsa04370:VEGF	32.9

miR-543	IVA (cytosolic, calcium-dependent) (PLA2G4A)			signaling pathway	2
hsa-miR-409-5p	calmodulin binding transcription activator 1 (CAMTA1)	-0.51	++	N/A	N/A

Table 4.2, continued

Chapter 5: Discussion

5.1 *ANXA7* potentially Regulates a Specific Set of MiRNAs

From the microarray miRNA results, it was found that the 16 microRNAs that had altered expression due to increased *ANXA7* expression have not been identified previously in miRNA profiling studies of prostate cancer. In addition, neither among these studies had overlapping miRNAs (Volinia *et al*., 2006; Porkka *et al*., 2007; Ambs *et al*., 2008; Ozen *et al*., 2008). The seemingly conflicting results between our data and data from other studies could possibly be due to the different approaches and methodology, for example platforms of microarray, type of samples and method for purification of RNA from samples (reviewed by Schaefer et al., 2009). Another possible explanation for this perhaps would be that each condition or altered gene expression (such as the case of ANXA7 in this study) would affect a specific set of microRNAs acting as a unique 'signature'. However, current miRNA data in prostate cancer is lacking as most profiling studies were only able to validate the dysregulation of a few microRNAs from microarray experiments with the more sensitive qRT-PCR (three in Ozen *et al.*, 2008, four in Ambs *et al*., 2008, one in Porrka *et al*., 2007). The number of studies looking at microRNAs that affect calcium signaling to date is very limited and the only one has been reported thus far (Wang *et al*., 2011). Expression of microRNAs in androgen-dependent LNCaP cells was studied. In this study, we used hormone-refractory prostate cancer cells. None of the miRNAs in the Wang's study (Wang *et al*., 2011) were common with this study and others mentioned previously (Volinia *et al*., 2006; Ambs *et al*., 2008; Ozen *et al*., 2008; Porkka *et al*., 2007). Therefore further studies involving groups of samples that are more stringently classified coupled

with high-throughput validation of miRNAs are warranted in order to accurately identify potential miRNA biomarkers.

5.2 Potential Regulation of Calcium Signaling by ANXA7 via Hsa-miR-874

Dysregulation in calcium signaling has been implicated in cancer progression where one of the key alterations is the change in the expression level of calcium channel and pump genes (Legrand *et al*., 2001). Examples of these alterations include the overexpression of TRPM8, a Ca^{2+}-permeable ion channel in some prostate cancers (Tsavaler *et al*., 2001; Zhang and Barritt, 2004). Calcium plays a dual function by acting as both a regulator of cell proliferation and an initiator of cell death during calcium overload (Monteith *et al.*, 2012). Even though overexpression of calcium channels often leads to a high turnover of calcium influx and reflux, unique calcium dysregulation mechanisms in cancer cells prevents a calcium overload from occurring which can lead to cell death. Based on previous reports, ANXA7 is a member of the annexin family of membrane proteins which operates in a Ca^{2+}-dependent manner and plays a major role in exocytosis (Geisow and Walker, 1986). In the current study, it was postulated that voltage-dependent Ca^{2+} channels are overexpressed in PC-3 and DU 145 prostate cancer cells due to mutated ANXA7 copies which indirectly regulates Ca^{2+} channel expression via miR-874 (Figure 5.1). A study by Nohata *et al*., 2011 indicated miR-874 as a tumor suppressor miRNA in maxillary sinus squamous cell carcinoma. In their study, they found miR-874 to have inhibitory effects on cell proliferation and invasion by directly regulating the PPP1CA (protein phosphatase 1, catalytic subunit, alpha isozyme) gene (Nohata *et al*., 2011). This

gene was also predicted as one of the targets of miR-874 in this study but was not included in our analysis as it did not pass the DAVID pathway enrichment filtering (section 3.2.18 and Table S4.6.1) and the focus of this study was on calcium signaling. However, this reinforced the possibility of miR-874 as a tumor suppressor miRNA in prostate cancer as well. Transfection of wt*ANXA7* copies into PC-3 and DU 145 cells increased the levels of miR-874 which suppress voltage-dependent Ca^{2+} channel overexpression. This was supported by *in silico* prediction of translational inhibition of calcium channel (CACNB2, CACNAE1, CACNA1D) and calcium binding protein p22 (CHP) mRNAs. A single microRNA could interact and regulate expression of multiple targets (Yun J. *et al*, 2011; Dong Q. *et al*, 2010). As a result of this inhibition, the rate of calcium influx was reduced and calcium-dependent transcription factors such as nuclear factor of activated T lymphocytes (NFAT) were deactivated. All these events have been reported to be involved in the control of cell cycle progression (Caetano *et al*., 2002; Lehen'kyi *et al*., 2007).

5.3 Putative modulation of MEF2C by miR-1284 and miR-874

The Myocyte Enhancer Factor 2 (MEF2) family of proteins which has four isoforms (MEF2A-D) was initially identified as a transcription factor that is involved in muscle cell differentiation. However, it was also found to be involved in the regulation of cell proliferation by functioning as a downstream player in signaling pathways activated by elevated levels of intracellular Ca^{2+} (Black and Olson, 1998). One member of this family, MEF2C, was a top predicted target that binds strongly to miR-1284 (Table 1). Elevated levels of MEF2C was associated with an aggressive leukemia phenotype (Schwieger *et al*.,

2009) and hepatocellular carcinoma phenotype (Bai *et al*., 2008). Another miR-1284 predicted target of interest was the transcriptional coactivator of MEF2C, the E1A binding protein p300 (EP300/p300). The p300 activates the transcription of MEF2 through its histone acetyltransferase activity (Ogryzko *et al*., 1996). Transcriptional corepressors on the other hand suppresses MEF2 activity by recruiting histone deacetylases. The histone deacetylase 4 (HDAC4) and p300 competes for binding to MEF2.The transcriptional repression activity of HDAC4 on MEF2 is regulated by Ca^{2+} (Youn *et al*., 2000). When Ca^{2+} is present, it competes with HDAC4 to bind to MEF2. Therefore MEF2 escapes from the inhibitory effects of HDAC4 and thus leads to increased transcriptional activity of MEF2 (Youn *et al*., 2000). Up-regulation of miR-1284 due to the overexpression of ANXA7 may inhibit transcriptional activity of MEF2C by directly inhibiting the expression of MEF2C itself or indirectly by inhibiting its transcriptional coactivator partner p300. It also allows transcription by releasing MEF2C from HDAC4 due to the presence of Ca^{2+}. Expression inhibition of voltage-dependent Ca^{2+} channels by miR-874 as mentioned above, leads to low level of Ca^{2+} and thus inhibition of MEF2C activity. The transcriptional activity of MEF2C is thereby putatively modulated indirectly by ANXA7 via the up-regulation of miR-1284 and miR-874 (Figure 5.1) leading to the magnified inhibition of MEF2C. Decreased transctiptional activity of MEF2C also reduces the transcription of *c-jun* (Kato *et al*., 1997) thus resulting in tumorigenesis inhibition.

5.4 Hsa-miR-543 and Phospholipase A2 Group 4A (PLA2G4A)

MiRNA-543 which was the most down-regulated miRNA in our list was predicted to target Phospholipase A2 Group IVA (PLA2G4A/hGIVA, $cPLA_2$-α). PLA2G4A is a member of a sub-group of lipid mediator enzymes (Ghosh *et al*., 2006) that is involved in the production of intracellular arachidonic acid for the production of eicosanoids (Laye and Gill, 2003). Production of biologically active eicosanoids such as prostaglandins (PGs) and hydroxyeicosatetraenoic acids (HETEs) are carried out by cyclooxygenase (COX) and lipoxygenase (LOX) and leads to various intracellular signal transduction (Patel *et al*., 2008a). The eicosanoid pathway was found to be activated in prostate cancer (Patel *et al*., 2008b; Nie *et al*., 2001). The Group IV PLA_2 enzymes are regulated by calcium and binds to intracellular proteins such as the annexins (Scott *et al*., 2010). It has been shown that PLA2G4A seems to have an oncogenic role (Sved *et al*., 2004) and the loss of PLA2G4A inhibitors such as ANX2 (Chetcuti *et al*., 2001) and ANX1 (Paweletz *et al*., 2000) has been found in prostate cancer. Inhibition of this enzyme slows the growth of prostate cancer cells both *in vitro* and *in vivo* with the corresponding reduction in cyclin D1 and Akt expression. The up-regulation of the phosphorylated form of PLA2G4A (p-PLA2G4A) was also found in three out of seven hormone-refractory prostate cancer samples examined (Patel *et al*., 2008). It would be interesting to elucidate this seemingly oncogenic effect of elevated levels of ANXA7 in PC-3 cells which lead to down-regulation of miR-543 and potential up-regulation of its putative target PLA2G4A which is oncogenic in prostate cancer. A key to explaining this relationship would be to investigate whether ANXA7 would also bind to and negatively regulate PLA2G4A like Annexins I and II (Wallner *et al*., 1986; Chetcuti *et al*., 2001) therefore suppressing the oncogenic effect of PLA2G4A. Down-regulation of

miR-543 via increased ANXA7 expression occurred possibly as a “balancing effect” to keep PLA2G4A levels at homeostatic levels (Figure 5.1). Further investigation is also needed to find out why only certain tissue samples showed increased levels of p-PLA2G4A when they acquire androgen-independence. A study with more samples and also looking at the expression levels of ANXA7 in relation to PLA2G4A expression levels could be carried out in the future to address this issue. However, it is interesting to note that increased ANXA7 led to the up-regulation of hsa-miR-543 in DU 145 cells which could potentially lead to the down-regulation of PLA2G4A and further investigation is required to explain the opposing expression pattern of hsa-miR-543 in PC-3 and DU 145 cells.

5.5 MicroRNA-409-5p and Calmodulin binding transcription activator 1 (CAMTA1)

CAMTAs are a family of proteins that can bind to calmodulin (CaM) and activate transcription in plants. They are also found in other multicellular organisms including humans but their physiologic roles remain to be elucidated (Bouché *et al*., 2002). The possible role of CAMTA1 in cell proliferation came from a study carried out in neuroblastomas whereby the reduced expression of CAMTA1 correlated with a poor prognosis suggesting a possible tumor suppressive role of CAMTA1 (Henrich *et al*., 2006).

In this study, hsa-miR-409-5p was predicted to bind to CAMTA1 and increased expression of ANXA7 led to hsa-miR-409-5p down-regulation in PC-3 cells. The down-regulation of hsa-miR-409-5p potentially reduces the negative regulatory effect of hsa-miR-409-5p on CAMTA1. This leads to increased expression of the CAMTA1 putative tumor suppressor gene. Calmodulin is a calcium-binding protein that regulates various

downstream transcription factors via the activation of Ca^{2+}/CaM-dependent kinase cascade when intracellular Ca^{2+} level increases (Ikura *et al*., 2002) and was found to bind to CAMTAs (Bouché *et al*., 2002). Modulation of CaM is recognized as an important event in malignant cell transformation (Sherbet 2001; Liu *et al*., 1996). Levels of CaM are elevated in various cancers as compared to their normal tissue counterparts (Liu *et al.*, 1996; Takemoto and Jilka, 1983; Wei *et al*., 1982) or unchanged (Moon *et al*., 1983). It is intriguing that there are currently no known functions for the binding of CaM to CAMTAs in humans. CaM binding is only postulated to act as a direct control of transcriptional activation, control of transport of CAMTA to the nucleus or control of DNA binding (Bouché *et al*., 2002). Further studies into the identification of the functions of CaM binding to CAMTA and the levels of CaM in PC-3 cells and DU 145 cells would be crucial to explain the pattern of up-regulation of hsa-miR-409-5p in DU 145 cells upon increased expression of ANXA7 as compared to PC-3 cells (Figure 5.1). Another interesting point to note would be the possible implications of miR-409-5p as a tumor suppressor whereby its expression was found to be lower in gliomas (Lages *et al*., 2011). However, more evidence is needed before miR-409-5p could be truly classified as a tumor suppressor and a clearer picture of ANXA7's relationship with miR-409-5p could be drawn.

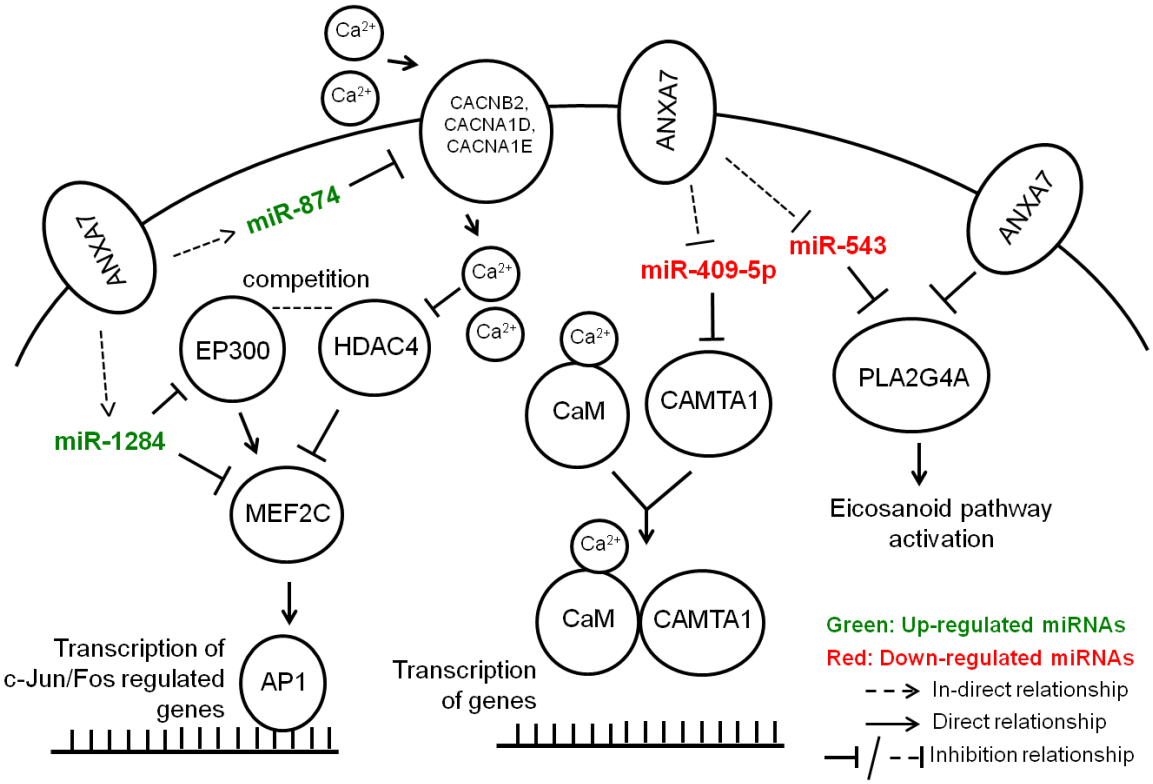

Figure 5.1: A hypothetical network illustrating the interaction of hsa-miR-874, hsa-miR-1284, hsa-miR-543 and hsa-miR-409-5p and their predicted targets following overexpression of wt*ANXA7* in PC-3 prostate cancer cells. Green denotes up-regulated miRNAs, whereas red denotes down-regulated miRNAs. Inhibitory relationships are denoted as flat arrow heads, direct interactions are denoted as solid arrows and in-direct interactions are denoted as dashed arrows.

Chapter 6: Conclusion

This study has demonstrated that ANXA7 leads to dysregulation in microRNA expression in prostate cancer cells. We also showed that the regulated microRNAs affected non-canonical pathways such as the calcium signaling pathways which are less studied compared to other well-known cancer-related pathways but are becoming more important in the study of cancer. The roles of non-canonical pathways are becoming more prominent in cancer as researchers are currently focusing their attention on novel biotherapeutics and biomarkers for development of more efficacious cancer treatment. Therefore our study provides a platform to methodically study the roles of these miRNAs in modulating calcium signaling in prostate cancer.

One limitation of this study is the use of cancer cell lines without tumor biopsy samples in the miRNA microarray. Prostate tumor biopsies with adjacent normal prostate biopsies allow for pairwise comparisons to be carried out. Pairwise comparison would give a more accurate representation of the miRNA expression in patients. Another limitation is the use of constitutive expression vector instead of inducible expression vector. Use of the latter allow for a time-point study of the change in miRNA expression levels when ANXA7 expression levels changes from low to high and maintained at high levels.

A better understanding in the interactions between miRNAs with their specific gene targets by experimentally confirming the relationship between the microRNA and their targets in the future can help us to delineate the molecular mechanism underlying the loss of ANXA7 in prostate cancer.

Future studies involving animal model and prostate cancer tissue samples would give a more comprehensive picture *in vivo*. It is our hope that our findings could be taken into a pre-clinical setting and to be ultimately developed into a potential therapeutic and/or diagnostic options and help in our war against cancer.

References

Abate-Shen C. and Shen M.M. (2000). Molecular genetics of prostate cancer. *Genes & Dev.* **14**:2410–34.

Altieri D.C., Languino L.R., Lian J.B., Stein J.L., Leav I. and van Wijnen A.J. *et al*. (2009). Prostate Cancer Regulatory Networks. *J. Cell. Biochem.* **107**:845-52.

Ambros V., Bartel B., Bartel D.P., Burge C.B., Carrington J.C., Chen X. *et al*. (2003). A uniform system for microRNA annotation. *RNA* **9**:277-99.

Ambs S., Prueitt R.L., Yi M., Hudson R.S., Howe T.M. and Petrocca F. *et al*. (2008). Genomic Profiling of MicroRNA and Messenger RNA Reveals Deregulated MicroRNA Expression in Prostate Cancer. *Cancer Res.* **68**:6162-70.

Aukerman M.J. and Sakai H. (2003). Regulation of flowering time and floral organ identity by a microRNA and its APETALA2-like target genes. *Plant Cell* **15**:2730-41.

Bai X., Wu L., Liang T., Liu Z., Li J. and Li D. (2008). Overexpression of myocyte enhancer factor 2 and histone hyperacetylation in hepatocellular carcinoma. *J. Cancer Res. Clin. Oncol.* **134**:83-91.

Bartel D.P. (2004). MicroRNAs: Genomics, Biogenesis, Mechanism, and Function. *Cell* **116**:281-97.

Bernstein E., Caudy A. A., Hammond S. M. and Hannon G. J. (2001). Role for a bidendate ribonuclease in the initiation step of RNA interference. *Nature* **409**:363-66.

Bentwich I., Avniel A., Karov Y., Aharonov R., Giladi S., Barad O. *et al*. (2005). Identification of hundreds of conserved and nonconserved human microRNAs. *Nature Genet.* **37**:766-70.

Bhatia-Gaur R., Donjacour A.A., Sciavolino P.J., Kim M., Desai N. and Young P. *et al*. (1999). Roles for Nkx3.1 in prostate development and cancer. *Gene Dev.* **13**:966-77.

Black B.L. and Olson E.N. (1998) Transcriptional control of muscle development by myocyte enhancer factor-2 (MEF2) proteins. *Annu. Rev. Cell Dev. Biol.* **14**:167-96.

Bohnsack M. T., Czaplinski K. and Görlich D. (2004). Exportin 5 is a RanGTP-dependent dsRNA-binding protein that mediates nuclear export of pre-miRNAs. *RNA* **10**: 185-91.

Borchert G.M., Lanier W. and Davidson B.L. (2006). RNA polymerase III transcribes human microRNAs. *Nat. Struct. Mol. Biol.* **13**:1097–101.

Bouché N., Scharlat A., Snedden W., Bouchez D. and Fromm H. A novel family of calmodulin-binding transcription activators in multicellular organisms. (2002). *J Biol. Chem.* **277**:21851-61.

Burns A.L., Magendzo K., Shirvan A., Srivastava M., Rojas E. and Alijani M.R. *et al*. (1989). Calcium channel activity of purified human synexin and structure of the human synexin gene. *Proc. Natl. Acad. Sci. USA.* **86**:3798-802.

Caetano M.S., Vieira-de-Abreu A., Teixeira L.K., Werneck M.B., Barcinski M.A. and Viola J.P. (2002). NFATC2 transcription factor regulates cell cycle progression during lymphocyte activation: evidence of its involvement in the control of cyclin gene expression. *FASEB J* **16**:1940-42.

Calin G.A., Dumitru C.D., Shimizu M., Bichi R., Zupo S. and Noch E. *et al*. (2002). Frequent deletions and down-regulation of micro-RNA genes *miR15* and *miR16* at 13q14 in chronic lymphocytic leukemia. *Proc. Natl. Acad. Sci. USA.* **99**:15524-29.

Calin G.A., Sevignani C., Dumitru C.D., Hyslop T., Noch E. and Yendamuri S. *et al*. (2004). Human microRNA genes are frequently located at fragile sites and genomic regions involved in cancers. *Proc. Natl. Acad. Sci. USA.* **101**: 2999–3004.

Calin G.A., Fabbri M., Iorio M.V., Ferracin M. and Shimizu M. et al. (2005). miR-15 and miR-16 induce apoptosis by targeting BCL2. *Proc. Natl. Acad. Sci. USA.* **102**:13944-49.

Cancer Research UK. (2010, September 29). CancerHelp UK: Prostate Cancer. Retrieved from http://www.cancerhelp.org.uk/type/prostate-cancer/about/the-prostate.

Caohuy H., Srivastava M. and Pollard H.B. (1996). Membrane fusion protein synexin (annexin VII) as a Ca^{2+}/GTP sensor in exocytotic secretion. *Proc. Natl. Acad. Sci. USA* **93**:10797-802.

Carthew R.W. and Sontheimer E.J. (2009). Origins and Mechanisms of miRNAs and siRNAs. *Cell* **136**:642-55.

Chang M., Tsuchiya K., Batchelor R.H., Rabinovitch P.S., Kulander
B.G. and Haggitt R.C. *et al*. (1994). Deletion mapping of chromosome 8p in colorectal carcinoma and dysplasia arising in ulcerative colitis, prostatic carcinoma, and malignant fibrous histiocytomas. *Am. J. Pathol.* **144**:1–6.

Chetcuti A., Margan S.H., Russell P., Mann S., Millar D.S., Clark S.J., Rogers J., Handelsman D.J. and Dong Q. (2001). Loss of Annexin II heavy and light chains in prostate cancer and its precursors. *Cancer Res.* **61**:6331-4.

Ciafre S.A., Galardi S., Mangiola A., Ferracin M., Liu C.G. and Sabatino G. *et al*. (2005). Extensive modulation of a set of microRNAs in primary glioblastoma. *Biochem. Biophys. Res. Commun*. **334**:1351-58.

Cimmino A., Calin G.A., Fabbri M., Iorio M.V., Ferracin M. and Shimizu M. *et al*. (2005). miR-15 and miR-16 induce apoptosis by targeting BCL2. *Proc. Natl. Acad. Sci. USA* **102**:13944-49.

Colombel M., Symmans F., Gil S., O'Toole K.M., Chopin D. and Benson M. *et al*. (1993). Detection of the apoptosis-suppressing oncoprotein bc1-2 in hormone-refractory human prostate cancers. *Am. J. Pathol.* **143**:390–400.

Cooney K.A., Wetzel J.C., Consolino C.M. and Wojno K.J. (1996). Identification and characterization of proximal 6q deletions in prostate cancer. *Cancer Res.* **56**:4150-53.

Cortez M.A., Bueso-Ramos C., Ferdin J., Lopez-Berestein G., Sood A.K. and Calin G.A. (2011). MicroRNAs in body fluids-the mix of hormones and biomarkers. *Nat. Rev. Clin. Oncol.* **8**:467-77.

Creutz C.E., Pazoles C.J. and Pollard H.B. (1978). Identification and Purification of an Adrenal Medullary Protein (Synexin) That Causes Calcium-dependent Aggregation of Isolated Chromaffin Granules. *J. Biol. Chem.* **253**: 2858-66.

Creutz C.E., Pazoles C.J. and Pollard H.B. (1979). Self-association of synexin in the presence of calcium. Correlation with synexin-induced membrane fusion and examination of the structure of synexin aggregates. *J. Biol. Chem.* **254**:553-58.

Culig Z., Hobisch A., Cronauer M.V., Radmayr C., Trapman J. and Hittmair, A. *et al*. (1994). Androgen receptor activation in prostatic tumor cell lines by insulin-like growth factor-I, keratinocyte growth factor, and epidermal growth factor. *Cancer Res.* **54**:5474–78.

Cullen B. R. (2004). Transcription and Processing of Human microRNA Precursors. *Mol. Cell* **16**:861-65.

Damber J.E. and Aus G. (2008). Prostate cancer. Lancet **371**:1710-21.

Denli A.M., Tops B.B., Plasterk R.H., Ketting R.F. and Hannon G.J. (2004). Processing of primary microRNAs by the Microprocessor complex. *Nature* **432**:231-35.

Department of Statistics Malaysia. (2009). Population Statistics, Malaysia Economics Statistics- Time Series 2009 (pp. 217-227). Malaysia: Department of Statistics Malaysia.

Dong Q., Meng P., Wang T., Qin W., Qin W. and Wang F. (2010). MicroRNA let-7a inhibits proliferation of human prostate cancer cells in vitro and in vivo by targeting E2F2 and CCND2. *PLoS One* **5**: e10147. doi: 10.1371/journal.pone.0010147.

Döring V, Schleicher M and Noegel AA. (1991). *Dictyostelium* annexin VII (synexin). cDNA sequence and isolation of a gene disruption mutant. *J. Biol. Chem.* **266**:17509-15.

Elo J.P., Kvist L., Leinonen K., Isomaa V., Henttu P. and Lukkarinen O. *et al*. (1995). Mutated human androgen receptor gene detected in a prostatic cancer patient is also activated by estradiol. *J. Clin. Endocrinol. Metab*. **80**:3494–3500.

Fabbri M., Ivan M., Cimmino A., Negrini M. and Calin G.A. (2007). Regulatory mechanisms of microRNAs involvement in cancer. *Expert Opin. Biol. Ther*. **7**:1009-19.

Ferlay J., Shin H.R., Bray F., Forman D., Mathers C. and Parkin D.M. GLOBOCAN 2008, Cancer Incidence and Mortality Worldwide: IARC CancerBase No. 10 [Internet]. Lyon, France: International Agency for Research on Cancer; 2010. Available from: http://globocan.iarc.fr

Fire A., Xu S., Montgomery M.K., Kostas S.A., Driver S.E. and Mello C.C. (1998). Potent and specific genetic interference by double-stranded RNA in *Caenorhabditis elegans*. *Nature* **391**:806-11.

Geisow M.J. and Walker J.H. (1986). New proteins involved in cell regulation by Ca2+ and phospholipids. *Trends Biochem. Sci.* **11**:420-23.

Ghosh M., Tucker D.E.,. Burchett S.A and Leslie C.C. (2006). Properties of the Group IV phospholipase A2 family. *Prog. Lipid Res.* **45**:487-510.

Gingrich J.R., Barrios R.J., Kattan M.W., Nahm H.S., Finegold M.J. and Greenberg N.M. (1997). Androgen-independent prostate cancer progression in the TRAMP model. *Cancer Res.* **57**:4687–91.

Giraldez A.J., Cinalli R.M., Glasner M.E., Enright A.J., Thomson J.M., Baskerville S. *et al*. (2005). MicroRNAs Regulate Brain Morphogenesis in Zebrafish. *Science* [DOI: 10.1126/science.1109020].

Gregory R.I., Yan K.P., Amuthan G., Chendrimada T., Doratotaj B., Cooch N. and Shiekhattar R. (2004). The Microprocessor complex mediates the genesis of microRNAs. *Nature* **432**:235-40.

Gregory R.I., Chendrimada T.P., Cooch N. and Shiekhattar R. (2005). Human RISC couples microRNA biogenesis and posttranscriptional gene silencing. *Cell* **123**:631–40.

Griffiths-Jones S., Bateman A., Marshall M., Khanna A. and Eddy S.R. (2003). Rfam: an RNA family database. *Nucleic Acids Res.* **31**:439-41.

Griffiths-Jones S. (2004). The microRNA Registry. *Nucleic Acids Res., Database issue* **32**:D109-11.

Griffiths-Jones S., Grocock R.J., van Dongen S., Bateman A. and Enright A.J. (2006). miRBase: microRNA sequences, targets and gene nomenclature. *Nucleic Acids Res.* **34**:140-44.

Grishok A., Pasquinelli A. E., Conte D., Li N., Parrish S., Ha I. *et al*. (2001). Genes and Mechanisms Related to RNA Interference Regulate Expression of the Small Temporal RNAs that Control *C. elegans* Developmental Timing. *Cell* **106**:24-34.

Hall T.A. (1999). BioEdit: a user-friendly biological sequence alignment editor and analysis program for Windows 95/98/NT. *Nucl. Acids. Symp. Ser.* **41**:95-8.

Han J., Lee Y., Yeom K.H., Kim Y.K., Jin H. and Kim V.N. (2004). The Drosha-DGCR8 complex in primary microRNA processing. *Genes Dev.* **18**:3016-27.

Hayashita Y., Osada H., Tatematsu Y., Yamada H., Yanagisawa K. and Tomida S. (2005). A polycistronic microRNA cluster, miR-17-92, is overexpressed in human lung cancers and enhances cell proliferation. *Cancer Res.* **65**:9628-32.

He H, Jazdzewski K., Li W., Liyanarachchi S., Nagy R. and Volinia S. *et al*. (2005). The role of microRNA genes in papillary thyroid carcinoma. *Proc. Natl. Acad. Sci. USA.* **102**:19075-80.

Henrich K.O., Fischer M., Mertens D., Benner A., Wiedemeyer R., Brors B., Oberthuer A., Berthold F., Wei J.S., Khan J., Schwab M. and Westermann F. (2006). Reduced expression of CAMTA1 correlates with adverse outcome in neuroblastoma patients. *Clin. Cancer Res.* **12**:131-8.

Hong K., Düzgüneş N. and Papahadjopoulos D. (1981). Role of synexin in membrane fusion. Enhancement of calcium-dependent fusion of phospholipid vesicles. *J. Biol. Chem.* **256**:3641-44.

Hong K., Düzgüneş N., Ekerdt R. and Papahadjopoulos D. (1982). Synexin facilitates fusion of specific phospholipid membranes at divalent cation concentrations found intracellularly. *Proc. Natl. Acad. Sci. USA.* **79**:4642-44.

Huang D.W., Sherman B.T. and Lempicki R.A. (2009a). Systematic and integrative analysis of large gene lists using DAVID Bioinformatics Resources. *Nature Protoc.* **4**:44-57.

Huang D.W., Sherman B.T. and Lempicki R.A. (2009b) Bioinformatics enrichment tools: paths toward the comprehensive functional analysis of large gene lists. *Nucleic Acids Res.* **37**:1-13.

Huggins C. and Hodges C.V. (1941). Studies in prostatic cancer. I. The effects of castration, of estrogen and of androgen injection of serum phosphatases in metastatic carcinoma of the prostate. *Cancer Res.* **1**:293–302.

Humphreys D.T., Westman B.J., Martin D.I. and Preiss T. (2005). Micro-RNAs control translation initiation by inhibiting eukaryotic initiation factor 4E/cap and poly(A) tail function. *Proc. Natl. Acad. Sci. USA.* **102**:16961–66.

Hutvagner G., McLachlan J., Pasquinelli A. E., Balint E., Tuschl T. and Zamore P. D. (2001). A Cellular Function for the RNA-Interference Enzyme Dicer in the Maturation of the let-7 Small Temporal RNA. *Science* **293**:834-38.

Hutvágner G. and Zamore P.D. (2002). A microRNA in a multiple-turnover RNAi enzyme complex. *Science* **297**:2056-60.

Hyytinen E.R., Frierson H.F. Jr, Boyd J.C., Chung L.W. and Dong J.T. (1999). Three distinct regions of allelic loss at 13q14, 13q21-22 and 13q33 in prostate cancer. *Genes Chromosomes Cancer* **25**:108-14.

Ikura M., Osawa M. and Ames J.B. (2002). The role of calcium-binding proteins in the control of transcription: structure to function. *Bioessays* **24**:625-36.

Isaacs W. and Kainu T. (2001). Oncogenes and tumor suppressor genes in prostate cancer. *Epidemiol Rev.* **23**:36-41.

Isaacs W.B. and Carter B.S. (1991). Genetic changes associated with prostate cancer in humans. *Cancer Surv.* **11**:15-24.

Jiang J., Lee E.J., Gusev Y. and Schmittgen T.D. (2005). Real-time expression profiling of microRNA precursors in human cancer cell lines. *Nucleic Acids Res.* **33**:5394–403.

Johnson S.M., Grosshans H., Shingara J., Byrom M., Jarvis R. and Cheng A. *et al*. (2005). RAS is regulated by the *let-7* microRNA family. *Cell* **120**:635-47.

Kanehisa M. and Goto S. (2000). KEGG: Kyoto Encyclopedia of Genes and Genomes. *Nucleic Acids Res.* **28**:27-30.

Kanehisa M., Goto S., Sato Y., Furumichi M. and Tanabe M. (2012). KEGG for integration and interpretation of large-scale molecular datasets. *Nucleic Acids Res*. **40**: D109-D114.

Kato Y., Kravchenko V.V., Tapping R.I., Han J., Ulevitch R.J. and Lee J.D.
(1997). BMK1/ERK5 regulates serum-induced early gene expression through transcription factor MEF2C. *EMBO J.* **16**:7054-66.
Kawamata T., Seitz H. and Tomari Y. (2009). Structural determinants of miRNAs for RISC loading and slicer-independent unwinding. *Nat. Struct. Mol. Biol.* **16**:953-60.

Kawamata T. and Tomari Y. (2010). Making RISC. *Trends Biochem. Sci.* **35**:368-76.

Ketting R.F., Fischer S.E.J., Berstein E., Sijen T., Hannon G.J. and Plasterk R.H.A. (2001). Dicer functions in RNA interference and in synthesis of small RNA involved in developmental timing in C. elegans. *Genes Dev*. **15**:2654-59.

Kleihues P., Schäuble B., zur Hausen A., Esteve J., and Ohgaki H. (1997). Tumors associated with p53 germline mutations: A synopsis of 91 families. *Am. J. Path*. **150**:1-13.

Lages E., Guttin A., El Atifi M., Ramus C., Ipas H. and Dupré I. (2011). MicroRNA and target protein patterns reveal physiopathological features of glioma subtypes. *PLoS One* **6**:e20600 doi:10.1371/journal.pone.0020600

Lagos-Quintana M., Rauhut R., Lendeckel W. and Tuschl T. (2001). Identification of Novel Genes Coding for Small Expressed RNAs. *Science* **294**: 853-58.

Lagos-Quintana M., Rauhut R., Yalcin A., Meyer J., Lendeckel W. and Tuschl T. (2002). Identification of Tissue-Specific MicroRNAs from Mouse. *Curr. Biol.* **12**:735-9.

Lagos-Quintana M., Rauhut R. and Meyer J. (2003). New microRNAs from mouse and human. *RNA* **9**: 175-9.

Latil A., Baron J.C., Cussenot O., Fournier G., Soussi T. and Boccon-Gibod L. *et al*. (1994). Genetic alterations in localized prostate cancer: Identification of a common region of deletion on chromosome arm 18q. *Genes Chromosomes Cancer* **11**:119–25.

Latil A., Cussenot O., Fournier G., Driouch K. and Lidereau, R. (1997). Loss of heterozygosity at chromosome 16q in prostate adenocarcinoma: Identification of three independent regions. *Cancer Res.* **57**:1058–62.

Lau N.C., Lim L.P., Weinstein E.G. and Bartel D.P. (2001). An Abundant Class of Tiny RNAs with Probable Regulatory Roles in *Caenorhabditis elegans*. *Science* **294**:858-62.

Laye J.P. and Gill J.H. (2003). Phospholipase A2 expression in tumours: a target for therapeutic intervention? *Drug Discov Today* **8**:710-6.

Legrand G., Humez S., Slomianny C., Dewailly E., Vanden Abeele F., Mariot P., Wuytack F. and Prevarskaya N. (2001). Ca2+ pools and cell growth. Evidence for sarcoendoplasmic Ca2+-ATPases 2B involvement in human prostate cancer cell growth control. *J Biol. Chem.* **276**:47608-47614.

Lehen'kyi V., Flourakis M., Skryma R. and Prevarskaya N. (2007). TRPV6 channel controls prostate cancer cell proliferation via Ca(2+)/NFAT-dependent pathways. *Oncogene* **26**:7380-85.

Le M.T., Teh C., Shyh-Chang N., Xie H., Zhou B. and Korzh V. *et al*. (2009). MicroRNA-125b is a novel negative regulator of p53. *Genes Dev.* **23**:862-76.

Lee R.C., Feinbaum R.L. and Ambros V. (1993). The *C. elegans* heterochronic gene *lin-4* encodes small RNAs with antisense complementarity to *lin-14*. *Cell* **75**:843-54.

Lee R. C. and Ambros V. (2001). An Extensive Class of Small RNAs in *Caenorhabditis elegans*. *Science* **294**:862-64.

Lee J.T., Lehmann B.D., Terrian D.M., Chappell W.H., Stivala F. and Libra M. *et al*. (2008). Targeting prostate cancer based on signal transduction and cell cycle pathways. *Cell Cycle* **7**:1745-62.

Lee Y., Jeon K., Lee J.T., Kim S. and Kim V.N. (2002). MicroRNA maturation: stepwise processing and subcellular localization. *EMBO J.* **21**:4663-70.

Lee Y., Ahn C., Han J., Choi H., Kim J. and Yim J. *et al*. (2003). The nuclear RNase III Drosha initiates microRNA processing. *Nature* **425**:415-19.

Lee Y., Kim M., Han J., Yeom K.H., Lee S. and Baek S.H. *et al*. (2004). MicroRNA genes are transcribed by RNA polymerase II. *EMBO J.* **23**:4051-60.

Lewis B.P., Burge C.B. and Bartel D.P. (2005). Conserved Seed Pairing, Often Flanked by Adenosines, Indicates that Thousands of Human Genes are MicroRNA Targets. *Cell* **120**:15-20.

Lim L.P., Lau N.C., Weinstein E.G., Abdelhakim A., Yekta S. and Rhoades M.W. *et al*. (2003). The microRNAs of *Caenorhabditis elegans*. *Genes Dev.* **17**:991-1008.

Liu G.X., Sheng H.F. and Wu S. (1996) A study on the levels of calmodulin and DNA in human lung cancer cells. *Br. J. Cancer.* **73**:899-901.

Llave C., Kasschau K.D., Rector M.A. and Carrington J.C. (2002a). Endogenous and Silencing-Associated Small RNAs in Plants. *Plant Cell* **14**:1605-19.

Llave C., Xie Z., Kasschau K.D. and Carrington J.C. (2002b). Cleavage of Scarecrow-like mRNA targets directed by a class of Arabidopsis miRNA. *Science* **297**:2053–56.

Lodygin D., Tarasov V., Epanchintsev A., Berking C., Knyazeva T. and Körner H. *et al*. (2008). Inactivation of miR-34a by aberrant CpG methylation in multiple types of cancer. *Cell Cycle* **7**:2591-600.

Lu J., Getz G., Miska E.A., Alvarez-Saavedra E., Lamb J. and Peck D. *et al*. (2005). MicroRNA expression profiles classify human cancers. *Nature* **435**:834-38.

Lund E., Güttinger S., Calado A., Dahlberg J.E. and Kutay U. (2004). Nuclear Export of MicroRNA Precursors. *Science* **303**:95-8.

Ma L., Teruya-Feldstein J. and Weinberg R.A. (2007). Tumour invasion and metastasis initiated by microRNA-10b in breast cancer. *Nature* **449**:682-8.

Maniataki E. and Mourelatos Z. (2005). A human, ATP-independent, RISC assembly machine fueled by premiRNA. *Genes Dev.* **19**:2979–90.

Martinez J., Patkaniowska A., Urlaub H., Luhrmann R., and Tuschl T. (2002). Single stranded antisense siRNAs guide target RNA cleavage in RNAi. *Cell* **110**:563–74.

Matranga C., Tomari Y., Shin C., Bartel D.P. and Zamore P.D. (2005). Passenger-strand cleavage facilitates assembly of siRNA into Ago2-containing RNAi enzyme complexes. *Cell* **123**:607-20.

Matsuyama H., Pan Y., Skoog L., Tribukait B., Naito K. and Ekman P. *et al*. (1994). Deletion mapping of chromosome 8p in prostate cancer by fluorescence in situ hybridization. *Oncogene* **9**:3071-76.

Mattie M.D., Benz C.C., Bowers J., Sensinger K., Wong L. and Scott G.K. *et al.* (2006). Optimized high-throughput microRNA expression profiling provides novel biomarker assessment of clinical prostate and breast cancer biopsies. *Molecular Cancer* **5:**24.

Meng F., Henson R., Wehbe-Janek H., Ghoshal K., Jacob S.T. and Patel T. (2007). MicroRNA-21 Regulates Expression of the PTEN Tumor Suppressor Gene in Human Hepatocellular Cancer. *Gastroenterology* **133**:647-58.

Metzler M., Wilda M., Busch K., Viehmann S. and Borkhardt A. (2004). High expression of precursor microRNA-155/BIC RNA in children with Burkitt lymphoma. *Genes Chromosomes Cancer* **39**:167-69.

Michael M.Z., O' Connor S.M., van Holst Pellekaan N.G., Young G.P. and James R.J. (2003). Reduced accumulation of specific microRNAs in colorectal neoplasia. *Mol. Cancer. Res.* **1**:882–91.

Monteith G.R., Davis F.M. and Roberts-Thomson S.J. (2012) Calcium channels and pumps in cancer: changes and consequences. *J Biol Chem.* **287**:31666-31673.

Morris J.P. 4th and McManus M.T. (2005). Slowing down the Ras lane: miRNAs as tumor suppressors? *Sci STKE.* **297**:pe41.

Moon T.D., Morley J.E., Vessella R.L., Levine A.S., Peterson G. and Lange P.H. (1983). The role of calmodulin in human renal cell carcinoma. *Biochem. Biophys. Res. Commun.* **114**;843-9.

Mourelatos Z., Dostie J., Paushkin S., Sharma A., Charroux B., Abel, L., *et al*. (2002). miRNPs: a novel class of ribonucleoproteins containing numerous microRNAs. *Genes Dev.* **16**:720–28.

Murakami Y., Yasuda T., Saigo K., Urashima T., Toyoda H. and Okanoue T. *et al*. (2006). Comprehensive analysis of microRNA expression patterns in hepatocellular carcinoma and non-tumorous tissues. *Oncogene* **25**:2537-45.

National Cancer Institute. (2008, November 20). Cancer Topics: Prostate Cancer. Retrieved from http://www.cancer.gov/cancertopics/types/prostate.

National Cancer Registry. (2002). The First Report Of The National Cancer Registry Cancer Incidence In Malaysia. Kuala Lumpur, Malaysia: Author.

National Cancer Registry. (2003). The Second Report Of The National Cancer Registry Cancer Incidence In Malaysia. Kuala Lumpur, Malaysia: Author.

National Cancer Registry. (2006). Malaysian Cancer Statistics-Data And Figure Peninsular Malaysia 2006. Kuala Lumpur, Malaysia: Author.

Nie D., Che M., Grignon D., Tang K., Honn K.V. (2001). Role of eicosanoids in prostate cancer progression. *Cancer Metastasis Rev.* **20**:195-206.

Nohata N., Hanazawa T., Kikkawa N., Sakurai D., Fujimura L. and Chiyomaru T. *et al*. (2011). Tumour suppressive microRNA-874 regulates novel cancer networks in maxillary sinus squamous cell carcinoma. *Br. J. Cancer* **105**:833-41.

Novina C.D. and Sharp P.A. (2004). The RNAi revolution. *Nature* **430**:161-64.

Nupponen N.N, Kakkola L., Koivisto P. and Visakorpi T. (1998). Genetic alterations in hormone-refractory recurrent prostate carcinomas. *Am. J. Pathol.* **153**:141-48.

O'Donnell K.A., Wentzel E.A., Zeller K.I., Dang C.V. and Mendell J.T. (2005). c-Myc-regulated microRNAs modulate E2F1 expression. *Nature* **435**:839-43.

Olive V., Jiang I. and He L. (2010). *mir-17-92*, a cluster of miRNAs in the midst of the cancer network. *Int. J. Biochem. Cell Biol.* **42**:1348–54.

Ogryzko V.V., Schiltz R.L., Russanova V., Howard B.H. and Nakatani Y. (1996). The transcriptional coactivators p300 and CBP are histone acetyltransferases. *Cell* **87**:953-59.

Ozen M., Creighton C.J., Ozdemir M. and M Ittmann M. (2008). Widespread deregulation of microRNA expression in human prostate cancer. *Oncogene* **27**:1788-93.

Park W., Li J., Song R., Messing J. and Chen X. (2002). CARPEL FACTORY, a Dicer Homolog, and HEN1, a Novel Protein, Act in microRNA Metabolism in *Arabidopsis thaliana*. *Curr. Biol.* **12**:1484-95.

Pasquinelli A.E., Reinhart B.J., Slack F., Martindale M.Q., Kuroda M.I. and Maller B. *et al* (2000). Conservation of the sequence and temporal expression of *let-7* heterochronic regulatory RNA. *Nature* **408**:86-9.

Patel M.I., Kurek C. and Dong Q. (2008a). The arachidonic acid pathway and its role in prostate cancer development and progression. *J Urol.* **1**:1668-75.

Patel M.I., Singh J., Niknami M., Kurek C., Yao M., Lu S., Maclean F., King N.J., Gelb M.H., Scott K.F., Russell P.J., Boulas J. and Dong Q. (2008b). Cytosolic phospholipase A2-alpha: a potential therapeutic target for prostate cancer. *Clin. Cancer Res*. **14:**8070-9.

Paweletz C.P., Ornstein D.K., Roth M.J., Bichsel V.E., Gillespie J.W. and Calvert V.S. *et al*. (2000). Loss of annexin 1 correlates with early onset of tumorigenesis in esophageal and prostate carcinoma. *Cancer Res.* **60**:6293-7.

Petersen C.P., Bordeleau M.E., Pelletier J., and Sharp P.A. (2006). Short RNAs repress translation after initiation in mammalian cells. *Mol. Cell* **21**:533–42.

Porkka K.P., Pfeiffer M.J., Waltering K.K., Vessella R.L., Tammela T.L.J. and Visakorpi T. (2007). MicroRNA Expression Profiling in Prostate Cancer. *Cancer Res*. **67**:6130-35.

Prostate Cancer Foundation. (2010). Understanding Prostate Cancer. Retrieved from http://www.pcf.org/site/c.leJRIROrEpH/b.5802023/k.B322/About_the_Prostate.htm

Provost P., Dishart D., Doucet J., Frendewey D., Samuelsson B. and Rådmark. (2002). Ribonuclease activity and RNA binding of recombinant human Dicer. *EMBO J.* **21**:5864–74.

Rand T.A., Petersen S., Du F. and Wang X. (2005). Argonaute2 cleaves the anti-guide strand of siRNA during RISC activation. *Cell* **123**:621-29.

Reinhart B.J, Slack F.J, Basson M., Pasquinelli A.E., Bettinger J.C., Rougvie A.E., Horvitz H.R. and Ruvkum G. (2000). The 21-nucleotide *let-7* RNA regulates developmental timing in *Caenorhabditis elegans*. *Nature* **403**:901-6.

Reinhart B.J., Weinstein E.G., Rhoades M.W., Bartel B. and Bartel D.P. (2002). MicroRNAs in Plants. *Genes Dev* **16**:1616-26.

Rhim J.S., Webber M.M., Bello D., Lee M.S., Arnstein P. and Chen L.S *et al*. (1994). Stepwise immortalization and transformation of adult human prostate epithelial cells by a combination of HPV-18 and v-Ki-*ras*. *Proc. Natl. Acad. Sci USA* **91**:11874-78.

Saric T., Brkanac Z., Troyer D.A., Padalecki S.S., Sarosdy M. and Williams K. *et al*. (1999). Genetic pattern of prostate cancer progression. *Int. J. Cancer* **81**:219–24.

Schaefer A., Jung M., Kristiansen G., Lein M., Schrader M. and Miller K. *et al*. (2010). MicroRNAs and cancer: current state and future perspectives in urologic oncology. *Urol. Oncol.* **28**:4-13.

Schwieger M., Schüler A., Forster M., Engelmann A., Arnold M.A. and Delwel R. (2009). Homing and invasiveness of MLL/ENL leukemic cells is regulated by MEF2C. *Blood* **114**:2476-88.

Scott K.F., Sajinovic M., Hein J., Nixdorf S., Galettis P., Liauw W., de Souza P., Dong Q., Graham G.G., Russell P.J. (2010) Emerging roles for phospholipase A2 enzymes in cancer. *Biochimie* **92**:601–10.

Sherbet G.V. (2001). Calcium signaling in cancer. *CRC Press*.

Shi X.B., Xue L., Yang J., Ma A.H., Zhao J. and Xu M. *et al*. (2007). An androgen-regulated miRNA suppresses Bak1 expression and induces androgen-independent growth of prostate cancer cells. *Proc. Natl. Acad. Sci. USA* **104**: 19983-88.

Srivastava M., Zhang-Keck Z.Y., Caohuy H., McPhie P. and Pollard H.B. (1996). Novel isoforms of synexin in Xenopus laevis : multiple tandem PGQM repeats distinguish mRNAs in specific adult tissues and embryonic stages. *Biochem. J.* **316**:729-35.

Srivastava M., Atwater I., Glasman M., Leighton X., Goping G. and Caohuy H. *et al*. (1999). Defects in inositol 1,4,5-trisphosphate receptor expression, Ca^{2+} signaling, and insulin secretion in the *anx7*(+/-) knockout mouse. *Proc Natl. Acad. Sci. USA.* **96**:13783-88.

Srivastava M., Bubendorf L., Nolan L., Glasman M., Leighton X. and Miller G. *et al*. (2001a). ANX7 as a bio-marker in prostate and breast cancer progression. *Dis. Markers* **17**:115-20.

Srivastava M., Bubendorf L., Srikantan V., Fossom L., Nolan L. and Glasman M. *et al*. (2001b). ANX7, a candidate tumor suppressor gene for prostate cancer. *Proc. Natl. Acad. Sci. USA.* **98**:4575-80.

Srivastava M., Montagna C., Leighton X., Glasman M., Naga S. and Eidelman O. *et al.* (2003). Haploinsufficiency of Anx7 tumor suppressor gene and consequent genomic instability promotes tumorigenesis in the Anx7(+/-) mouse. *Proc. Natl. Acad. Sci. USA.* **100**:14287-92.

Srivastava M., Bubendorf L., Raffeld M., Bucher C., Torhorst J. and Sauter G. *et al*. (2004). Prognostic Impact of ANX7-GTPase in Metastatic and HER2-Negative Breast Cancer Patients. *Clin. Cancer Res.* **10**:2344-50.

Srivastava M., Torosyan Y., Raffeld M., Eidelman O., Pollard H.B. and Bubendorf L. (2007). ANXA7 expression represents hormone-relevant tumor suppression in different cancers. *Intl. J. Cancer* **121**:2628-36.

Suzuki H.I., Yamagata K., Sugimoto K., Iwamoto T., Kato S. and Miyazono K. (2009). Modulation of microRNA processing by p53. *Nature* **460**:529-33.

Sved P., Scott K.F., McLeod D., King N.J., Singh J., Tsatralis T., Nikolov B., Boulas J., Nallan L., Gelb M.H., Sajinovic M., Graham, G.G., Russell P.J. and Dong Q. (2004). Oncogenic action of secreted phospholipase A2 in prostate cancer. *Cancer Res*. **64**:6934-40.

Takahashi S., Shan A.L., Ritland S.R., Delacey K.A., Bostwick D.G. and Lieber, M.M. *et al*. (1995). Frequent loss of heterozygosity at 7q31.1 in primary prostate cancer is associated with tumor aggressiveness and progression. *Cancer Res.* **55**:4114–19.

Takamizawa J., Konishi H., Yanagisawa K., Tomida S., Osada H. and Endoh H. *et al*. (2004). Reduced expression of the let-7 microRNAs in human lung cancers in association with shortened postoperative survival. *Cancer Res.* **64**:3753–56.

Takemoto D. and Jilka C. (1983). Increased content of calmodulin in human leukemia cells. *Leuk. Res.* **7**:97-100.

Tam W. (2001). Identification and characterization of human BIC, a gene on chromosome 21 that encodes a noncoding RNA. *Gene* **274**:157-67.

Tam W., Hughes S.H., Hayward W.S. and Besmer P. (2002). Avian *bic*, a Gene Isolated from a Common Retroviral Site in Avian Leukosis Virus-Induced Lymphomas That Encodes a Noncoding RNA, Cooperates with *c-myc* in Lymphomagenesis and Erythroleukemogenesis. *J. Virol.* **76**:4275-86.

Tsavaler L., Shapero M.H., Morkowski S. and Laus R. (2001) Trp-p8, a novel prostate-specific gene, is up-regulated in prostate cancer and other malignancies and shares high homology with transient receptor potential calcium channel proteins *Cancer Res.* **61**:3760-3769.

Tu S.M., McConnell K., Marin M.C., Campbell M.L., Fernandez A. and von Eschenbach A.C. *et al*. (1995). Combination adriamycin and suramin induces apoptosis in bcl-2 expressing prostate carcinoma cells. *Cancer Lett*. **93**:147–55.

Veldscholte J., Berrevoets C.A., Ris-Stalpers C., Kuiper G.G., Jenster G. and Trapman, J. *et al*. (1992). The androgen receptor in LNCaP cells contains a mutation in the ligand binding domain which affects steroid binding characteristics and response to antiandrogens. *J. Steroid Biochem. Mol. Biol.* **41**:665–69.

Volinia S., Calin G.A., Liu C.G., Ambs S., Cimmino A. and Petrocca F. *et al*. (2006). A microRNA expression signature of human solid tumors defines cancer gene targets. *Proc. Natl. Acad. Sci. USA.* **103**: 2257–61.

Wakiyama M., Takimoto K., Ohara O., and Yokoyama S. (2007). Let-7 microRNA-mediated mRNA deadenylation and translational repression in a mammalian cell-free system. *Genes Dev.* **21**:1857–62.

Wallner B.P., Mattaliano R.J., Hession C., Cate R.L., Tizard R., Sinclair K.L., Foeller C., Chow E.P., Browning J.L., Ramachandran K.L. and Pepinsky R.B. (1986). Cloning and expression of human lipocortin, a phospholipase A2 inhibitor with potential anti-inflammatory activity. *Nature (Lond.)* **320**:77– 81.

Wang W.L., Chatterjee N., Chittur S.V., Welsh J. and Tenniswood M.P. (2011). Effects of 1α,25 dihydroxyvitamin D3 and testosterone on miRNA and mRNA expression in LNCaP cells. *Mol. Cancer* **10**:doi: 10.1186/1476-4598-10-58.

Wei J.W., Morris H.P. and Hickie R.A. (1982). Positive correlation between calmodulin content and hepatoma growth rates. *Cancer Res.* **42**:2571-4.

Wienholds E., Kloosterman W.P., Miska E., Alvarez-Saavedra E., Berezikov E., de Brujin E. *et al*. (2005). MicroRNA Expression in Zebrafish Embryonic Development. *Science* **309**:310-11.

Wightman B., Bruglin T.R., Gatto J., Arasu P. and Ruvkun G. (1991). Negative regulatory sequences in the *lin-14* 3'-untranslated region are necessary to generate a temporal switch during *Caenorhabditis elegans* development. *Genes Dev.* **5**:1813-24.

Winter J., Jung S., Keller S., Gregory R.I. and Diederichs S. (2009). Many roads to maturity: microRNA biogenesis pathways and their regulation. *Nat. Cell Biol.* **11**:228-34.

Wu H., Xu H., Miraglia L.J. and Crooke S.T. (2000). Human RNase III Is a 160-kDa Protein Involved in Preribosomal RNA Processing. *J. Biol. Chem.* **275**:36957–65.

Yoda M., Kawamata T., Paroo Z., Ye X., Iwasaki S., Liu Q. *et al*. (2010). ATP-dependent human RISC assembly pathways. *Nat. Struct. Mol. Biol.* **17**:17-23.

Youn H.D., Grozinger C.M. and Liu J.O. (2000) Calcium regulates transcriptional repression of myocyte enhancer factor 2 by histone deacetylase 4. *J Biol. Chem*. **275:**22563-67.

Yun J., Frankenberger C.A., Kuo W.L., Boelens M.C., Eves E.M. and Cheng N. *et al*., (2011). Signalling pathway for RKIP and Let-7 regulates and predicts metastatic breast cancer. *EMBO J.* **30**:4500-14.

Zeng Y. and Cullen B. R. (2004). Structural requirements for pre-microRNA binding and nuclear export by Exportin 5. *Nucleic Acids Res.* **32**:4776-85.

Zenklusen J.C., Thompson J.C., Troncoso P., Kagan J. and Conti C.J. (1994). Loss of heterozygosity in human primary prostate carcinomas: A possible tumor suppressor gene at 7q31.1. *Cancer Res.* **54**:6370–73.

Zhang H., Kolb F.A., Jaskiewicz L., Westhof E. and Filipowicz W. (2004). Single processing center models for human Dicer and bacterial RNase III. *Cell* **118**:57-68.

Zhang-Keck Z.Y, Burns A.L. and Pollard H.B. (1993). Mouse synexin (annexin VII) polymorphisms and a phylogenetic comparison with other synexins. *Biochem J.* **289**:735-41.

Zhang L. and Barritt G. J. (2004) Evidence that TRPM8 is an androgen-dependent Ca2+ channel required for the survival of prostate cancer cells. *Cancer Res*. **64**:8365–8373.

Appendix A

Supplementary Materials

S4.1 Full length PCR Amplification of the *ANXA7* gene

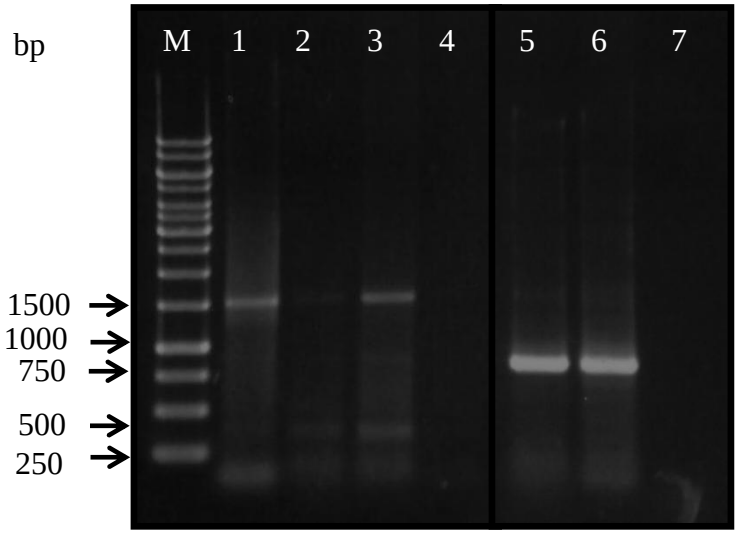

Figure S4.1. 1: PCR amplification of *ANXA7* using A7P2 primer pair. Successful amplification of *ANXA7* was carried out using the A7P2 primers on PC-3 cell line cDNA (lane 3) but the attempt to amplify *ANXA7* using the same primers on normal prostate epithelium cDNA (lane 2) failed. An amplification from a previous successful amplification reaction was also carried out (lane 1) as a positive control. To ensure the integrity of both normal prostate epithelium cDNA and PC-3 cell line cDNA, amplification of β-actin was carried out in parallel (lane 5 & 6, respectively). No-template amplification was carried out as negative controls (lane 4 & 7).

S4.2 Construction of Cloning and Expression Vectors containing ANXA7.

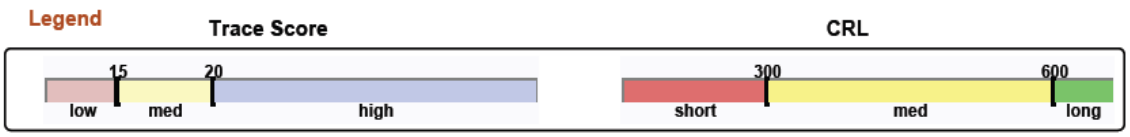

Trace File Name	Well#	Cap#	Trace Score	CRL	QV20+	Signal Intensity A	C	G	T	Comments
T5c1_M13F.ab1	C12	92	46	1063	1050	445	449	330	480	
T5c1_M13R.ab1	G5	35	47	1020	1012	197	218	141	235	
T5c2_M13F.ab1	D12	90	45	1012	1030	446	437	340	448	
T5c2_M13R.ab1	H5	33	47	969	949	180	194	133	214	
T5c3_M13F.ab1	E12	88	46	1064	1058	278	267	214	270	
T5c3_M13R.ab1	C11	91	46	1031	1045	421	379	305	473	Re-Cyc RxnID661510
T5c4_M13F.ab1	F12	86	46	1059	1048	449	505	347	499	
T5c4_M13R.ab1	B6	46	47	1086	1076	268	321	180	356	
T5d1_M13F.ab1	G12	84	46	1062	1057	324	340	291	312	
T5d1_M13R.ab1	D11	89	47	953	949	136	114	104	144	Re-Cyc RxnID661514
pGEM_M13F.ab1	A10	80	48	1066	1055	380	442	366	494	

Figure S4.2. 1: Quality check on pENTR/*ANXA7* construct sequences returned from sequencing. The sequence files of each cloning construct (T5c1-T5c4 & T5d1) was exported into Sequence Scanner (Applied Biosystems, USA) to generate a quality control report containing information on Trace score and Contiguous Read Length (CRL) of each clone. Each clone is sequenced in the forward (M13F) and in the reverse (M13F) directions as shown in the Trace File Name. All clones had sequences that are called accurately (Trace score >40) and able to cover whole *ANXA7* insert (CRL >600) Trace Score represents the accuracy of the basecall, Trace score >40 is equivalent to 99.99% accuracy. CRL represents the longest stretch of bases with high QV (quality value) QV>20 is equivalent to a high quality base. The full length sequence of the *ANXA7* in each construct was obtained by combining the forward and the reverse sequence of each construct. pGEM_M13F acted as a sequencing control.

T5c2 (1448 letters)

Query ID lcl|51085
Description T5c2
Molecule type nucleic acid
Query Length 1448

Database Name Human Genome (all assemblies) (3 databases)
Description ▹See details
Program BLASTN 2.2.26+ ▹Citation

Sequences producing significant alignments:

Accession	Description	Max score	Total score	Query coverage	E value	Max ident
NT_030059.13	Homo sapiens chromosome 10 genomic contig, GRCh37.p5 Pri	379	2718	99%	2e-102	100%
NW_001837987.2	Homo sapiens chromosome 10 genomic contig, alternate asse	379	2718	99%	2e-102	100%

T5c3 (1439 letters)

Query ID lcl|933
Description T5c3
Molecule type nucleic acid
Query Length 1439

Database Name Human Genome (all assemblies) (3 databases)
Description ▹See details
Program BLASTN 2.2.26+ ▹Citation

Sequences producing significant alignments:

Accession	Description	Max score	Total score	Query coverage	E value	Max ident
NT_030059.13	Homo sapiens chromosome 10 genomic contig, GRCh37.p5 Pri	379	2716	99%	2e-102	100%
NW_001837987.2	Homo sapiens chromosome 10 genomic contig, alternate asse	379	2716	99%	2e-102	100%

T5c4 (1439 letters)

Query ID lcl|5833
Description T5c4
Molecule type nucleic acid
Query Length 1439

Database Name Human Genome (all assemblies) (3 databases)
Description ▹See details
Program BLASTN 2.2.26+ ▹Citation

Sequences producing significant alignments:

Accession	Description	Max score	Total score	Query coverage	E value	Max ident
NT_030059.13	Homo sapiens chromosome 10 genomic contig, GRCh37.p5 Pri	379	2716	99%	2e-102	100%
NW_001837987.2	Homo sapiens chromosome 10 genomic contig, alternate asse	379	2716	99%	2e-102	100%

T5d1 (1438 letters)

Query ID lcl|30151
Description T5d1
Molecule type nucleic acid
Query Length 1438

Database Name Human Genome (all assemblies) (3 databases)
Description ▹See details
Program BLASTN 2.2.26+ ▹Citation

Sequences producing significant alignments:

Accession	Description	Max score	Total score	Query coverage	E value	Max ident
NT_030059.13	Homo sapiens chromosome 10 genomic contig, GRCh37.p5 Pri	379	2663	98%	2e-102	100%
NW_001837987.2	Homo sapiens chromosome 10 genomic contig, alternate asse	379	2663	98%	2e-102	100%

Figure S4.2. 2: Analysis of *ANXA7* sequence in pENTR/*ANXA7* constructs using NCBI BLAST. The full length sequences of the pENTR/*ANXA7* cloning constructs (T5c2-T5c4 & T5d1) was compared to sequences in the Human BLAST Assembled RefSeq Genomes. All sequences had a 100% identity (Max ident: 100%) to a region in Homo sapiens chromosome 10. The human genome build 37.3 with two genomic contig assemblies was referred to during the analysis (Accession number NT 030059.13 and NW 001837987.2)

```
                    500       510       520       530       540       550       560       570       580       590       600
Anx7 mRNA variant 1 CCTAGTCAG-------------------------------------------------------------CCTGCCACAGTGACTCAGGTCACTCAA
Anx7 mRNA variant 2 CCTAGTCAGATCAATACAGATTCTTTTTCTTCCTATCCTGTTTTCTCTCCTGTTTCTTTGGATTATAGCAGTGAACCTGCCACAGTGACTCAGGTCACTCAA
T5c1                CCTAGTCAG-------------------------------------------------------------CCTGCCACAGTGACTCAGGTCACTCAA
T5c2                CCTAGTCAG-------------------------------------------------------------CCTGCCACAGTGACTCAGGTCACTCAA
T5c3                CCTAGTCAG-------------------------------------------------------------CCTGCCACAGTGACTCAGGTCACTCAA
T5c4                CCTAGTCAG-------------------------------------------------------------CCTGCCACAGTGACTCAGGTCACTCAA
T5d1                CCTAGTCAG-------------------------------------------------------------CCTGCCACAGTGACTCAGGTCACTCAA
```

Figure S4.2. 3: Alignment of *ANXA7* sequences with cloning construct sequences using Bioedit. The full length sequences from the cloning constructs (T5c1-T5c4 & T5d1) were aligned with both *ANXA7* variant 1 (top) and *ANXA7* variant 2 (second from top) sequences using the ClustalW Multiple Alignment option. All cloning constructs (T5c1-T5c4 & T5d1) had *ANXA7* variant 1 sequence and not the variant 2 sequence. *ANXA7* variant 2 contains a region (base 508 to base 575) not present in variant 1. Only the region that matches to variant 1 but not to variant 2 was shown. The numbers above the sequences indicate the base number in the sequence.

a)

Legend

Trace Score: 15 (low) – 20 (med) – high

CRL: 300 (short) – 600 (med) – long

Trace File Name	Well#	Cap#	Trace Score	CRL	QV20+	Signal Intensity A	C	G	T	Comments
LR1b4_BGH reverse_run 1.ab1	H6	34	43	957	1020	196	241	138	248	
LR1b4_BGH reverse_run 2.ab1	G6	36	46	949	990	180	211	135	221	
LR1b4_T7 promoter_run 1.ab1	D12	90	42	973	1010	271	313	194	285	
LR1b4_T7 promoter_run 2.ab1	H4	18	45	1081	1083	427	539	343	415	Re-Cyc RxnID672910
pGEM_M13F.ab1	D12	90	46	1055	1056	498	606	403	558	

b)

LR1B4_full sequence_run 2 (1464 letters)

Query ID lcl|59139
Description LR1B4_full sequence_run 2
Molecule type nucleic acid
Query Length 1464

Database Name Human Genome (all assemblies) (3 databases)
Description ▹See details
Program BLASTN 2.2.26+ ▹Citation

Sequences producing significant alignments:

Accession	Description	Max score	Total score	Query coverage	E value	Max ident
NT_030059.13	Homo sapiens chromosome 10 genomic contig, GRCh37.p5 Pri	379	2718	98%	2e-102	100%
NW_001837987.2	Homo sapiens chromosome 10 genomic contig, alternate asse	379	2718	98%	2e-102	100%

Figure S4.2. 4a & b: Quality check of sequencing results and analysis of *ANXA7* sequence in pcDNA3.1/*ANXA7* construct. a) The clone LR1B4 containing the *ANXA7* sequence inserted into the pcDNA3.1/nV5-DEST™ vector was sequenced for a second time (run 2) to ensure accuracy of the sequencing and each clone is sequenced in the forward (T7 promoter) and reverse (BGH reverse) direction and checked according to Figure S4.2.1. **b)** The full length sequence of the clone was then subjected to BLAST according to Figure S4.2.2.

S4.3 Transfer of *ANXA7* from pcDNA3.1/ANXA7 to pIRES2-AcGFP1 vector

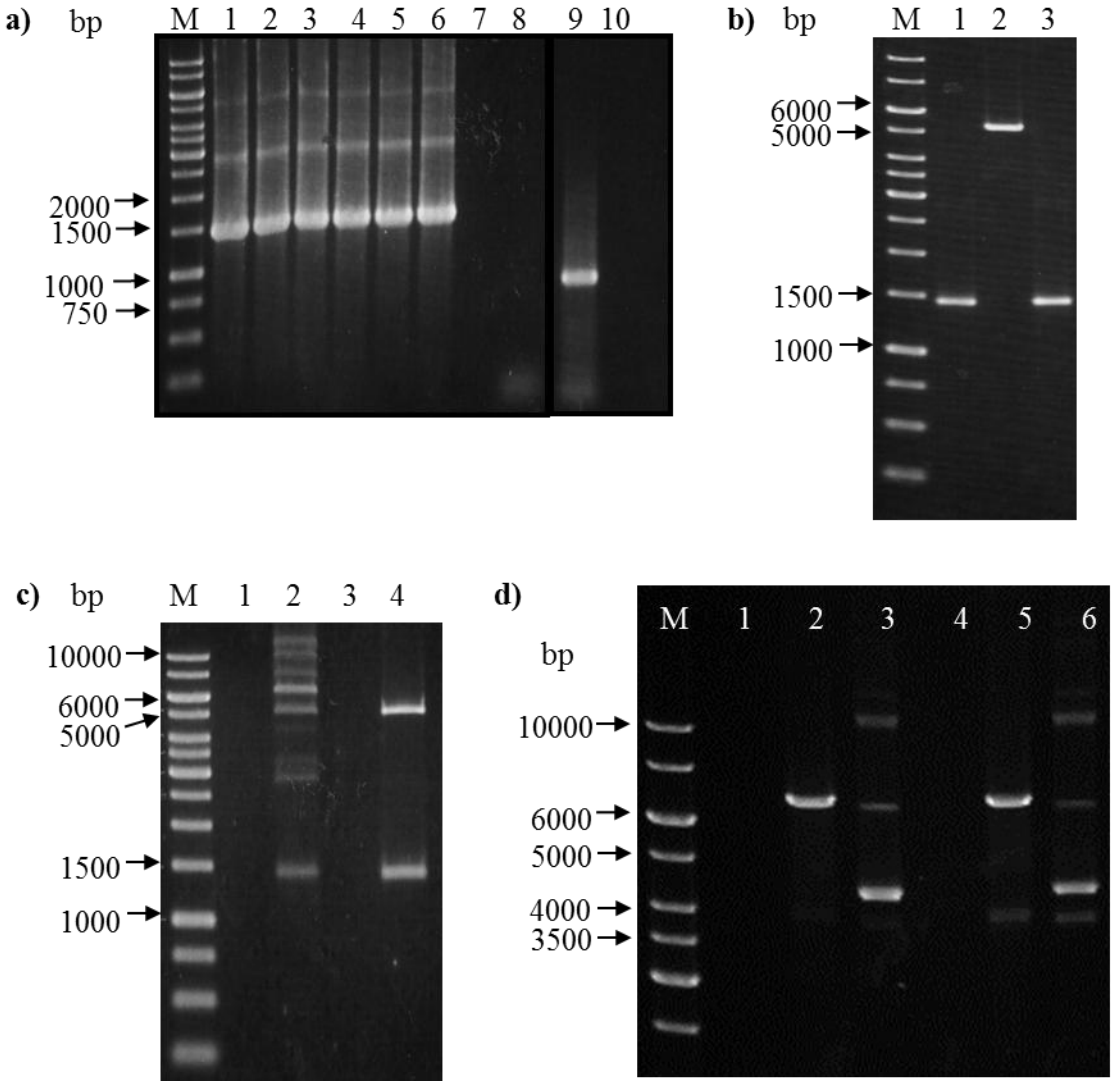

Figure S4.3. 1: Cloning of the *ANXA7* insert in pcDNA3.1/ANXA7 into pIRES2-AcGFP1 vector. a) PCR amplification of *ANXA7* from pcDNA3.1/ANXA7 vector with annealing temperatures of 53°C (lane 1), 56°C (lane 2), 59°C (lane 3), 62°C (lane 4), 65°C (lane 5) and 68°C (lane 6). The expected PCR product has a band size of about 1500bp. No-template amplification (lanes 8 & 10) and β-actin amplification (lane 9) was carried out as controls. Lane 7 was left empty.

Figure S4.3. 1 continued,: b) *BamHI* and *EcoRI* enzyme digestion of purified PCR product from a) (lane 1) and pIRES2-AcGFP1 vector (lane 2). A no-enzyme digestion (lane 3) was carried out as a control. A 0.8% agarose gel was used. **c)** Restricted PCR product and vector from b) was then ligated (lane 2) with the desired product of about 6800bp. A no-ligase reaction (lane 4) was carried out as a control. A 0.8% agarose gel was used. Lane 3 was left empty. **d)** *EcoRI* restriction enzyme digestion (lanes 2 & 5) of plasmids purified from colonies that carry a vector with the correct insert size screened via colony PCR (Figure 3.3.1). Restricted plasmids have an expected linear size of 6800bp.

a)

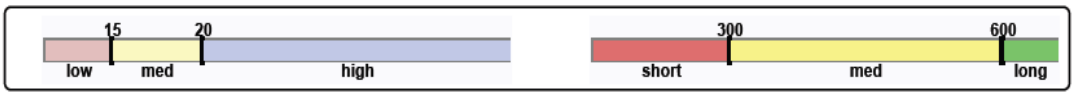

Trace File Name	Well#	Cap#	Trace Score	CRL	QV20+	Signal Intensity A	C	G	T	Comments
pIRES2-Anx7_1_F-pIRES2(run 1).ab1	C7	59	44	1188	1211	265	261	303	223	
pIRES2-Anx7_1_F-EcoRI(run 1).ab1	H3	17	37	764	857	187	219	206	195	
pIRES2-Anx7_1_R-BamHI(run 1).ab1	A4	32	38	806	947	297	280	261	243	
pIRES2-Anx7_1_R-pIRES2(run 1).ab1	E6	40	43	681	694	218	289	133	179	Re-Cyc RxnID884284
pIRES2-Anx7_1_F-pIRES2(run 2).ab1	E7	55	44	1133	1193	252	246	287	216	
pIRES2-Anx7_1_F-EcoRI(run 2).ab1	B4	30	31	854	989	257	238	247	196	
pIRES2-Anx7_1_R-BamHI(run 2).ab1	E12	88	45	907	957	197	166	132	164	RunID9568#4C. Re-Run RxnID878026, RunID9568
pIRES2-Anx7_1_R-pIRES2(run 2).ab1	H10	66	46	510	492	200	309	136	150	Re-Cyc RxnID884286
pIRES2-Anx7_2_F-pIRES2(run 1).ab1	G7	51	45	1193	1223	333	337	393	294	
pIRES2-Anx7_2_F-EcoRI(run 1).ab1	D4	26	29	808	924	257	234	243	202	
pIRES2-Anx7_2_R-BamHI(run 1).ab1	E4	24	37	880	1016	340	314	284	284	
pIRES2-Anx7_2_R-pIRES2(run 1).ab1	A11	95	45	627	610	291	420	187	229	Re-Cyc RxnID884288
pIRES2-Anx7_2_F-pIRES2(run 2).ab1	A8	64	45	1194	1222	351	371	418	308	
pIRES2-Anx7_2_F-EcoRI(run 2).ab1	F4	22	33	781	938	224	214	214	194	
pIRES2-Anx7_2_R-BamHI(run 2).ab1	G4	20	42	1027	1078	252	257	220	244	
pIRES2-Anx7_2_R-pIRES2(run 2).ab1	F6	38	42	645	654	188	245	115	153	Re-Cyc RxnID884290

b)

pIRES2/Anx7-clone 1 (1435 letters)

Query ID lcl|55517
Description pIRES2/Anx7-clone 1
Molecule type nucleic acid
Query Length 1435

Database Name Genome (all assemblies)
Description Homo sapiens build 37.3 genome database (reference assembly GRCh37.p5 [GCF_000001405.17] and alternate assemblies HuRef [GCF_000002125.1] and CRA_TCAGchr7v2 [GCF_000002135.2])
Program BLASTN 2.2.26+ ▷Citation

Sequences producing significant alignments:

Accession	Description	Max score	Total score	Query coverage	E value	Max ident	Links
NT_030059.13	Homo sapiens chromosome 10 genomic contig, GRCh37.p5 Pri	379	2716	100%	4e-102	100%	
NW_001837987.2	Homo sapiens chromosome 10 genomic contig, alternate asse	379	2716	100%	4e-102	100%	

pIRES2/Anx7-clone 2 (1435 letters)

Query ID lcl|2023
Description pIRES2/Anx7-clone 2
Molecule type nucleic acid
Query Length 1435

Database Name Genome (all assemblies)
Description Homo sapiens build 37.3 genome database (reference assembly GRCh37.p5 [GCF_000001405.17] and alternate assemblies HuRef [GCF_000002125.1] and CRA_TCAGchr7v2 [GCF_000002135.2])
Program BLASTN 2.2.26+ ▷Citation

Sequences producing significant alignments:

Accession	Description	Max score	Total score	Query coverage	E value	Max ident	Links
NT_030059.13	Homo sapiens chromosome 10 genomic contig, GRCh37.p5 Pri	379	2716	100%	4e-102	100%	
NW_001837987.2	Homo sapiens chromosome 10 genomic contig, alternate asse	379	2716	100%	4e-102	100%	

Figure S4.3. 2a & b: Quality check of sequencing results for pIRES2/ANXA7 clones and *ANXA7* sequence analysis.

Figure S4.3. 2a & b, continued: The sequencing covers the full length of the *ANXA7* sequence using four primers (F-pIRES2, F-EcoRI, R-BamHI and R-pIRES2 in 5' to 3' direction of *ANXA7*) and each clone sequenced twice (run 1 & run 2). One of the sequence returned had a CRL of less than 600 (marked as yellow) but the quality of the sequence was not affected and the full length of the *ANXA7* could still be covered by other sequences that have sequences which overlapped with this sequence. **b)** Both clones were subjected to BLAST according to Figure S4.2.2.

S4.4 Stable transfection of PC-3 and DU 145 cells with pIRES2/ANXA7

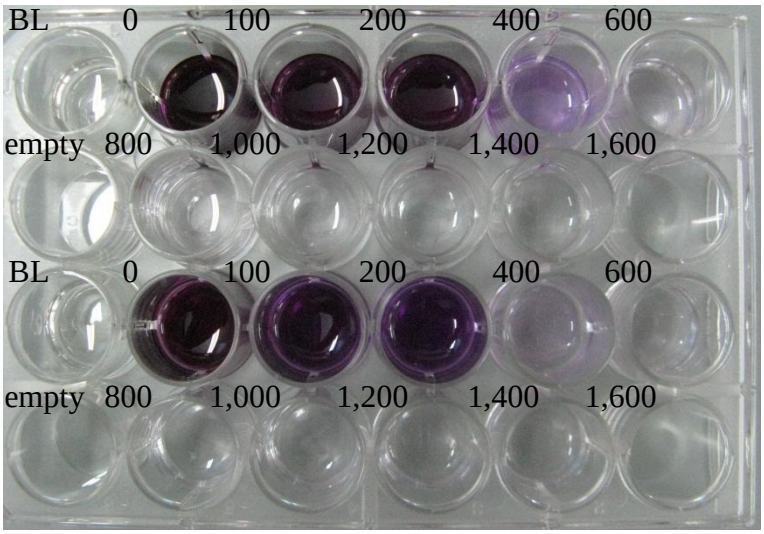

Figure S4.4. 1: Determination of G418 antibiotic concentration for selection of stable transfected cells. DU 145 (top two row of wells) and PC-3 (bottom two row of wells) cells were grown in a 24-well plate with an initial seeding number of 5 x 10^4 cells and allowed to attached overnight. Cells were then grown in complete medium with the addition of different G418 antibiotic concentration (100 μg/ml to 1,600 μg/ml) for 7 days with medium change every 3 days. After seven days, cell viability was visually assessed using MTT. Viable cells are indicated by the formation of purple solution. Concentration of G418 (in μg/ml) used are shown by the numbers at the top left of each well. BL, blank control; empty, empty well; 0 μg/ml, cells grown in medium without addition of G418.

4.5 MiRNA Profile of PC-3 and DU 145 Cells following *ANXA7* Overexpression

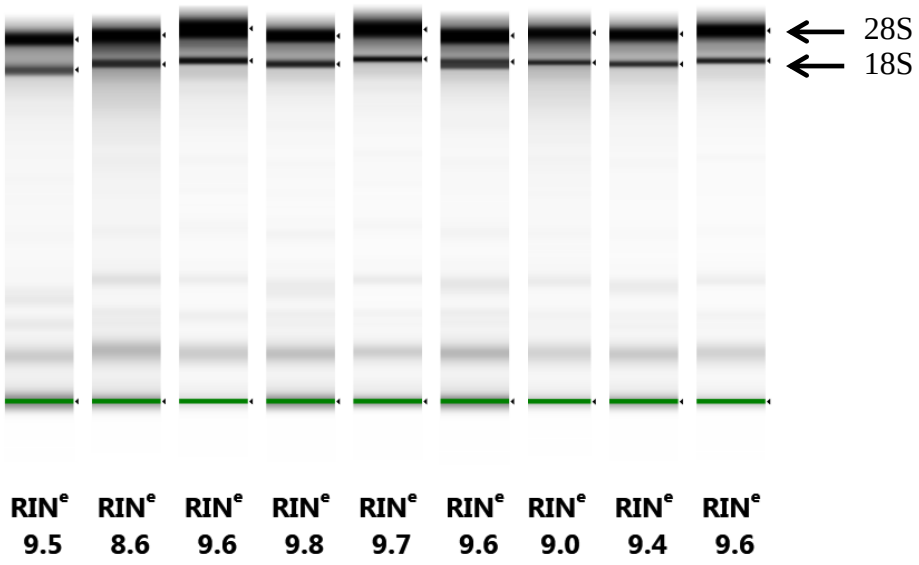

Figure S4.4. 2: Assessment of total RNA Integrity. The quality of the total RNA purified was determined using the Agilent 2200 Tapestation system according to manufacturer's protocol (Agilent Technologies, USA). Intact RNA is observed from the presence of two rRNA bands in each lane (top: 28S; bottom: 18S) in addition to a RNA Integrity Number (RIN) being assigned to each sample RNA (bottom of each lane). The RIN value ranges from 0 to 10 with a larger number indicating a high quality RNA.

S4.6 Predicted Genes and Pathways Targeted by ANXA7 Dysregulated miRNAs

Table S4.6. 1: List of miRNA gene targets and related pathways as obtained using TargetScan 6.2 software and KEGG pathway. MiRNA with gene targets that do not meet various score threshold criteria were designated as (N/A). * Targets obtained from TargetScan 6.2, with total context scores ≤ -0.25. ** Pathways obtained from KEGG Pathway Database. † Strength of binding where, -0.25 ≥ + ≥ -0.39 and -0.40 ≥ ++ ≥ -0.59. †† False discovery rate, with FDR ≤ 50.0.

miRNA	Target Genes (Gene symbol) *	Total Context Score *	Binding Strength †	KEGG Pathways**	FDR††
hsa-miR-346	N/A	N/A	N/A	N/A	N/A
hsa-miR-1237	N/A	N/A	N/A	N/A	N/A
hsa-miR-363	N/A	N/A	N/A	N/A	N/A
hsa-let-7b	N/A	N/A	N/A	N/A	N/A
hsa-miR-874	calcium channel, voltage-dependent, beta 2 subunit (CACNB2); R type, alpha 1E subunit (CACNA1E); L type, alpha 1D subunit (CACNA1D)	-0.4 / -0.36 / -0.39	++ / + / +	hsa04010:MAPK signaling pathway	0.38
	calcium binding protein P22 (CHP)	-0.31	+		
	protein phosphatase 5, catalytic subunit (PPP5C)	-0.35	+		
hsa-miR-133a	protein phosphatase 2, catalytic subunit, alpha isozyme (PPP2CA); beta isozyme (PPP2CB)	-0.49 / -0.41	++ / ++	hsa04310:Wnt signaling pathway hsa04010:MAPK signaling pathway	19.58 45.50
	transducin (beta)-like 1X-linked (TBL1X)	-0.25	+		
	epidermal growth factor receptor (EGFR)	-0.28	+		
	TAO kinase 1 (TAOK1)	-0.38	+		
	transforming growth factor, beta 2 (TGFB2)	-0.25	+		
	fibroblast growth factor 1 (acidic) (FGF1)	-0.35	+		

hsa-miR-551a	N/A	N/A	N/A	N/A	N/A
hsa-miR-1284	notch 3 (NOTCH3)	-0.34	+	hsa04330:Notch signaling pathway hsa04010:MAPK signaling pathway hsa04310:Wnt signaling pathway hsa04350:TGF-beta signaling pathway	0.84 0.91 2.56 40.99
	E1A binding protein p300 (EP300)	-0.28	+		
	myocyte enhancer factor 2C (MEF2C)	-0.43	++		
	TAO kinase 1 (TAOK1)	-0.43	++		
	frizzled family receptor 5 (FZD5)	-0.29	+		
	inhibitor of DNA binding 4, dominant negative helix-loop-helix protein (ID4)	-0.28	+		
hsa-miR-448	serine/threonine kinase 4 (STK4)	-0.25	+	hsa04010:MAPK signaling pathway hsa04350:TGF-beta signaling pathway	11.94 30.44
	mitogen-activated protein kinase kinase kinase 7 (MAP3K7)	-0.47	++		
	growth differentiation factor 6 (GDF6)	-0.46	++		
	SMAD specific E3 ubiquitin protein ligase 1 (SMURF1)	-0.31	+		
hsa-miR-382	N/A	N/A	N/A	N/A	N/A
hsa-miR-487b	N/A	N/A	N/A	N/A	N/A
hsa-miR-940	v-src sarcoma (Schmidt-Ruppin A-2) viral oncogene homolog (avian) (SRC)	-0.55	++	hsa04012:ErbB signaling pathway hsa04010:MAPK signaling pathway hsa04310:Wnt signaling pathway	0.58 3.04 4.27
	calcium binding protein P22 (CHP)	-0.32	+		
	mitogen-activated protein kinase 8 interacting protein 1 (MAPK8IP1)	-0.30	+		
	dishevelled, dsh homolog 3 (Drosophila) (DVL3)	-0.45	++		
	frizzled family receptor 4 (FZD4)	-0.37	+		
	calcium binding protein P22 (CHP)	-0.32	+		

Table S4.6.1, continued

hsa-miR-376a	N/A	N/A	N/A	N/A	N/A
hsa-miR-193a-3p	v-Ki-ras2 Kirsten rat sarcoma viral oncogene homolog (KRAS)	-0.41	++	hsa04010:MAPK signaling pathway hsa04310:Wnt signaling pathway	1.06 15.59
	mitogen-activated protein kinase kinase kinase 3 (MAP3K3)	-0.30	+		
	TAO kinase 1 (TAOK1)	-0.26	+		
	son of sevenless homolog 2 (Drosophila) (SOS2)	-0.53	++		
	stathmin 1 (STMN1)	-0.34	+		
	dual specificity phosphatase 7 (DUSP7)	-0.29	+		
	transforming growth factor, beta 2 (TGFB2)	-0.28	+		
	transducin (beta)-like 1 X-linked receptor 1 (TBL1XR1)	-0.30	+		
	presenilin 1 (PSEN1)	-0.30	+		
	seven in absentia homolog 1 (Drosophila) (SIAH1)	-0.36	+		
hsa-miR-409-5p	calmodulin binding transcription activator 1 (CAMTA1)	-0.51	++	N/A	N/A
hsa-miR-543	phospholipase A2, group IVA (cytosolic, calcium-dependent) (PLA2G4A)	-0.26	+	hsa04370:VEGF signaling pathway	32.92

Table S4.6.1, continued